Versatile Use of Liquid Chromatography and Mass Spectrometry in Drug Metabolism Studies

Bohumila Suchanová

Department of Biochemical Sciences
Faculty of Pharmacy in Hradec Králové
Charles University in Prague
Czech Republic

2007

Supervised by:

Doc. Ing. Vladimír Wsól, Ph.D.
Department of Biochemical Sciences
Faculty of Pharmacy in Hradec Králové
Charles University in Prague
Czech Republic

Opponents:

Prof. RNDr. Petr Solich, CSc.
Department of Analytical Chemistry
Faculty of Pharmacy in Hradec Králové
Charles University in Prague
Czech Republic

????

List of original publications

This dissertation is based on the following five papers, which are referred to in the text by their Roman numerals (**I-V**):

I. Vladimir Wsol, Barbora Szotakova, Vendula Baliharova, Ludek Sispera, Michal Holcapek, Lenka Kolarova, Bohumila Suchanova, Miroslav Kuchar, and Lenka Skalova: **The phase I biotransformation of potential antileukotrienic drug quinlukast in rat microsomes and hepatocytes.** *Collect. Czech. Chem. Commun.* 69 (2004) 689-702.

II. Kati S. Hakala, Bohumila Suchanova, Leena Luukkanen, Raimo A. Ketola, Moshe Finel, and Risto Kostiainen: **Rapid simultaneous determination of metabolic clearance of multiple compounds catalyzed in vitro by recombinant human UDP-glucuronosyltransferases.** *Anal. Biochem.* 341 (2005) 105–112.

III. Marek Link, Romana Novotna, Bohumila Suchanova, Lenka Skalova, Vladimir Wsol, and Barbora Szotakova: **The stereoselective biotransformation of the anti-obesity drug sibutramine in rat liver microsomes and in primary cultures of rat hepatocytes.** *J. Pharm. Pharmacol.* 57 (2005) 405-410.

IV. Bohumila Suchanova, Ludek Sispera, and Vladimir Wsol: **Liquid chromatography–tandem mass spectrometry in chiral study of amlodipine biotransformation in rat hepatocytes.** *Anal. Chim. Acta* 573-574 (2006) 273-283.

V. Bohumila Suchanova, Risto Kostiainen, and Raimo A. Ketola: **Characterization of in vitro metabolic profile of amlodipine using tandem mass spectrometry and accurate mass measurement.** *J. Mass Spectrom.* – submitted for publication.

Abbreviations

AML	amlodipine
APCI	atmospheric pressure chemical ionization
API	atmospheric pressure ionization
ATP	adenosine triphosphate
CE	capillary electrophoresis
Da	Dalton
ESI	electrospray ionization
FTMS	Fourier transform mass spectrometry
GC	gas chromatography
ITMS	ion trap mass spectrometry
LC	liquid chromatography
LLE	liquid-liquid extraction
m/z	mass to charge ratio
MRM	multiple reaction monitoring
MS	mass spectrometry
MS/MS	tandem mass spectrometry
MS^n	multiple stage mass spectrometry
NCEs	new chemical entities
NMR	nuclear magnetic resonance
QqQ	triple quadrupole = triple stage mass spectrometer
Q-TOF	quadrupole time-of-flight mass spectrometer
RAM	restricted access media
RIA	radioimmunoassay
SIM	selected ion monitoring
SPE	solid phase extraction
SRM	selected reaction monitoring
UGT	UDP-glucuronosyltransferase
UV	ultraviolet

Summary

Human organism has always been exposed to a vast array of chemicals encountered in the environment. Chemical revolution has significantly influenced biological evolution of humans leading to serious unpredictable toxicities. In response to continual chemical stress they have developed a variety of enzymes to transform these xenobiotics. Xenobiotics are mostly highly lipophilic and cannot readily be excreted from the body without metabolism to more hydrophilic, water-soluble metabolites. Not only environmental chemicals represent xenobiotics but also drugs, dietary components etc.

Biotransformation studies play an important role in the drug discovery and development process. Usually data from drug metabolism is required before a new substance can advance towards the development stages of a new therapeutic agent. Data on metabolism is frequently used to optimize drug candidates, suggest more active compounds or support toxicology studies. The increased flux of new chemical entities into drug discovery has placed an increased need for fast and reliable information on the metabolism of these substances. Liquid chromatography coupled with mass spectrometry can meet demands for rapid drugs and metabolites analysis imposed by modern drug discovery strategies.

This dissertation thesis presents an evidence of versatile usability of liquid chromatography and mass spectrometry in drug metabolism study and brings new approaches to solve questions of drug metabolism. Metabolites of quinlukast and sibutramine were characterized using a direct infusion of samples into the ion trap mass spectrometer. Coupling of liquid chromatography and mass spectrometry enabled study of amlodipine metabolism in detail. Differences in amlodipine metabolism from the chiral point of view, i.e. differences in metabolism of *rac*-, R- and S-amlodipine were specified. Further the metabolic profile of amlodipine was investigated and metabolic pathways yielding twenty-one characterized metabolites suggested. Liquid chromatography coupled with mass spectrometry was utilized in combination with “cocktail strategy”, in which a mixture of substrates is incubated at once, and the metabolites of the substrates are determined within a single assay. This combination enabled to develop rapid and reliable quantitative method for determination of glucuronides and human recombinant UDP-glucuronosyltransferases *in vitro*.

Summary in Czech

Lidský organismus byl od nepaměti vystaven škále chemikálií, které se vyskytují v životním prostředí. Chemická revoluce výrazně ovlivnila biologickou evoluci lidí a vedla k vážnému nepředvídatelnému toxickému působení těchto chemických látek. Odpovědí na neustálý chemický stres byl vývoj široké palety různých enzymů, které jsou schopné přeměňovat xenobiotika. Xenobiotika jsou obvykle vysoce lipofilní, a proto nemohou být vyloučeny z těla bez předchozí biotransformace na hydrofilní, ve vodě rozpustné metabolity. Mezi xenobiotika řadíme nejen chemické látky životního prostředí, ale také léčiva, složky potravy a další látky cizí organismu.

Biotransformační studie hrají důležitou roli ve výzkumu i ve vývoji léků. Údaje o metabolismu léčiv jsou obvykle vyžadovány předtím, než nová látka projde všemi vývojovými stádii a stane se lékem. Informace o metabolismu jsou často využívány ke zlepšování vlastností budoucích léčiv, umožňují navrhnout účinnější sloučeniny, nebo jsou využívány v rámci toxikologických studií. Se vzrůstajícím počtem nově vyvíjených látek stoupají nároky na rychlé získání spolehlivých informací o metabolismu těchto látek. Spojení kapalinové chromatografie a hmotnostní spektrometrie naplňuje požadavek na rychlost a spolehlivost analýzy léčiv a jejich metabolitů, který udává strategie moderního výzkumu.

Tato disertační práce předkládá důkaz o mnohostranné využitelnosti kapalinové chromatografie a hmotnostní spektrometrie pro studium metabolismu léčiv a přináší nové přístupy při řešení otázek biotransformace léčiv. Pomocí hmotnostní spektrometrie byly charakterizovány metabolity quinlukastu a sibutraminu po přímém nástřiku vzorků do iontové pasti. Spojení kapalinové chromatografie a hmotnostní spektrometrie umožnilo detailní studium metabolismu amlodipinu. Byly určeny rozdíly v metabolismu amlodipinu z chirálního hlediska, tedy rozdíly v metabolismu *rac*-, R-, a S-amlodipinu. Byl prostudován metabolický profil amlodipinu a navrženy metabolické cesty vedoucí ke vzniku jednadvaceti charakterizovaných metabolitů. Spojení kapalinové chromatografie s hmotnostní spektrometrií bylo využito v kombinaci s „koktejlovou strategií“, při které je najednou inkubována směs substrátů a metabolity těchto substrátů jsou determinovány během jediné analýzy. Tato kombinace umožnila vyvinout rychlou a spolehlivou kvantitativní metodu pro stanovení koncentrace glukuronidů a enzymové aktivity lidských rekombinantních UDP-glukuronosyltranferas *in vitro*.

Table of contents

1. INTRODUCTION

A vast array of chemicals is encountered in the modern environment, where the chemical revolution has outpaced biological evolution of humans leading to serious unpredictable toxicities. Organisms have always been exposed to environmental chemicals, and they have developed a variety of enzymes to transform these xenobiotics. The majority of xenobiotics is highly lipophilic and cannot readily be excreted from the body without metabolism to more hydrophilic, water-soluble species. Not only environmental chemicals represent xenobiotics but also drugs, dietary components etc.

Biotransformation studies play an important role in the drug discovery and development process. Usually data from drug metabolism is required before a new substance can advance towards the development stages of a new therapeutic agent. Data on metabolism is frequently used to optimize drug candidates, suggest more active compounds or support toxicology studies. The increased flux of new chemical entities (NCEs) into drug discovery due to combinatorial chemistry and high-throughput screening techniques has placed an increased need for fast and reliable information on the metabolism of these substances. Determination of the metabolic fate of drugs is thus an essential and important part of the drug development process. The study of how a drug is absorbed, distributed, metabolized, and eliminated by the body is vital but costly and time-consuming step in the drug discovery process. Thus biotransformation studies are commonly performed in the early drug discovery to determine metabolic pathways and to detect and characterize phase I and phase II metabolites. Metabolism can dictate the rate of absorption into the body, lead to the production of new species with possibly adverse effect, or activate the drug. Until recently, drug metabolism studies only took place once a compound had been chosen for drug development. However, the discovery of toxic metabolite can set a research program back significantly.

Liquid chromatography coupled with mass spectrometry can meet the demands for rapid drug metabolite profiling imposed by modern drug discovery strategies by decreasing sample preparation steps, and automating metabolite identification and making the analysis of polar molecules feasible without the need for derivatization. The technique is well suited to the direct identification of drug metabolites. Owing to the selectivity and specificity of the mass spectrometry and to high efficiency of liquid chromatography, LC-MS allows the separation and identification of the analytes even in complex matrices, like urine or plasma.

1.1 Drug metabolism

Drugs are xenobiotics to living organisms and are metabolized by organisms as a protection. There are a number of enzymes in humans and animals, which are capable to biotransform lipid-soluble xenobiotics in such way as to render them more water-soluble. Drug metabolism reactions are commonly divided into phase I, phase II, and phase III reactions. In phase I reactions functional groups are added to or generated in the molecule, while in phase II reactions the molecule is conjugated with some endogenous component. Transport of metabolites of xenobiotics may be considered as phase III of the detoxification mechanisms. Phase I reactions are involved in hydrolysis, oxidation, and reduction reactions whereas phase II type reactions have been referred to as conjugative reactions. The principal enzymes responsible for phase I reactions are the cytochrome P450s (Gibson and Skett, 2001; Guengerich, 2006; Sheweita, 2000), although other enzyme systems such as the flavin-containing monooxygenases (Cashman, 2005; Cashman and Zhang, 2006; Krueger and Williams, 2005), alcohol dehydrogenases belonging to medium-chain dehydrogenase/reductase superfamily (Gallego *et al.*, 2006), members of short-chain dehydrogenase/reductase (Kallberg *et al.*, 2002; Oppermann *et al.*, 2001), aldo-keto reductase superfamilies (Jez *et al.*, 1997b; Jez *et al.*, 1997a; Jin and Penning, 2006), and enzymes catalyzing peroxidation of xenobiotics i.e., prostaglandin synthase, lipoxygenase, and peroxidase (Kulkarni, 2001a; Kulkarni, 2001b; Vogel, 2000), may also serve this function for certain substrates. Phase I reactions introduce or unmask a functional group (-OH, -NH_2, -COOH, etc.) and make the compound more water soluble. If the metabolites of phase I reactions are sufficiently polar, they may be readily excreted at this point. Phase II reactions have been referred to as conjugative reactions, which include glucuronidation, sulfation, acetylation, methylation, conjugation with glutathione (mercapturic acid synthesis), and conjugation with amino acids (e.g., glycine, taurine, and glutamic acid) (Gibson and Skett, 2001). Phase III reactions are usually mediated by ATP dependent transporters. They can be found in a variety of tissues. ATP dependent transporters are often involved in tumour resistance to chemotherapy and may function as energy dependent efflux pump (Bodo *et al.*, 2003; Suzuki *et al.*, 2001).

The net result of the combined phase I, II and III reactions is generally to detoxify and eliminate xenobiotics from the body. However, the same pathways can also carry out the activation of most toxic and carcinogenic chemicals to electrophilic forms, which can react irreversibly with macromolecules as proteins and nucleic acids (Goldstein and Faletto, 1993).

In the theory, a balance between the cytochrome P450 and conjugation enzymes is responsible for either the detoxification or the accumulation of toxic metabolites in the body (King *et al.*, 2000).

1.2 Systems for studies of drug metabolism

Systemic metabolism is the leading drug disposition pathway, thus major emphasis is placed on a comprehensive assessment of drug metabolism. *In vivo* experiments are performed with animals or humans and the metabolites are analyzed in urine, plasma, bile, and feces samples (Kostiainen *et al.*, 2003). Studies on living subjects have many limitations and drawbacks. Of principle importance is the issue of risk to human subjects. Increasingly stringent regulatory requirements for the control and pre-marketing studies, as well as scientific needs for appropriate design and sample size cause these studies to be costly and time-consuming. Therefore well designed *in vitro* methodologies are essential. Because it is not possible to use humans in long-term toxicological studies, the use of animal models will continue.

In vitro methods play a critical role during the pre-clinical drug development phase as well as in non-clinical studies conducted post-approval and launch of the drug. During the pre-clinical phase of drug development such studies asses the metabolic stability, metabolic phenotyping (elucidation of specific enzymes involved in phase I and II metabolism), metabolic profiling (identification and structural characterization of the metabolites), and drug interaction issues pertaining to enzyme inhibition and induction. Such studies are now increasingly being used for qualitative and quantitative prediction of drug biotransformation in humans and in the identification of likely determinants of metabolism following drug administration to humans, including possible drug interactions. Results from a multitude of such experiments help in identifying/optimizing a lead compound and sorting out compounds that are likely to be problematic with regards to causing toxicity or adverse drug-drug interactions (Hariparsad *et al.*, 2006; Masimirembwa *et al.*, 2003).

The liver is the major organ involved in the biotransformation of drug, though also extrahepatic organs intestine, kidneys, lungs, brain or skin contribute to metabolism of drugs (Krishna and Klotz, 1994; Schwenk, 1988). The availability of human liver tissue dropped due to extensive use for transplantation and thus animal tissues are often used and results extrapolated. There are 2 basic categories of *in vitro* methods for the examination of liver drug metabolism. The first group of *in vitro* methods consists of the cellular models, which

include primary hepatocytes, liver slices, and cell lines. The second group is the use of preparations of the drug-metabolizing enzymes such as tissue homogenates, subcellular fractions – microsomes, cytosol, S9, and isolated (recombinant) enzymes (Hariparsad *et al.*, 2006; Wrighton *et al.*, 1995).

1.3 Analysis of drug metabolites

The metabolism of a drug can be extremely complex, involve multiple enzymatic pathways, and lead to a range of metabolites with varying concentrations. Other drugs can have one or two major metabolic pathways that dominate their metabolism, but several minor pathways can produce at least one metabolite. The information required to determine the metabolic fate of an NCE includes detection of metabolites, structure characterization and quantitative analysis. In some cases the concentrations of the metabolites may be extremely low and highly specific and sensitive analytical methods are then required. Several methods have been applied in the analysis of drugs and their metabolites, such as radioimmunoassay (RIA), gas chromatography/mass spectrometry (GC/MS), and liquid chromatography (LC) with ultraviolet (UV), fluorescence, radioactivity and mass spectrometric detection (MS).

MS has emerged as an ideal technique for the identification of such structurally diverse metabolites. After the introduction of the atmospheric pressure ionization (API) techniques, electrospray and atmospheric pressure chemical ionization (APCI), it was possible to couple liquid chromatography with mass spectrometry (LC/MS). The technique is extremely robust, rapid, sensitive, and easily automated. LC/MS and especially liquid chromatography coupled with tandem mass spectrometry (LC/MS/MS) have become the methods of choice for drug metabolism studies, yielding concentration versus time data for drug compounds as well as information on structure of metabolite from complex biological samples.

Concerning LC, good separation is often required for sufficient specificity of the LC/MS analysis. The selection of an LC method depends on the complexity of the sample matrix and also on the specificity of the mass spectrometric detection method. In the case of quantitative analysis of a parent drug or a few metabolites in a simple *in vitro* matrix, the speed of the LC method is a key issue to ensure high sample throughput. Good resolution has clear benefits in drug and metabolite analysis, because co-eluting matrix components may decrease the signal owing to competition in the ionization process, further the metabolism of a drug may lead to the formation of several isobaric compounds that should be separated prior

to quantitation, and labile metabolites, such as N-oxide, glucuronides and sulfates, may degrade to give the original drug either by in-source dissociation or by thermal degradation in the heated capillary. In this case, co-elution of the metabolites with the original drug will interfere with quantitation. Reversed-phase LC is most often used in metabolite analysis owing to the universality and its good compatibility with APCI- and ESI-MS. Nevertheless, for routine use of LC/MS separations should be developed using volatile eluting solvents and buffers.

The analytical strategy for metabolite analysis is dependent on the information sought. In the early stage of drug discovery, metabolic stability, drug-drug interactions and enzyme kinetic studies are based on the quantitative analysis of a parent drug or a few of its metabolites. In these types of analyses the key issue is high throughput and therefore the analytical method should be as fast as possible. However, the determination of metabolite profiles is usually performed for a limited number of lead molecules and in these experiments the key issues are high specificity and sensitivity rather than a speed. The first step in metabolite profiling is to identify all the possible metabolites. The second step is their structural characterization and finally quantitation. An analytical strategy for metabolite profiling by LC/API-MS is presented in Scheme 1.

Mass spectrometric detection of ionized metabolites by can be carried out in a linear mode or in the more selective and sensitive mode called selected ion monitoring (SIM). In the linear mode a range of mass to charge ratio (*m/z*) is constantly monitored. In SIM a particular ion (or ions) of a specific m/z value is selected for monitoring. Sensitivity of identification of metabolites in the full-scan MS using QqQ may not exert sufficient sensitivity, which can be achieved by ion trap mass spectrometer (ITMS) and time-of-flight mass spectrometer (TOF-MS) (Clarke *et al.*, 2001).

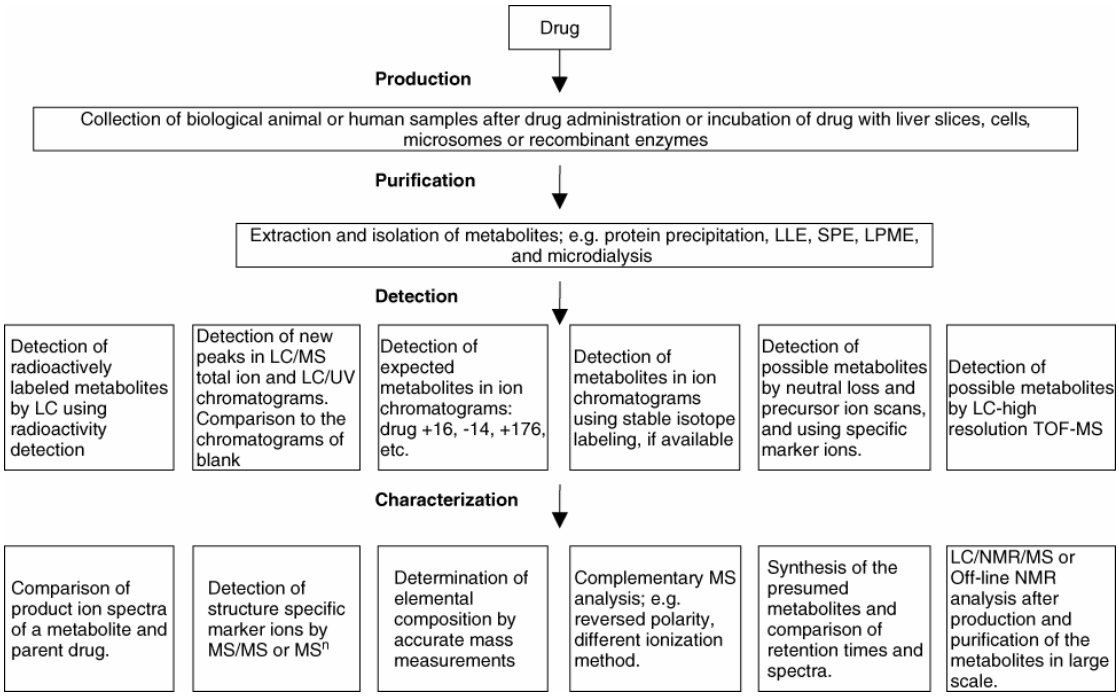

Scheme 1. Strategy and possibilities for metabolite profiling by LC/MS. Reprinted with permission from Kostiainen *et al.*, 2003.

1.3.1 Metabolites identification

Identifying metabolites remains a time-consuming process because a range of instrumental techniques and software applications are needed to obtain the appropriate data. The analyst must be quite experienced to handle these various instruments and software packages. Data is rarely obvious or completely conclusive, but rather requires previous experience to unravel it. For all these reasons, interpreting the data is typically the largest bottleneck in metabolite identification.

A common method in metabolite identification includes the production of metabolites by *in vitro* or *in vivo* experiments, collection of samples at different time points including blank sample at time-point zero and analysis of samples by using full-scan MS. The metabolites are identified by comparison of the full scan ion chromatograms of the blank, control and the full samples. The comparison might be achieved manually, which is usually enormously time-consuming, or by means of software for metabolite identification.

Manual interpretation of the data is still a major drawback in the metabolite identification process because it is so time consuming. These new approaches to data acquisition have led to many more samples being run in the same time period, which, in turn, increase the amount of data. Software that can reduce operator workload by using a series of

criteria to analyze data and report apparent metabolites significantly improves throughput in metabolite identification.

Instrument manufacturers are creating software packages that facilitate the metabolite identification process such as Metabolynx (Micromass), Metabolite ID (PE Sciex), and the new Metabolite Data Browser (Thermo Finnigan). These packages automatically perform functions that researchers presently complete by hand such as the background subtraction of a control data file or the application of an isotope cluster analysis for chlorine- and bromine-containing compounds. At a minimum, the software searches for a list of expected metabolites from full-scan data and returns a list of possible hits. This allows discarding noise responses automatically.

As these packages evolve, they will handle correlation analysis of tandem MS data and data-dependent tandem MS acquisition of potential metabolites. All of these factors aid in reducing the data set that the analyst has to examine, thereby increasing throughput. The new direction for metabolite identification is the integration of automated data interpretation with LC/MS/MS in combination with the protocols described in this report. This approach significantly accelerates metabolite identification.

To improve the reliability of metabolite identification by full-scan MS, stable isotopic labeling (^{2}H, ^{13}C, ^{15}N, ^{18}O, ^{34}S) has been used. The disadvantage is a time-consuming and expensive synthesis step. A mixture of known amounts of labeled and nonlabeled drug is used for the metabolic experiments. The samples collected after certain time periods are analyzed by LC/MS. The identification of a metabolite is then based on criteria that two peaks with identical shapes and retention times must be recorded in the ion chromatograms, the mass difference of the two peaks must be the same as the mass difference between the labeled and the unlabeled parent drug; and the relative abundance ratio of the peaks must be the same as the concentration ratio of the labeled and the unlabeled parent drug. These criteria can be linked also to specific software packages aimed at the identification of the metabolites. The labeling is not necessary in the cases where the compound includes one or more chlorine or bromine atom, which will show abundant M+2 isotopes with known abundance ratios in the mass spectra (Kostiainen *et al.*, 2003).

Tandem MS (MS/MS) is the keystone of metabolite characterization and it offers more specific detection of metabolites in complex matrices than unit resolution full-scan MS. When tandem mass spectrometry is used, there is a possibility of combining linear and SIM modes at the different stages within the instrument. In a typical triple stage quadrupole mass spectrometer (QqQ), four main detection modes (precursor ion scan, constant neutral loss

scan, product ion scan, and selected reaction monitoring) are possible and will be discussed further (Oliveira and Watson, 2000). Tandem mass spectrometers usually contain an isolation stage and a fragmentation stage within the same device. Although many different ways exist to complete a tandem MS experiment, all of them follow the same basic series of events. First, the ion of interest is isolated on the basis of its *m*/*z* ratio and then passed into the collision cell - a region of local high pressure. In trapping instruments, the isolation and fragmentation normally take place within the same space, and the stages are separated by time rather than space. In order to facilitate interpretation, the parent compound standard is normally infused into the mass spectrometer in a separate experiment and forced to undergo collisional fragmentation. The resulting fragment ions can then be compared with the unknown and used as a guide during interpretation (Clarke *et al.*, 2001).

Precursor ion and constant neutral-loss scans

A unique feature of QqQ is its capability to identify families of metabolites by using constant neutral loss and precursor ion scans. These two scanning modes are especially important in early drug discovery because they provide a large amount of information and require very little knowledge regarding the structure of metabolites.

Precursor ion scanning experiments identify likely metabolites by determining if they contain an unaltered portion of the parent molecule or an expected alteration (e.g., +16 Da for oxidation). The power of such an approach is that the operator only needs to know the fragmentation pattern of the parent compound, not the alteration to the parent compound (Clarke *et al.*, 2001). This detection strategy is also used when there is the need to determine or to ascertain the origin of a particular product ion. It operates with the first quadrupole in linear mode and the second in SIM mode which means that the first quadrupole is set to scan linearly within a range covering the fragment of interest up to higher masses, while the second quadrupole operates in SIM mode at *m/z* of the product ion in question (Oliveira and Watson, 2000).

Constant neutral-loss experiments require no knowledge of the parent compound. This scanning technique searches for expected neutral losses from the analyte of interest. In a metabolite identification study, the neutral losses normally are the characteristic losses detected when a conjugate moiety is broken apart from a conjugated metabolite (e.g., loss of 176 Da from a glucuronide conjugate). This technique provides data on the molecular weights of the conjugated metabolites (Busch *et al.*, 1988). The first quadrupole and the third quadrupole both operate in linear scan mode. The first one operates with a mass range that

covers *m/z* ratios of target analytes. Ions are fragmented in the collision cell of the second quadrupole. The third quadrupole operates with mass range that differs from the first by a mass that corresponds to the loss of a particular fragment. In this mode, all components of the sample reaching the detector share the same fragmentation pattern (Oliveira and Watson, 2000).

These two scanning techniques are incredibly effective at detecting molecules that closely resemble the dosed drug and greatly reduce the amount of data the operator has to analyze. Reducing the data set size narrows the list of possible metabolites for further study. While the triple quadrupole is the only instrument that possesses the hardware to perform precursor ion and constant neutral loss experiments in real time, software is being developed to allow rapid evaluation of data "on-the-fly" and to provide this type of information on other types of mass spectrometers in "pseudo real-time" (within the run time of the LC) (Clarke *et al.*, 2001).

Product ion scans

In this detection mode the first quadrupole is operated in SIM mode to select ions with mass to charge ratios corresponding to the precursor (also called parent) ions that fragment to generate product ions of the target analytes. The selected ion (or ions) monitored by the first quadrupole is then fragmented in the collision cell of the second quadrupole while the third quadrupole operates in linear scan mode to detect the product ions – ions generated by fragmentation of a parent ion and exiting the collision cell. This mode affords abundant structural information, which can further be used to set up more selective and sensitive detection strategies for quantitative analysis such as selected (SRM) or multiple (MRM) reaction monitoring (Oliveira and Watson, 2000).

Multiple stage mass spectrometry

Multiple stages (MS^n) of MS can provide large amounts of structural information regarding each analyte, thereby allowing for a more detailed characterization of the metabolites. Completing MS^n experiments requires a mass spectrometer that can capture and store ions (Louris *et al.*, 1987). While the ions are stored, they can be subjected to excitation and collisional fragmentation. The trapping instrument can then capture the resultant fragment ions, which can then be forced to undergo further fragmentation. The second-generation mass spectrum will now give structural information regarding the isolated fragment, allowing easier characterization of that ion. Because this procedure can be applied to each of the initial parent

ion fragments, detailed structural information can be acquired rapidly. This technique often allows the isolation of a small region of the parent ion molecule that has been modified and, in some cases, even the individual atom that are different.

At present, the Fourier transformation (FTMS) and the ion trap mass spectrometers are the only trapping mass spectrometers available. FTMS instruments are not yet capable of high throughput on a regular basis because they are expensive and require skilled operators. Thus, cheaper and simpler quadrupole ion trap mass spectrometers are typically used for these types of trapping experiments.

Although MS^n experiments can often pinpoint the site of modification very accurately, occasionally a metabolite fragments in a manner that does not provide the required information to identify the type of modification. This is typically the case when an expected fragment ion appears as a modified entity within the tandem MS/MS spectrum, but the modification cannot be explained by a common metabolic alteration (e.g., M+4 to a dimethylbenzene ring). In these cases, the answer can sometimes be determined by using accurate mass measurement, which, in turn, allows the calculation of an empirical formula for the fragment (Clarke *et al.*, 2001).

Accurate mass measurements

The use of accurate mass measurements in metabolite detection and structure characterization has increased significantly since the introduction of enhanced performance API-TOF mass spectrometers. TOF and hybrid quadrupole-TOF (Q-TOF) nowadays make accurate mass measurements a feasible part of routine metabolite identification. The current commercial instruments provide fast mass spectral speed with high full-scan sensitivity and resolution 5 000-10 000. Continuous internal mass calibration provides accurate mass measurements with mass errors better than 10 ppm in the accurate mass TOF experiments. Accurate MS/MS measurements for determining empirical formulae of fragment ions were also reported (Williams and Scrivens, 2005).

When using Q-TOF, the accurate mass measurements are corrected using a reference compound. Different methodologies to introduce the reference compound, used as a lock mass, have been investigated. The most basic one is continuous post-column infusion, where the lock mass is continuously introduced using a syringe pump into the chromatographic effluent. However, this configuration suffers from many drawbacks, the main one being an alteration of both the reference and the unknown compound ionization efficiencies. This is particularly true when gradient LC is used, and results in poor control of their relative

response. Some instruments have been designed with dual electrospray ion sources to allow intermittent introduction of calibration standard. The use of a double sprayer circumvents solvent and gradient elution effects while eliminating potential mass interferences. Also a new technique was described, where flow injection analysis of the lock mass compound was performed into the LC column effluent so that the reference compound band partially overlaps that of the investigated analyte at the ionization source (Charles, 2003).

Recently, a new technique using a hybrid linear ion trap/orbitrap mass spectrometer for accurate mass full scan MS and MS/MS measurements has been reported (Peterman *et al.*, 2006).

Data-dependent acquisition

In conventional LC/MS/MS experiments a sample is initially analyzed to identify the molecular ions of the peaks of interest. The sample is then further analyzed by performing product ion MS/MS scans on the selected peaks. This is a time-consuming process because the sample needs to be run at least twice and the MS/MS data is only recorded for a limited number of components. In data-dependent acquisition the mass spectrometer performs the MS and MS^n scans without any user intervention. ITMS is particularly well suited to this sort of experiment, not only due to its inherent sensitivity in full scan mode but also because of the ease of switching between MS and MS^n analyses. The experimental process is greatly simplified, since the ITMS uses the same helium gas at the same pressure to both collect ion and perform fragmentation.

1.3.2 Metabolites quantitation

Quantitative analysis of the parent drug or its metabolites is needed in the early stage of drug discovery for example in fast screening of metabolic stability, in enzyme activity studies and in drug-drug interaction studies. The quantitative method in metabolite analysis must be sensitive, selective, reliable, robust and fast. It is widely accepted that LC/MS fulfils these requirements.

The main advantages of LC/MS are high selectivity and sensitivity that allow the quantitative analysis of drugs and their metabolites at very low concentrations in complex biological matrices. QqQ using SRM or MRM is most often used in quantitative LC/MS analysis, but ITMS, TOF, and Q-TOF have also been widely and increasingly used.

In SRM or MRM, single or multiple precursors to product ion pairs can be monitored. In addition, SRM or MRM mode is the best way to maximize signal/noise ratio of

compounds. When the fragmentation pattern of the analyte of interest is known, the first quadrupole can be used in SIM mode to filter the precursor ion (ions) of target analyte (analytes). Fragmentation is then induced in the collision cell of the second quadrupole and the third stage is also operated in SIM mode to filter only one product ion for each analyte. In this way, particular MS/MS transition can be monitored. If for example the glucuronide of a parent drug is expected, the transition M-177 (corresponding to the loss of a glucuronic acid moiety) can be used to detect this metabolite. This detection is extremely powerful, especially with complex matrices such as biological samples, where sensitivity and selectivity are particularly important. MRM is primarily used for quantitation studies (Oliveira and Watson, 2000).

1.3.3 Sample preparation

Although detection modes such as SRM or MRM used in LC/MS/MS can provide very selective and sensitive analysis for drug and metabolites present in complex biological matrices, sample preparation step is still an important step in LC/MS analysis, especially when tandem mass spectrometry is not available (Henion *et al.*, 1998). Interfering matrix compounds, such as proteins, salts and endogenous and background compounds, must be removed in sample pretreatment, not only to avoid clogging of columns and capillaries but also to improve the selectivity, sensitivity and reliability of analysis. Common pretreatment methods for biological samples include protein precipitation and centrifugation followed by liquid–liquid extraction (LLE) or solid-phase extraction (SPE). Attention must be paid to precipitation of proteins with acids, since it may catalyze the hydrolysis of some conjugates such as glucuronides and sulfates. This can be avoided by using organic solvents in the precipitation. Also, care must be taken that the highly polar or ionic compounds with low retention factors are not lost in reversed-phase SPE. In addition to these well known methods, new, interesting sample pretreatment techniques, such as on-line column switching with a restricted access media (RAM) column (Keski-Hynnila *et al.*, 2001; Kubalec and Brandsteterova, 1999), liquid-phase membrane extraction (LPME) and microdialysis have also been introduced for metabolite analysis (Bergstrom and Markides, 2002; Kuuranne *et al.*, 2003).

2. AIMS OF THE STUDY

The primary aim of the study was to evaluate the applicability and feasibility of different analytical techniques employing liquid chromatography and mass spectrometry in the study of drug metabolism.

Specifically, the aims of the research were

- to elucidate structure of the principal metabolites of quinlukast (**I**)
- to develop rapid LC/MS/MS method for determination of glucuronides in biological matrices (**II**)
- to elucidate structures of the major sibutramine metabolites (**III**)
- to study amlodipine metabolism from the chiral point of view using LC-UV and LC/MS/MS (**IV**)
- to characterize metabolic profile of amlodipine using LC/MS/MS and accurate mass measurements (**V**)

3. MATERIALS AND METHODS

Materials, samples, instrumentation and analytical conditions are briefly described in this section. More detailed information can be found in reprints of original publications **II-V**. In original publication **I** no detailed information on the method is given, thus it is described thoroughly in this section.

3.1 Reagents and samples

Chemicals and standard compounds used in the studies **I-V** are listed in Table 1. Structures of studied compounds are shown in Figure 1. Several *in vitro* models were utilized in studies. Quinlukast and sibutramine were incubated with rat microsomes and hepatocytes in paper **I** and **III**. In paper **II**, a mixture of substrates was incubated with human recombinant UDP-glucuronosyltransferases (UGTs). In paper **IV** and **V** amlodipine (AML) was incubated with primary culture of rat hepatocytes.

Table 1. List of chemicals and standards used in the studies I-V.

Compound	Source	Paper
2-(aminoethoxy)methyl-4-(2-chlorophenyl)-3-ethoxycarbonyl-5-methoxy-carbonyl-6-methylpyridine	Research Institute for Pharmacy and Biochemistry*	IV, V
4 - (2 - chlorophenyl) - 3 -ethoxy-carbonyl-5-methoxycarbonyl-2(carboxymethoxy)methyl-6-methyl-1,4-dihydropyridine	Research Institute for Pharmacy and Biochemistry*	IV, V
4 - (2- chlorophenyl) - 3- ethoxycarbonyl - 5- methoxycarbonyl-2(carboxymethoxy)methyl-6-methylpyridine	Research Institute for Pharmacy and Biochemistry*	IV, V
4-methylumbelliferone	Sigma-Aldrich Chemie (Steinheim, Germany)	II
4-methylumbelliferyl-β-D-glucuronide	Sigma-Aldrich Chemie (Steinheim, Germany)	II
Acetonitrile	Riedel-deHaen (Seelze, Germany)	I
Acetonitrile	Merck (Darmstadt, Germany)	III
Acetonitrile	Sigma-Aldrich (Prague, Czech Republic)	IV
Ammonium acetate (NH4Ac)	J.T. Baker (Deventer, Netherland)	IV, V
Ammonium hydroxide	J.T. Baker (Deventer, Netherland)	IV, V
Antibiotics	Sigma-Aldrich (Prague, Czech Republic)	I, III-V
Collagen	Sigma-Aldrich (Prague, Czech Republic)	I, III-V
Collagenase	Sevapharma (Prague, Czech Republic)	I, III-V
Desmethylsibutramine	Dept. of Organic Chemistry, Faculty of Pharmacy **	III
Didesmethylsibutramine	Dept. of Organic Chemistry, Faculty of Pharmacy **	III
Dimethyl sulfoxide	Riedel-deHaen (Seelze, Germany)	I
Disodium hydrogen phosphate dihydrate	Merck (Darmstadt, Germany)	II
D-saccharic acid 1,4-lactone	Sigma-Aldrich Chemie (Steinheim, Germany)	II
Entacapone	Orion Pharma (Espoo, Finland)	II
Entacapone-3-O-glucuronide	Dept. of Pharmaceutical Chemistry, Faculty of Pharmacy***	II
Estriol	Sigma-Aldrich Chemie (Steinheim, Germany)	II
estriol-16α-(β-D-glucuronide)	Sigma-Aldrich Chemie (Steinheim, Germany)	II
estriol-17β-(β-D-glucuronide)	Sigma-Aldrich Chemie (Steinheim, Germany)	II
Ethyl acetate	Merck (Darmstadt, Germany)	III
Fetal calf serum	Sigma-Aldrich (Prague, Czech Republic)	I, III-V
Formic acid (98–100%) (FA)	Sigma-Aldrich Chemie (Steinheim, Germany)	II
Ham F12 medium	Sigma-Aldrich (Prague, Czech Republic)	I, III-V

Compound	Source	Paper
Insulin	Sigma-Aldrich (Prague, Czech Republic)	I, III-V
Magnesium chloride hexahydrate	Merck (Darmstadt, Germany)	II
Methanol	Riedel-deHaen (Seelze, Germany)	I
Methanol	J.T. Baker (Deventer, Netherland)	II
Methanol	Merck (Darmstadt, Germany)	III
Metoprolol	ICN Biomedicals (Costa Mesa, CA, USA)	V
NADPH	Sigma-Aldrich (Prague, Czech Republic)	I
Paracetamol	Orion Pharma (Espoo, Finland)	II
paracetamol glucuronide	Sigma-Aldrich Chemie (Steinheim, Germany)	II
Perchloric acid (70–72%)	Merck (Darmstadt, Germany)	II
p -nitrophenol	Sigma Chemicals Co. (St. Louis, USA)	II
p -nitrophenyl-β-D-glucuronide	Sigma Chemicals Co. (St. Louis, USA)	II
Quinlukast	Research Institute for Pharmacy and Biochemistry*	I
R- and S-sibutramine enantiomers	Research Institute for Pharmacy and Biochemistry*	III
Rac -, R-, S- amlodipine	Research Institute for Pharmacy and Biochemistry*	IV, V
Sibutramine	Dept. of Organic Chemistry, Faculty of Pharmacy)**	III
Sodium dihydrogen phosphate dihydrate	Fluka Chemie (Buchs, Germany)	II
Tolcapone	Orion Pharma (Espoo, Finland)	II
Tolcapone-3-O-glucuronide	Dept. of Pharmaceutical Chemistry, Faculty of Pharmacy***	II
Toluene	Merck (Darmstadt, Germany)	III
Umbelliferone	Sigma-Aldrich Chemie (Steinheim, Germany)	II
Umbelliferone glucuronide	Ultrafine (Manchester, UK)	II
uridine 5'-diphosphoglucuronic acid	Sigma-Aldrich Chemie (Steinheim, Germany)	II
William's E medium	Sigma-Aldrich (Prague, Czech Republic)	I, III-V
α-naphtol	Sigma Chemicals Co. (St. Louis, USA)	II
α-naphtyl-β-D-glucuronide	Sigma Chemicals Co. (St. Louis, USA)	II

* Research Institute for Pharmacy and Biochemistry (Prague, Czech Republic)
** Dept. of Organic Chemistry, Faculty of Pharmacy (Hradec Kralove, Czech Republic) synthesized according to (Jeffery *et al.*, 1996)
*** Dept. of Pharmaceutical Chemistry, Faculty of Pharmacy (Helsinki, Finland), (Luukkanen *et al.*, 1999)

3.2 Instrumentation

The studies were carried using different instruments. The instrumentation and conditions for the studies are summarized in Table 2. All MS experiments were performed with ESI and positive ionization.

Characterization of major metabolites of quinlukast (I)

Fractions of major metabolites of quinlukast were collected separately into glass test tubes after chromatographic separation using the conditions described in the paper **I**. After the extraction and evaporation the residues were reconstituted and directly infused into the ITMS using a syringe pump. Quinlukast and its metabolites showed better ionization in positive mode. The parameters of measurement were: a spray voltage of 4.2 kV, capillary heater temperature was held at 280ºC and capillary voltage of 35 V. Product ion spectra were collected, fragmentation pattern of quinlukast studied and tentative structures of metabolites suggested. Structures of quinlukast sulfoxide and quinlukast sulfone were confirmed by comparison with retention times of synthetically prepared standards.

Rapid simultaneous quantitation of multiple glucuronides *in vitro* (II)

A rapid, sensitive, and selective liquid chromatography tandem mass spectrometry method was developed for the analysis of samples produced by single-substrate and *n*-in-one (a mixture of seven substrates: entacapone, 17β-estriol, umbelliferone, 4-methylumbelliferone, tolcapone, hydroxyquinoline, and paracetamol) incubations with different recombinant UGTs. The main ion optics parameters - declustering potential, collision energy, and collision cell exit potential - were optimized for each multiple reaction monitoring (MRM) transition to find the best sensitivity. The method was validated and used to test the applicability of *n*-in-one incubations in the determination of intrinsic clearance as the slope of the linear portion of the Michaelis–Menten curve where substrate concentrations were low.

Characterization of major metabolites of sibutramine (III)

Fractions of major metabolites of sibutramine were collected separately into glass test tubes after chromatographic separation using the conditions in the paper **III**. After the extraction and evaporation the residues were dissolved in a mixture of H_2O–MeOH (2:3 v/v) and analyzed using ITMS with ion source parameters: spray voltage of 4.5 kV, capillary heater temperature was held at 280ºC, capillary voltage 29 V. Ions were sampled into the mass spectrometer at a maximum injection time of 300 ms. Full scan and product ion spectra were recorded, interpreted, and tentative structures suggested.

Study of metabolism of *rac*-, R-, and S-AML (IV)

LC-UV and LC/MS/MS method was developed for study of metabolism of amlodipine from the chiral point of view. Structures of eight major metabolites of amlodipine were characterized using data dependent LC/MS/MS. The characterized metabolites were semiquantitated using LC-UV and the rate of metabolism compared separately for rac-, R-, and S-amlodipine.

Metabolic profile of AML using LC/MS/MS and accurate mass measurements (V)

LC/MS/MS and accurate mass measurements were used to identify and characterize as many metabolites of amlodipine as possible. In the first step, full scan spectra of samples, blanks, and control were measured and compared to identify metabolites. In the second step, the product ion spectra of identified metabolites were obtained, interpreted and tentative structures of metabolites suggested. In the third step the tentative structures were confirmed.

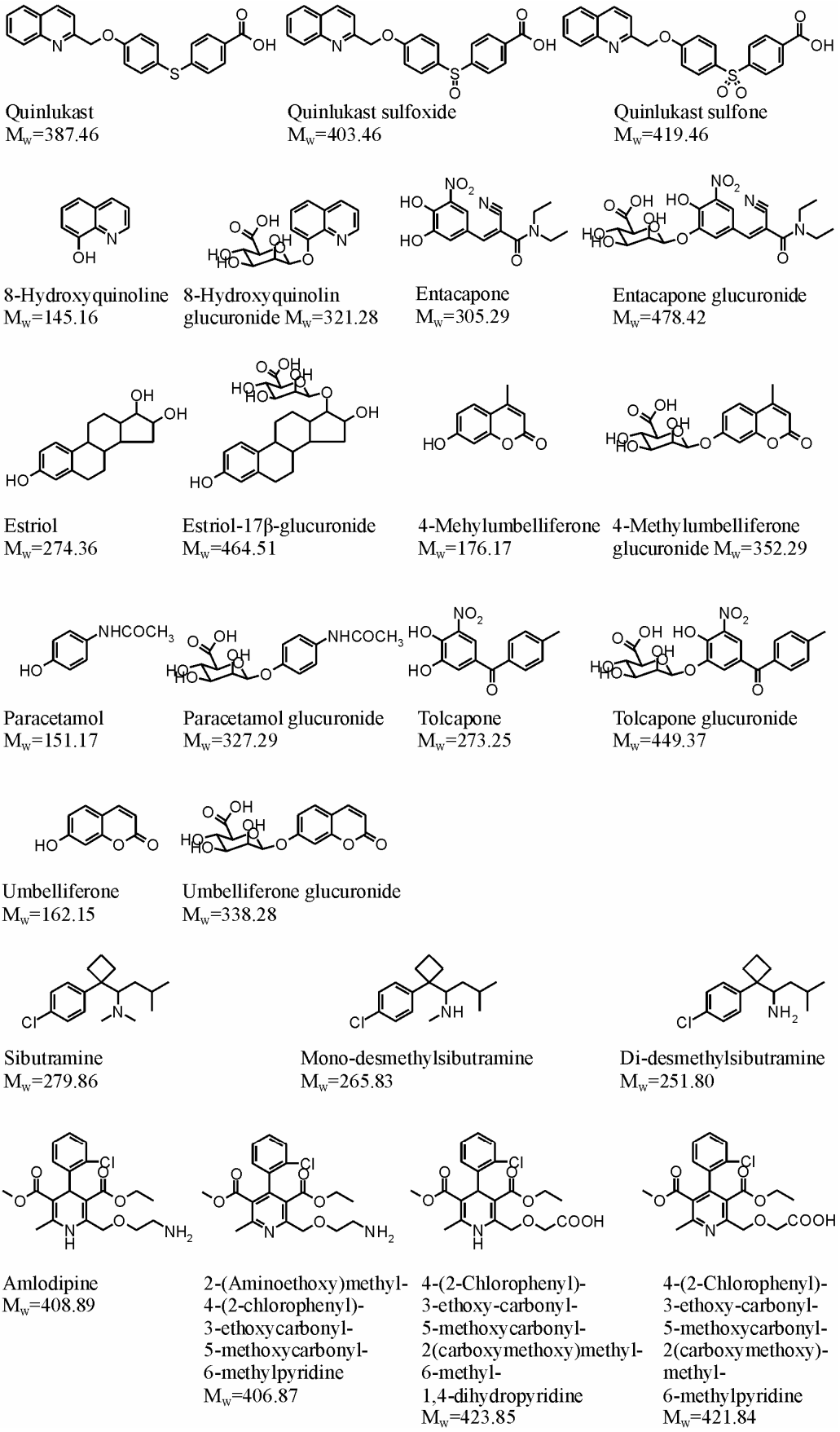

Fig. 1. Structures of studied compounds. M_w, molecular weight (g/mol).

Table 2. Instrumentation and conditions used in qualitative and quantitative analyses of drug metabolites.

Paper	LC or syringe pump	Column	Eluent* / Solvent**	Mass Spectrometer
I, III	Built-in syringe pump		H_2O-MeOH (1:1, v/v)	LCQ Advantage (ThermoFinnigan, USA)
II	Agilent 1100 HPLC (Agilent Technologies, Germany)	Purospher STAR RP-18 55×4 mm., 3 µm (Merck, Germany)	A: 0.1% FA B: 0.1% FA in MeOH two-steps B gradient: 5%→90% (3 min), 90% (1 min), 90%→5% (1min)	Sciex API 3000 (Sciex, Canada)
III	Built-in syringe pump		H_2O-MeOH (2:3, v/v)	LCQ Advantage (ThermoFinnigan, USA)
IV	Surveyor HPLC system (ThermoFinnigan, USA), LC-UV: Shimadzu HPLC-UV system (Prague, Czech Republic)	BDS Hypersil C_{18} 150×2.1 mm, 5 µm, BDS Hypersil C_8 guard 10 mm × 4 mm, 5 µm (Thermo Electron Corporation, USA)	A: 10 mM NH_4Ac pH 4.8 B: 10 mM NH_4Ac pH 4.8 in 60% MeCN linear B gradient: 16%→84% (40 min), 16% (1 min)	LCQ Advantage (ThermoFinnigan, USA)
V	Agilent 1100 HPLC (Agilent Technologies, Germany)	Symmetry Shield C_{18} 100 mm × 2.1 mm, 3.5 µm, Symmetry C_{18} Sentry Guard 10 mm × 2.1 mm, 3.5 µm	A: 10 mM NH_4Ac pH 4.8 B: 10 mM NH_4Ac pH 4.8 in 60% MeCN three-steps B gradient: 16%→25% (5 min), 25%→75% (5 min), 75%→84% (5 min), 84%→16% (1 min)	Sciex API 3000 (Sciex, Canada), Q-TOF micro (Waters Micromass, UK)

* If LC employed

** If direct infusion via syringe pump employed

4. RESULTS AND DISCUSSION

The main results achieved in the papers **I-V** are briefly described and discussed. More detailed information on the experimental conditions, analytical procedures and achieved results can be found in reprints of original publication. Structures of studied compounds are presented in Figure 1.

4.1 Interpretation of product ion spectra

Major metabolites of quinlukast (**I**), sibutramine (**III**) and amlodipine (**IV**, **V**) were structurally characterized in original papers. ESI-MS in positive mode was utilized. In the papers **I** and **III**, the samples were infused directly using a syringe pump whereas in the papers **IV** and **V**, the samples were separated using liquid chromatography prior to introduction into the mass spectrometer.

4.1.1 Quinlukast metabolites (I)

Four metabolites were found in incubation of quinlukast with microsomes. Two of them were found to be identical with synthetically prepared standards quinlukast sulfoxide and quinlukast sulfone (Figure 1). Two isobaric metabolites were found yield protonated molecules at *m/z* 422 and methanol adduct ions $[M+H+MeOH]^+$ at *m/z* 454. Their product ion spectra differed only in relative abundances of several product ions. Based on spectra interpretations they were suggested to be quinlukast dihydrodiols as explained in the paper **I**. In hepatocytes culture medium yet another polar metabolite was found with protonated molecule at *m/z* 564. The polar character and higher mass increase indicated conjugation. Product ion spectrum yielded fragments supporting the glucuronidation of quinlukast. A product ion at *m/z* 546 corresponded to loss of water $[M+H-H_2O]^+$ and a product ion at *m/z* 484 was explained by loss of two molecules of water and decarboxylation of glucuronic acid moiety. The spectrum further showed abundant product ion at *m/z* 388 formed by the cleavage of glucuronic acid moiety (Glu), $[M+H-Glu]^+$ from the ester quinlukast glucuronide. The most abundant product ion of the spectra at *m/z* 370 was explained by successive loss of water $[M+H-H_2O-Glu]^+$. A product ion at *m/z* 342 resulted from subsequent loss of carbon oxide. The interpretation of product ion spectra is illustrated in the Figure 2.

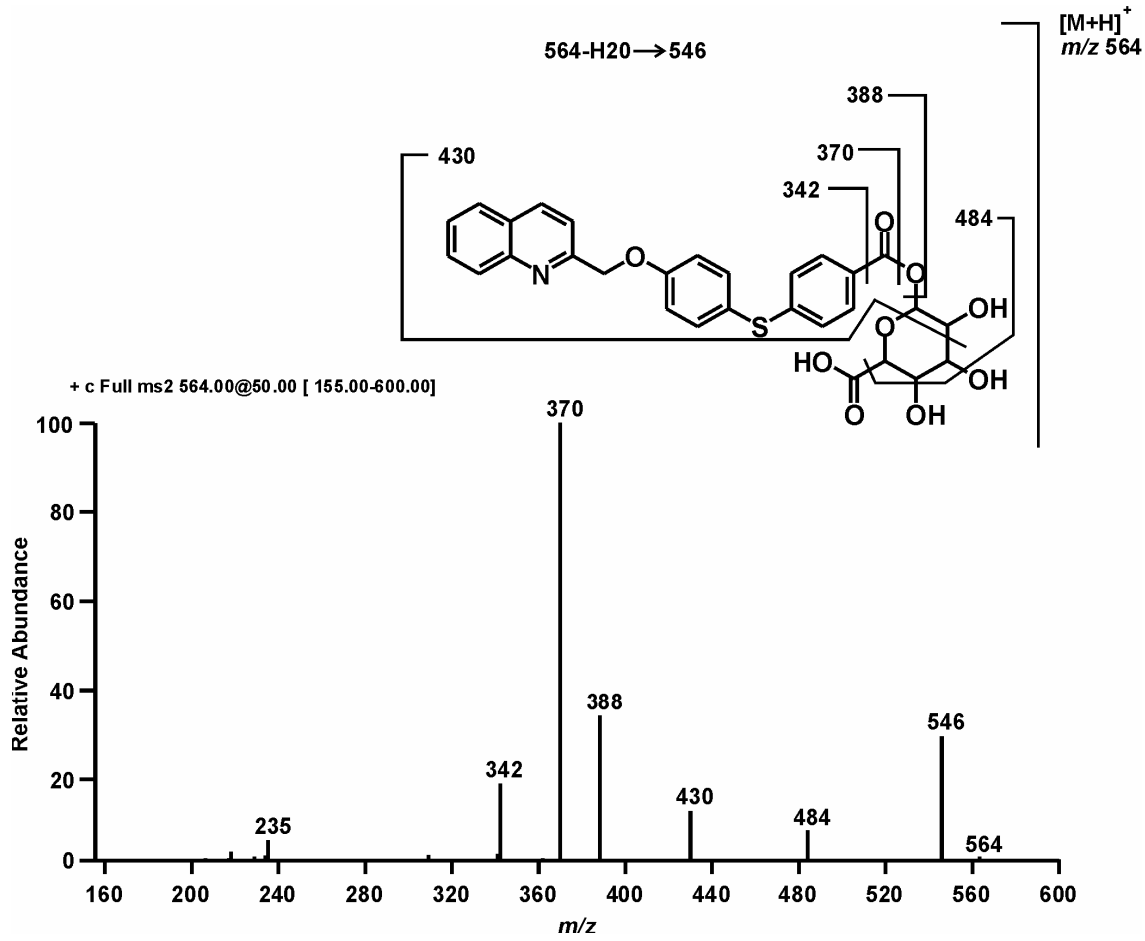

Figure 2. Proposed structure of quinlukast metabolite and explanation of product ions.

4.1.2 Sibutramine metabolites (II)

Product ion spectra were obtained using direct infusion via syringe pump into the mass spectrometer. Sibutramine and synthesized metabolites mono-desmethylsibutramine and di-desmethylsibutramine (Figure 1) exerted better ionization in positive mode due to the basic character. Therefore ITMS in positive mode was employed. Full scan and product ion spectra presented in Figure 2 were collected for the metabolites marked M_1, M_2 and M_3 in the paper **II**. M_1 and M_2 were found to be already described mono- and di-desmethylsibutramine (Figure 1). Since the interpretation of product ion spectra is absent in the paper **II**, it is discussed more thoroughly here. M_1 and M_2 showed same retention times and product ion spectra as the synthetic standards and thus their structures were confirmed unambiguously. M_3 was characterized by interpretation of the first (MS^2), the second (MS^3) and the third (MS^4) generation of product ion spectra (Figure 3). In the MS^2 product ion spectra a product ion at *m/z* 250 is explained by loss of H_2O and a product ion at *m/z* 233 is created by successive loss of NH_3. A product ion at *m/z* 194 results from loss of $CH_3CH(CH_3)CH_2OH$ though the po-

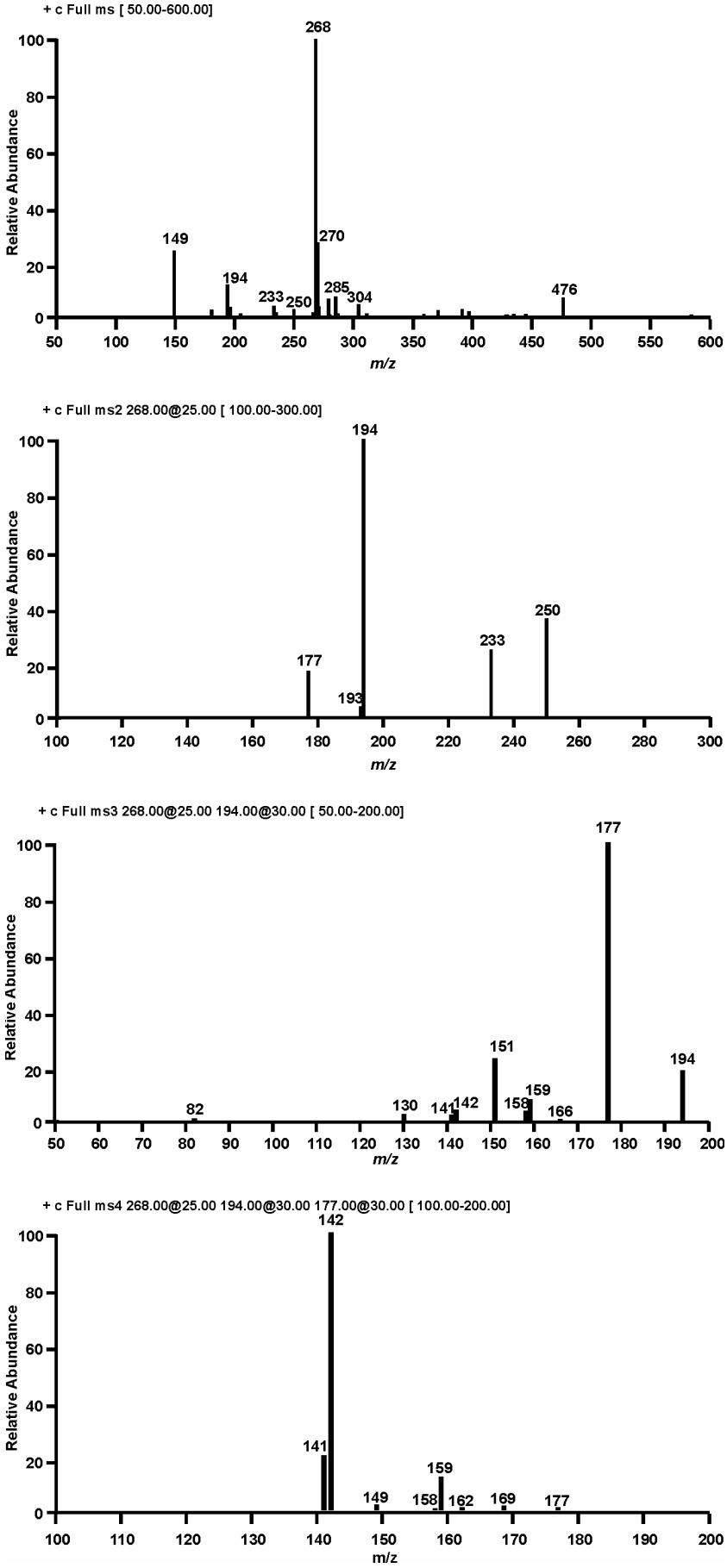

Fig. 3. Full scan and product ion spectra of the first, second and third generation of sibutramine metabolite.

sition of hydroxyl cannot be pointed out unambiguously. In this case MS^3 and MS^4 product ion spectra only confirm the interpretation of product ions of the first generation, but do not pinpoint the position of hydroxyl which is readily cleft as H_2O. A product ion at *m/z* 177 results from cleavage of the product ion at *m/z* 194 by opening of the cyclobutyl ring and loss of NH_3 as can be observed in the MS^3 product ion spectrum.

4.1.3 Amlodipine metabolites (IV, V)

Metabolic behavior of amlodipine in primary culture of rat hepatocytes was studied thoroughly in the papers **IV** and **V**. Data-dependent LC/ESI-tandem MS in time (LC/ESI-MS/MS in time) analysis was utilized in the paper **IV** in order to obtain product ion spectra of eight major amlodipine metabolites chosen for the quantitation (described in 4.2.2) within one run. Basically two types of metabolites were detected, reduced type – dihydropyridine metabolites and oxidized type – pyridine metabolites. Product ion spectra of AML and synthetic derivatives of AML whose structures are shown in Fig. 1 were measured in order to determine a characteristic fragmentation pattern of AML derivatives. The product ion spectra of metabolites were compared with product ion spectra of known compound and product ions observed were interpreted. Characteristic product ions seen for synthetic derivatives of AML designated here as D_1-D_3, AML itself, and metabolites M_1-M_8 together with identification and retention times are summarized in Table 3. From the tentative structures of metabolites metabolic pathways were proposed as presented in the paper **IV** (Fig. 6).

Nevertheless, the eight characterized metabolites were not the only identified metabolites. The structure of AML enables variety of metabolic modifications and their combinations as demonstrated in the paper **V** (Fig. I). The aim of the study was to characterize metabolic profile of AML *in vitro*, i.e. to identify all possible metabolites which can be also present in very low amounts. Identification was based on comparison of the incubation sample with blank and control samples, incubation of rat hepatocytes without AML and incubation of AML without rat hepatocytes, respectively, as well as on the presence of chlorine M+2 isotopic peaks in the mass spectra and revealed twenty-one AML metabolites. Product ion spectra of all identified metabolites were measured and interpreted. The interpretation was facilitated using fragmentation pattern of AML and its synthetic derivatives. The structure characterization of AML metabolites is in detail discussed in the paper **V**. Being short, in the first step the structures of metabolites were suggested based on product ion spectra interpretation, in the second step the tentative structures were confirmed

using accurate mass measurement and determination of empirical formula, which was more accurate than 4 ppm.

Table 3. LC-MS/MS characteristics of synthetic derivatives D1–D3, AML, and metabolites M1–M8.

Analyte	t_R MS (min)	M_w	Precursor ion *m/z*	Product ions *m/z*
D_1	25.3	421	422	376 (-C_2H_5OH); 346 (-$OHCH_2COOH$); 318 (-$OHCH_2COOH$; -C_2H_4); 286 (-CH_3OH; -C_2H_4; -$OHCH_2COOH$)
D_2	29.4	423	424	392 (-CH_3OH); 378 (-C_2H_5OH); 348 (-$OHCH_2COOH$); 320 (-$OHCH_2COOH$; -C_2H_2); 288 (-C_2H_5OH;-CH_3OCH_2COOH); 244 (-C_2H_5OH; -CH_3OCH_2COOH; -CO_2)
D_3	29.7	406	407	390 (-NH_3); 364 (-$C_2H_2NH_3$); 346 (-$OHC_2H_4NH_2$); 318 (-$OHC_2H_4NH_2$; -C_2H_4); 286 (-$OHC_2H_4NH_2$; -OHC_2H_3O)
AML	33.8	408	409	392 (-NH_3); 366 (-$C_2H_3NH_2$); 348 (-$OHC_2H_4NH_2$); 320 (-$OHC_2H_4NH_2$; -C_2H_4); 288 (-$OHC_2H_4NH_2$; -C_2H_3OH; -CH_4)
M_1	10.1	392	393	376 (-NH_3); 350 (-$C_2H_3NH_2$); 332 (-$OHC_2H_4NH_2$); 304 (-$OHC_2H_4NH_2$; -C_2H_4); 286 (-$OHC_2H_4NH_2$; -C_2H_5OH); 280 (-$C_2H_3OC_2H_2NH_2$; -C_2H_2); 260 (-$OHC_2H_4NH_2$;-$HCOOC_2H_3$); 168 (-C_6H_5Cl; -$HCOOC_2H_3$; -C_2HNH_2); 149 (-C_6H_5Cl; -OC_2H_2NH; -NH_3; -CHCOOH)
M_2	23.6	394	395	352 (-$C_2H_3NH_2$); 334 (-$OHC_2H_4NH_2$); 306 (-$OHC_2H_4NH_2$; -C_2H_4)
M_3	24.2	424	425	393 (-CH_3OH); 382 (-$C_2H_3NH_2$); 346 (-$OHC_2H_4NH_2$; -H_2O); 320 (-$OHC_2H_4NH_2$; -C_2H_3OH); 310 (-$OHC_2H_4NH_2$; -H_2O; HCl); 286 (-$OHC_2H_4NH_2$; -CH_4; -OHC_2H_4OH); 276 (-$HCOOC_2H_4OH$; -$OC_2H_3NH_2$); 252 (-C_6H_5Cl; -NH3; -C_2H_3OH); 238 (-C_6H_5Cl; CH_3OH; -$C_2H_3NH_2$); 229 (-$C_6H_4ClC_2H_2COOCH_3$)
M_4	26.0	422	423	391 (-CH_3OH); 377 (-OCHOH); 347 (-CH_3OH); 338 (-C_2H_3OH; -$C_2H_3NH_2$)
M_5	28.4	436	437	419 (H20); 393 (-CH4; -C2H4); 352 (-$C_2H_3NHCOCH_3$); 308 (-H_2O; -$OHC_2H_2NHCOCH_3$)
M_6	29.7	406	407	390 (-NH_3); 364 (-$C_2H_2NH_3$); 346 (-$OHC_2H_4NH_2$); 318 (-$OHC_2H_4NH_2$; -C_2H_4); 286 (-$OHC_2H_4NH_2$; -OHC_2H_3O)
M_7	34.3	448	449	431 (-H_2O); 417 (-CH_3OH); 407 (-C_2H_2O); 390 (-NH_2COCH_3); 364 (-$C_2H_3NHCOCH_3$); 346 (-$OHC_2H_4NHCOCH_3$); 318 (-$OHC_2H_4NHCOCH_3$; C_2H_4); 286 (-$OHC_2H_4NHCOCH_3$; C_2H_4; CH_3OH)
M_8	39.3	450	451	419 (-CH_3OH); 366 (-$C_2H_3NHCOCH_3$); 348 (-$OHC_2H_4NHCOCH_3$); 334 (-CH_3OH; -$C_2H_3NHCOCH_3$)

Besides already reported metabolites in dog, rat and human *in vivo* (Beresford *et al.*, 1989; Beresford *et al.*, 1988b; Beresford *et al.*, 1988a; Stopher *et al.*, 1988), new metabolites were found in primary culture of rat hepatocytes. No N-acetylated metabolites of AML were published. The structures of all characterized metabolites are shown in proposed metabolic pathways of AML *in vitro* in the paper **V** (Fig. 4).

4.2 Determination of drug metabolites

The papers **II** and **IV** dealt with determination of drug metabolites *in vitro*. In the paper **II** a quantitative LC/MS/MS method was developed and validated for determination of glucuronides. In the paper **IV** metabolites of *rac*-, R-, S-AML were semiquantitated employing LC-UV. There are many validation guidelines to choose from, each with numerous parameters to evaluate. The thoroughness of a validation procedure should be in reasonable proportion to the intended use of the method. Parameters tested in these works were limits of detection (**II**), limit of semiquantitation (**IV**), linearity (**II, IV**), intra-day and inter-day repeatability (**II, IV**) (in paper **II** called within- and between-day repeatability). Also a repeatability of retention times (**II**) recovery of extraction (**IV**) and stability (**IV**) were evaluated.

4.2.1 Simultaneous quantitation of multiple glucuronide conjugates (II)

A rapid, sensitive, and selective liquid chromatography tandem mass spectrometry (LC/MS/MS) method was developed for the analysis of samples produced by single-substrate and *n*-in-one (cocktail of seven substrates) incubations with UDP-glucuronosyltransferases (UGTs). All of the glucuronides produced an intense protonated molecule, which was chosen as precursor ion for positive ion MS/MS studies. All of the glucuronides produced an intense protonated molecule, which was chosen as precursor ion for positive ion MS/MS studies. All of the MS/MS spectra except that for estriol glucuronide showed abundant product ion formed by the cleavage of glucuronic acid moiety (Glu), $[M+H\text{-}Glu]^+$, which was chosen for the MRM. In estriol glucuronide, most intense product ions, $[M+H\text{-}H_2O]^+$ and $[M+H\text{-}H_2O\text{-}Glu]^+$, were monitored in MRM.

The validation parameters of the method are listed in the paper **II** (Table 1). The LC method was robust, with repeatable peak shape. Very good repeatability was obtained for the retention times, with the relative standard deviations (RSDs) being within 0.3–1% for all of the glucuronides. The method was applied to *n*-in-one incubations of seven substrates with UGTs and kinetic parameters maximal reaction rate of metabolite formation (V_{max}) and

Michaelis constant (K_m) and intrinsic clearance (Cl_{int}) as V_{max}/K_m were determined. The kinetic parameters determined from *n*-in-one incubations correlated well to kinetic parameters determined from single-substrate incubation as shown in the paper **II** (Tables 2 and 3). The combination of newly developed LC/MS/MS method for multiple glucuronides determination and *n*-in-one incubation could significantly decrease the time needed for experiments to screen metabolic properties of new substrates in the early phase of drug discovery.

4.2.2 Semiquantitative determination of amlodipine metabolites (IV)

UV detection and fluorescent detection were employed to identify peaks of metabolites in LC analysis. Data acquired at 240 nm were used for semiquantitation. Due to inaccessibility of analytical standards an alternative approach to method validation was applied and biological quality control (BCQ) samples were used instead of spiked quality control (SQC) samples to control quality of the data generated. The amounts of metabolites were expressed as amlodipine equivalent concentration units. The evaluated parameters are stated in the paper **IV** (Table 2 and 3). The performance of the method was evaluated and was found to be acceptable for biological samples. The developed LC-UV semiquantitative method was applied to primary rat hepatocytes samples incubated with *rac*-, *S*-, and *R*-AML and kinetic study was performed for four different concentrations of substrates and five different time intervals. The rates of metabolites formation were compared and different rates were found for individual metabolites formation in *rac*-, *S*-, and *R*-AML as shown in the paper **IV** (Table 8). Not only quantitative but also qualitative difference in the metabolism and pharmacokinetics were found for S-AML and R-AML as presented in the paper **IV** (Tables 4-7).

5. CONCLUSIONS

Variety of drug metabolism studies was performed employing liquid chromatography and mass spectrometry. LC/MS was successfully applied to identification, structure characterization and quantitative analysis of drug metabolites owing to its superior sensitivity, specificity and efficiency. LC/MS is a versatile technique allowing high sample throughput.

Together with the *n*-in-one incubations, the determination of Cl_{int} values as the slope of the linear part of the Michaelis–Menten fitting, LC/MS/MS as an analytical method proved to be effective approach for increasing throughput in the first-phase screening of metabolic properties.

Structures of new metabolites of quinlukast and sibutramine were characterized using direct infusion of collected fraction into the ion trap mass spectrometer. Liquid chromatography data-dependent tandem mass spectrometry employing ion trap mass spectrometer enabled to collect product ion spectra of major metabolites of amlodipine within one analytical run and thus significantly decreased the total time needed for the study. Metabolic profile of amlodipine was further investigated in detail using combination of structural information provided by product ion spectra measured by triple quadrupole and information on elemental compositions of metabolites provided by accurate mass determination with Q-TOF. The combined approach enabled to characterize the twenty-one metabolites of amlodipine and to propose *in vitro* metabolic pathways in rat.

6. REFERENCES

Beresford, A. P., Macrae, P. V., Alker, D., and Kobylecki, R. J.: Biotransformation of amlodipine. Identification and synthesis of metabolites found in rat, dog and human urine/confirmation of structures by gas chromatography-mass spectrometry and liquid chromatography-mass spectrometry. *Arzneim. Forsch.* 39 (1989) 201-209.

Beresford, A. P., Macrae, P. V., and Stopher, D. A.: Metabolism of amlodipine in the rat and the dog: a species difference. *Xenobiotica* 18 (1988a) 169-182.

Beresford, A. P., McGibney, D., Humphrey, M. J., Macrae, P. V., and Stopher, D. A.: Metabolism and kinetics of amlodipine in man. *Xenobiotica* 18 (1988b) 245-254.

Bergstrom, S. K. and Markides, K. E.: On-line coupling of microdialysis to packed capillary column liquid chromatography-tandem mass spectrometry demonstrated by measurement of free concentrations of ropivacaine and metabolite from spiked plasma samples. *J. Chromatogr., B: Anal. Technol. Biomed. Life Sci.* 775 (2002) 79-87.

Bodo, A., Bakos, E., Szeri, F., Varadi, A., and Sarkadi, B.: The role of multidrug transporters in drug availability, metabolism and toxicity. *Toxicol. Lett.* 140-141 (2003) 133-143.

Busch, K. L., Glish, G. L., and McLuckey, S. A. In *Mass spectrometry/mass spectrometry techniques and applications of Tandem mass spectrometry*, VCH Publishers, New York, N.Y (1988).

Cashman, J. R.: Some distinctions between flavin-containing and cytochrome P450 monooxygenases. *Biochem. Biophys. Res. Commun.* 338 (2005) 599-604.

Cashman, J. R. and Zhang, J.: Human flavin-containing monooxygenases. *Annu. Rev. Pharmacol. Toxicol.* 46 (2006) 65-100.

Charles, L.: Flow injection of the lock mass standard for accurate mass measurement in electrospray ionization time-of-flight mass spectrometry coupled with liquid chromatography. *Rapid Commun. Mass Spectrom.* 17 (2003) 1383-1388.

Clarke, N. J., Rindgen, D., Korfmacher, W. A., and Cox, K. A.: Systematic LC/MS metabolite identification in drug discovery. *Anal. Chem.* 73 (2001) 430A-439A.

Gallego, O., Belyaeva, O. V., Porte, S., Ruiz, F. X., Stetsenko, A. V., Shabrova, E. V., Kostereva, N. V., Farres, J., Pares, X., and Kedishvili, N. Y.: Comparative functional analysis of human medium-chain dehydrogenases, short-chain dehydrogenases/reductases and aldo-keto reductases with retinoids. *Biochem. J.* 399 (2006) 101-109.

Gibson G.G., Skett P. In *Introduction to drug metabolism*, 3rd ed.; Nelson Thornes Publishers, Cheltenham, UK (2001).

Goldstein, J. A. and Faletto, M. B.: Advances in mechanisms of activation and deactivation of environmental chemicals. *Environ. Health Perspect.* 100 (1993) 169-176.

Guengerich, F. P.: Cytochrome P450s and other enzymes in drug metabolism and toxicity. *AAPS. J.* 8 (2006) E101-E111.

Hariparsad, N., Sane, R. S., Strom, S. C., and Desai, P. B.: In vitro methods in human drug biotransformation research: implications for cancer chemotherapy. *Toxicol. In Vitro* 20 (2006) 135-153.

Henion, J., Brewer, E., and Rule, G.: Sample preparation for LC/MS/MS: analyzing biological and environmental samples. *Anal. Chem.* 70 (1998) 650A-656A.

Jeffery, J. E., Kerrigan, F., Miller, T. K., Smith, G. J., and Tometzki, G. B.: Synthesis of sibutramine, a novel cyclobutylalkylamine useful in the treatment of obesity, and its major human metabolites. *Journal of the Chemical Society-Perkin Transactions* 1 (1996) 2583-2589.

Jez, J. M., Bennett, M. J., Schlegel, B. P., Lewis, M., and Penning, T. M.: Comparative anatomy of the aldo-keto reductase superfamily. *Biochem. J.* 326 (1997a) 625-636.

Jez, J. M., Flynn, T. G., and Penning, T. M.: A new nomenclature for the aldo-keto reductase superfamily. *Biochem. Pharmacol.* 54 (1997b) 639-647.

Jin, Y. and Penning, T. M.: Aldo-Keto Reductases and Bioactivation/Detoxication. *Annu. Rev. Pharmacol. Toxicol.* (2006)

Kallberg, Y., Oppermann, U., Jornvall, H., and Persson, B.: Short-chain dehydrogenases/reductases (SDRs). *Eur. J. Biochem.* 269 (2002) 4409-4417.

Keski-Hynnila, H., Raanaa, K., Forsberg, M., Mannisto, P., Taskinen, J., and Kostiainen, R.: Quantitation of entacapone glucuronide in rat plasma by on-line coupled restricted access media column and liquid chromatography-tandem mass spectrometry. *J. Chromatogr., B: Biomed. Sci. Appl.* 759 (2001) 227-236.

King, C. D., Rios, G. R., Green, M. D., and Tephly, T. R.: UDP-glucuronosyltransferases. *Curr. Drug Metab.* 1 (2000) 143-161.

Kostiainen, R., Kotiaho, T., Kuuranne, T., and Auriola, S.: Liquid chromatography/atmospheric pressure ionization-mass spectrometry in drug metabolism studies. *J. Mass Spectrom.* 38 (2003) 357-372.

Krishna, D. R. and Klotz, U.: Extrahepatic metabolism of drugs in humans. *Clin. Pharmacokinet.* 26 (1994) 144-160.

Krueger, S. K. and Williams, D. E.: Mammalian flavin-containing monooxygenases: structure/function, genetic polymorphisms and role in drug metabolism. *Pharmacol. Ther.* 106 (2005) 357-387.

Kubalec, P. and Brandsteterova, E.: Determination of propafenone and its main metabolite 5-hydroxypropafenone in human serum with direct injection into a column-switching chromatographic system. *J. Chromatogr., B: Biomed. Sci. Appl.* 726 (1999) 211-218.

Kulkarni, A. P.: Lipoxygenase - a versatile biocatalyst for biotransformation of endobiotics and xenobiotics. *Cell Mol. Life Sci.* 58 (2001a) 1805-1825.

Kulkarni, A. P.: Role of biotransformation in conceptal toxicity of drugs and other chemicals. *Curr. Pharm. Des* 7 (2001b) 833-857.

Kuuranne, T., Kotiaho, T., Pedersen-Bjergaard, S., Einar, R. K., Leinonen, A., Westwood, S., and Kostiainen, R.: Feasibility of a liquid-phase microextraction sample clean-up and liquid chromatographic/mass spectrometric screening method for selected anabolic steroid glucuronides in biological samples. *J. Mass Spectrom.* 38 (2003) 16-26.

Louris, J. N., Cooks, R. G., Syka, J. E. P., Kelley, P. E., Stafford, G. C., and Todd, J. F. J.: Instrumentation, Applications, and Energy Deposition in Quadrupole Ion-Trap Tandem Mass-Spectrometry. *Anal. Chem.* 59 (1987) 1677-1685.

Luukkanen, L., Kilpelainen, I., Kangas, H., Ottoila, P., Elovaara, E., and Taskinen, J.: Enzyme-assisted synthesis and structural characterization of nitrocatechol glucuronides. *Bioconjug. Chem.* 10 (1999) 150-154.

Masimirembwa, C. M., Bredberg, U., and Andersson, T. B.: Metabolic stability for drug discovery and development: pharmacokinetic and biochemical challenges. *Clin. Pharmacokinet.* 42 (2003) 515-528.

Oliveira, E. J. and Watson, D. G.: Liquid chromatography-mass spectrometry in the study of the metabolism of drugs and other xenobiotics. *Biomed. Chromatogr.* 14 (2000) 351-372.

Oppermann, U. C., Filling, C., and Jornvall, H.: Forms and functions of human SDR enzymes. *Chem. Biol. Interact.* 130-132 (2001) 699-705.

Peterman, S. M., Duczak, J., Kalgutkar, A. S., Lame, M. E., and Soglia, J. R.: Application of a Linear Ion Trap/Orbitrap Mass Spectrometer in Metabolite Characterization Studies: Examination of the Human Liver Microsomal Metabolism of the Non-Tricyclic Anti-

Depressant Nefazodone Using Data-Dependent Accurate Mass Measurements. *J. Am. Soc. Mass Spectrom.* 17 (2006) 363-375.

Schwenk, M.: Mucosal biotransformation. *Toxicol. Pathol.* 16 (1988) 138-146.

Sheweita, S. A.: Drug-metabolizing enzymes: mechanisms and functions. *Curr. Drug Metab.* 1 (2000) 107-132.

Stopher, D. A., Beresford, A. P., Macrae, P. V., and Humphrey, M. J.: The metabolism and pharmacokinetics of amlodipine in humans and animals. *J. Cardiovasc. Pharmacol.* 12 (1988) S55-S59.

Suzuki, T., Nishio, K., and Tanabe, S.: The MRP family and anticancer drug metabolism. *Curr. Drug Metab.* 2 (2001) 367-377.

Vogel, C.: Prostaglandin H synthases and their importance in chemical toxicity. *Curr. Drug Metab.* 1 (2000) 391-404.

Williams, J. P. and Scrivens, J. H.: Rapid accurate mass desorption electrospray ionisation tandem mass spectrometry of pharmaceutical samples. *Rapid Commun. Mass Spectrom.* 19 (2005) 3643-3650.

Wrighton, S. A., Ring, B. J., and Van den Branden, M.: The use of in vitro metabolism techniques in the planning and interpretation of drug safety studies. *Toxicol. Pathol.* 23 (1995) 199-208.

Acknowledgements

I am most grateful to my supervisor Doc. Ing. Vladimír Wsól, Ph.D. for giving me the chance to carry out the doctoral studies and providing excellent facilities for my work at the Department of Biochemical Sciences, Faculty of Pharmacy in Hradec Králové, Charles University. I would like to thank all recent and former members of the Department of Biochemical Sciences who provided besides a professional scientific also personal atmosphere that made working in the lab even more enjoyable. Especially, I would like to thank Prof. Jaroslav Dršata, Doc. Ing. Barbora Szotáková, Ph.D., Doc. Ing. Lenka Skálová, Ph.D., Alena Pakostová, Ing. Luděk Šišpera, CSc, PharmDr. Radim Král, Ph.D., Helena Kaiserová, Yogeeta Babú, Michal Šavlík, Iva Boušová and Marek Link. I deeply appreciate Doc. Ing. Michal Holčapek, Ph.D. from Department of Analytical Chemistry, Faculty of Chemical Technology, University of Pardubice for teaching me the art of decipherment of mass spectra.

My deepest gratitude goes to Doc. Raimo A. Ketola and Prof. Risto Kostiainen for their excellent ideas, endless enthusiasm and door being always open for discussions of all kinds. Further I wish to express words of thanks to other collaborators from the Department of Pharmaceutical Chemistry, Faculty of Pharmacy, University of Helsinki. Huge thanks go to Kati Hakala for her patient tuition and familiarizing me with mass spectrometry and liquid chromatography.

I warmly thank all my Czech friends living in Finland for making my days in Finland much easier and happier. I would like thank my parents Bohumil Suchan and Zdeňka Suchanová for their moral support especially during my residency in Finland.

Financial support from the former Research Centre LN00B125, Faculty of Pharmacy, and the Mobility Fund of Charles Faculty, as well as from the Academy of Finland and the Centre for International Mobility, is gratefully acknowledged.

I

THE PHASE I BIOTRANSFORMATION OF THE POTENTIAL ANTILEUKOTRIENIC DRUG QUINLUKAST IN RAT MICROSOMES AND HEPATOCYTES

Vladimír Wsól[a1,b,*], Barbora Szotáková[a2,b], Vendula Baliharová[b1], Luděk Šišpera[b2], Michal Holčapek[c1], Lenka Kolářová[c2], Bohumila Suchanová[b3], Miroslav Kuchař[d] and Lenka Skálová[a3,b]

[a] *Department of Biochemical Sciences, Faculty of Pharmacy, Charles University, Heyrovského 1203, 500 05 Hradec Králové, Czech Republic; e-mail: [1] wsol@faf.cuni.cz, [2] szotako@faf.cuni.cz, [3] skaloval@faf.cuni.cz*

[b] *Research Centre LN00B125, Faculty of Pharmacy, Charles University, Heyrovského 1203, 500 05 Hradec Králové, Czech Republic; e-mail: [1] baliharova@faf.cuni.cz, [2] sispera@faf.cuni.cz, [3] suchanova@faf.cuni.cz*

[c] *Department of Analytical Chemistry, Faculty of Chemical Technology, University of Pardubice, nám. Čs. legií 565, 532 10 Pardubice, Czech Republic; e-mail: [1] michal.holcapek@upce.cz, [2] lenka.kolarova@upce.cz*

[d] *Research Institute for Pharmacy and Biochemistry, U Kabelovny 130, 102 37 Prague 10, Czech Republic; e-mail: miroslav.kuchar@zentiva.cz*

Received September 23, 2003
Accepted January 29, 2004

Dedicated to the 50th anniversary of the foundation of the Department of Biochemistry, the first biochemical department in Czechoslovakia.

The phase I metabolism of quinlukast (VÚFB 19363, Q; 4-{[4-(2-quinolylmethoxy)phenyl]-sulfanyl}benzoic acid), a new antiasthmatic drug with significant antileukotriene effects, was investigated in rat microsomes and hepatocytes. Quinlukast, incubated with rat liver microsomal fraction under oxidative conditions, generated four metabolites, M2–M5. Based on comparison with synthetically prepared standards, metabolites M2 and M4 were identified as sulfoxide and sulfone of the parent compound, respectively. Metabolites M3 and M5 were identified as quinlukast dihydrodiols. For all the metabolites the apparent kinetic parameters K'_m, V'_{max} and metabolic efficiency Cl_{int} were calculated. No metabolite was found in rat liver cytosol. In vitro studies with primary cultures of isolated hepatocytes were designed to evaluate time dependent (2, 4, 8 and 24 h) and concentration dependent (0.005–0.1 mmol/l) formation of metabolites of quinlukast. Four metabolites were detected in culture medium. Three of them were identical to metabolites found in incubation of quinlukast with microsomes (M2, M3 and M5) and another, the most polar metabolite, M1, was detected. The basic metabolic pathways were proposed for quinlukast in rats.

Keywords: Antiasthmatics; Drug metabolism; Metabolic pathways; Hepatocytes; Microsomes; Enzyme kinetics; Kinetic parameters; LC-MS; Biotransformations; Antihistaminics; Metabolites.

Antileukotriene drugs inhibit the formation or action of leukotrienes, which are potent lipid mediators. Leukotrienes LTB_4 and cysteine-containing leukotrienes (Cys-LT), LTC_4, LTD_4 and LTE_4, originate from oxidative metabolism of arachidonic acid through a key enzyme, 5-lipoxygenase, in lung tissue and in a number of inflammatory cells[1]. It is now widely recognized that Cys-LTs play an important role in asthma, participating both in the bronchoconstriction and in the chronic inflammatory component of the disease[2]. In human tissues, effects of these leukotrienes are mediated by activation of Cys-LT_1 receptors. Consequently, the number of structurally different Cys-LT_1 antagonists has been expanding[3] in the last years and some are already available for clinical use (zafirlukast, pranlukast and montelukast)[4,5].

New original compounds – derivatives of (arylsulfanyl)benzoic acid – with significant antileukotrienic effects were prepared in the Research Institute for Pharmacy and Biochemistry (Prague, Czech Republic). Of them, quinlukast (VÚFB 19363, Q), 4-{[4-(2-quinolylmethoxy)phenyl]sulfanyl}-benzoic acid (Fig. 1), is considered to be the most promising[6].

The IC_{50} value for Q in inhibition of binding to leukotriene D_4 receptors is comparable to montelukast and zafirlukast, while leukotriene B_4 biosynthesis inhibition by Q is much more effective than that of montelukast and zafirlukast (*manuscript in preparation*). The main advantage of Q is its multiple antileukotrienic, anti-inflammatory and antiasthmatic effect.

With respect to promising biological activities further pre-clinical trials of Q have been initiated. Biotransformation study represents an integral and important part of development of each new drug. The study described in this paper was designed to characterize the phase I in vitro metabolism of Q in rats and to identify the principal Q metabolites. The kinetics of metabolites formation was studied in primary cultures of rat hepatocytes and in subcellular fractions of rat liver homogenate.

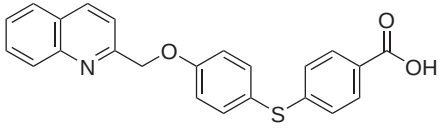

FIG. 1
Chemical structure of quinlukast

EXPERIMENTAL

Chemicals

Quinlukast (VÚFB 19363, Q) and its potential metabolites, Q sulfoxide and Q sulfone, were obtained from the Research Institute for Pharmacy and Biochemistry (Prague, Czech Republic). Enzymatic tests were performed using NADPH from Sigma–Aldrich (Prague, Czech Republic). Acetonitrile (MeCN), methanol (MeOH) and dimethyl sulfoxide (DMSO) (all HPLC grade) were obtained from Riedel–deHaen (Seelze, Germany). Collagenase was purchased from Sevapharma (Prague, Czech Republic). The Ham F12 medium, William's E medium, foetal calf serum, antibiotics, insulin and collagen were supplied by Sigma–Aldrich (Prague, Czech Republic). All other chemicals were of the highest purity commercially available.

Animals

Male Wistar rats (10–12 weeks) were obtained from the BioTest (Konárovice, Czech Republic). They were kept on standard rat food with free access to tap water, in animal quarters under a 12-h light-dark cycle. Rats were cared for and used in accordance with the Guide for the Care and Use of Laboratory Animals (Protection of Animals from Cruelty Act. No. 246/92, Czech Republic).

Isolation of Microsomal and Cytosolic Fractions

Livers of male Wistar rats (10–12 weeks) were used as source of cytosol and microsomes. Livers were homogenized in 0.1 M Na phosphate buffer, pH 7.4. The microsomal and cytosolic fractions were obtained by fractional ultracentrifugation of the homogenate[7]. A rewashing step (followed by second ultracentrifugation) was added at the end of the microsomes preparation procedure. Microsomes were finally resuspended in the homogenization buffer containing 20% glycerol (v/v) and stored at –80 °C. The protein content was determined according to Lowry with 0.1% SDS [8].

Isolation of Hepatocytes

Hepatocytes were obtained by the two-step collagenase method[9]. In the first step, the liver was washed with 150–200 ml of a solution without calcium, with the aim to remove the rest of blood and make the cell–cell junction weaker. In the second step, hepatocytes were released by action of collagenase (50 mg/100 ml) in perfusion solution with calcium. Second perfusion took 5–6 min (recirculation system). Isolated hepatocytes were washed three times and mixed with culture medium. The culture medium consisted of a 1:1 mixture of Ham F12 and Williams' E, supplemented as described earlier[10,11]. The viabilities of cells measured by Trypan Blue staining according to the Sigma protocol were 85–90%. Three million of viable cells in 3 ml of culture medium were placed into 60-mm plastic dishes precoated with collagen. The foetal calf serum was added in culture medium (5%) to promote cell attachment during the first four hours after plating. Then the medium was exchanged for fresh one without serum. The cultures were maintained at 37 °C in a humid atmosphere with 5% CO_2.

Cytotoxicity Assay

Cytotoxicity was assayed by using the MTT (3-(4,5-dimethylthiazol-2-yl)-2,5-diphenyl-2*H*-tetrazolium bromide) test as described[12]. Cells, seeded in 96-well plates, were incubated with Q at different concentrations (0.005–0.1 mmol/l) for 24 h, followed by incubation with MTT. An amount of 25 μl of a MTT solution in phosphate buffer (3 mg/ml) per well was applied without removal of the medium; after 2.5 h the medium was discarded and cells were lysed with 0.08 M HCl in propan-2-ol (50 μl/well). Absorbance of the formazane product was measured at 595 nm. The absorbance of formazane in cells treated with Q was compared to that in control cells exposed to medium with 0.5% DMSO alone.

Incubation of Microsomal and Cytosolic Fractions with Quinlukast

A liver microsomal suspension (50 μl corresponding to 50 mg of wet tissue) was incubated in Eppendorf microtubes with quinlukast as substrate (final concentrations ranging from 0.01 to 1 mmol/l) and 0.5 mM NADPH or NADH in a total buffer volume of 0.3 ml. The liver cytosolic fraction (50 μl corresponding to 7 mg of wet tissue) was incubated in Eppendorf microtubes with quinlukast as substrate (final concentrations 0.05, 0.2 and 0.5 mmol/l) and 0.5 mM NADPH in a total buffer volume of 0.3 ml. Incubations were performed for 30 min at 37 °C. All incubations were terminated by cooling to 0 °C and addition of 10 μl of 1 M HCl. Quinlukast and its metabolites were extracted twice with two volumes of ethyl acetate–*n*-heptane mixture (1:3, v/v), and the combined extracts were evaporated to dryness in vacuum. The dry samples were dissolved in 5 mM phosphate buffer, pH 7.0, prior to their HPLC injection.

Incubation of Hepatocytes Primary Culture with Quinlukast

A stock solution of Q dissolved in DMSO was added to fresh medium. The final concentration of DMSO in medium was 0.1%.

Hepatocyte monolayers (18–24 h after isolation) were incubated with 50 or 100 μM Q. Aliquots of the medium (0.5 ml) were collected in the intervals of 0, 2, 4, 8 and 24 h. For kinetic study various concentrations (0, 5, 10, 25, 50, 75, 100 μmol/l) of the substrate were used and incubation proceeded for 24 h. All medium samples were stored frozen at –80 °C prior to their solid-phase extraction and HPLC analyses.

Solid-Phase Extraction

SPE of the hepatocyte samples were performed on Sep-Pak Light tC18 cartridges (145 mg sorbent; Waters, Prague, Czech Republic). The cartridges were conditioned with methanol (2 ml) and a washing solution, 10 mM phosphate buffer (2 ml, pH 7.0), before applying the samples. Hepatocyte samples (500 μl) prepared as described above were manually loaded onto the cartridges which were purged with washing solution (4.5 ml). Finally, all SPE cartridges were eluted with 1 ml of methanol. The eluting solvents were evaporated, and dry samples reconstituted in 120 μl of solution consisting of 5 mM phosphate buffer, pH 7.0, in MeCN–H_2O (40:60, v/v) and prepared for HPLC injection.

HPLC Assay for Quinlukast and Its Metabolites

Quinlukast and its metabolites were measured with an HPLC system consisting of an LC-10 AD_{VP} gradient pump, SIL-10 AD_{VP} autoinjector, FCV-10 AL_{VP} solvent mixer, CTO-10 AC_{VP} column oven, SCL-10 A_{VP} system controller and SPD-M10 A_{VP} UV-VIS photodiode array detector with detection set at 220–300 nm range (285 nm for metabolites). Data from these chromatographic runs were processed using the Chromatography Laboratory Automated Software System Class VP (version 6.12) from Shimadzu (Prague, Czech Republic). The assay was performed on a Purospher RP18e analytical column (5 μm, 125 × 3 mm; Merck, Prague, Czech Republic) equipped with a Hypersil BDS C18 guard column (5 μm, 4 × 4 mm; Agilent, Prague, Czech Republic). The HPLC method involved the following gradient system using 8 mM H_3PO_4 in H_2O–MeOH–MeCN (70:16.5:13.5, v/v/v) as mobile phase A and 8 mM H_3PO_4 in H_2O–MeOH–MeCN (10:49.5:40.5, v/v/v) as mobile phase B. The flow rate was set at 0.7 ml/min. From 0 to 13 min, the ratio of mobile phase A to B was linearly changed from 73:27 to 51:49. Mobile phase B was then increased to 80% at 13.5 min. Mobile phase B was held at 80% for 6.5 min, after which it was reverted back to 27% at 20.5 min. The equilibration time was 15.5 min. All chromatographic runs were performed at 25 °C. The blank medium spiked with M2 was used for calibration. Weighted linear regression analysis was performed by plotting the peak area versus analyte concentration (0.08–8.00 μmol/l). Regression line parameters were used to calculate concentrations of other metabolites in all biological samples. The limit of reliable quantification (coefficient of variation, CV ≤ 20%) was taken as 80 nmol/l for all three metabolites. Intra-day variability was assessed by quadruple analyses of incubated samples. The CV values did not exceed 4.9% (M2), 5.1% (M3) and 7.2% (M5). Absolute recovery of M2 from medium was 84.7 ± 2.6% at the 2.4 μmol/l level. Figure 2 illustrates the resolution of Q and its metabolites in male rat hepatocytes.

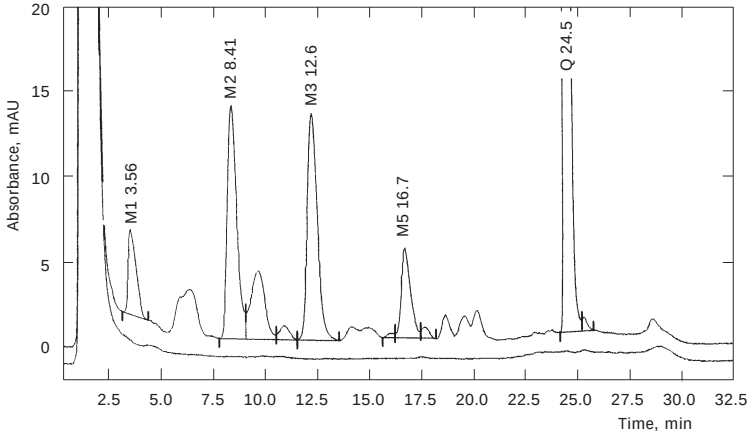

FIG. 2
HPLC chromatogram of the rat hepatocyte medium. 24-h incubation with 100 μM Q as substrate is shown together with blank sample of hepatocytes. HPLC conditions are described in Experimental

HPLC/MS

The equipment used consisted of a Model 616 pump with a quaternary gradient system, a Model 996 diode-array UV detector, a Model 717+ autosampler, a thermostatted column compartment and a Millennium chromatography manager (all from Waters, Milford, MA, U.S.A.). The UV detector outlet of the liquid chromatograph was connected to the ion trap analyser Esquire3000 (Bruker Daltonics, Bremen, Germany) using electrospray ionization (ESI) in both the positive- and negative-ion mode. Data were acquired in the mass range *m/z* 50–1000. The pressure of the nebulising gas was 414 kPa, the flow rate and temperature of the drying gas was 11 l/min and 365 °C, respectively. The ion trap analyser was tuned to give an optimum response for *m/z* 400. The isolation width for MS/MS experiments was *m/z* 4, and the collision amplitude was 1 V. The compound stability was 100% (first experiments) and 20%.

RESULTS

Metabolism of Quinlukast in Rat Microsomes and Cytosol

Q in a saturated solution (0.5 mmol/l) was incubated with microsomes under aerobic or anaerobic conditions. NADH or NADPH was used as a coenzyme. Composition of the incubation mixture was analysed by HPLC. Four metabolites (M2–M5) were detected in the incubation mixture after aerobic incubation with NADPH. When NADH coenzyme was used substantially lower amounts of metabolites were formed. Only a negligible amount of metabolites was found in samples incubated under anaerobic conditions (data are not shown). Metabolites M2 and M4 were compared with synthetically prepared standards and identified as Q sulfoxide and Q sulfone, respectively. While Q sulfoxide was the principal metabolite of Q in rat microsomes, Q sulfone was only a minor one the concentration of which was near the limit of detection. Using HPLC/MS with positive-ion ESI, the first-stage mass spectra of Q and of all four discussed metabolites showed protonated molecules without any fragmentation, which enabled an easy molecular weight determination (see the spectrum of M3 in Fig. 3a). Following MS/MS spectra of $[M + H]^+$ ions (Fig. 3b) yielded the characteristic fragment ions supporting the structure assignment of M3 and M5. The mass spectra of M3 and M5 differ solely in the relative abundances of some fragment ions in MS/MS spectra, hence only one example illustrates an identification (Fig. 3). Cleavage of a bond between the sulfur atom and the benzene ring leads to the *m/z* 269 ion and subsequent neutral loss of water corresponds to the *m/z* 251 ion. Similarly, the cleavage of the bond between the etheric oxygen and the CH_2 group leads to the *m/z* 177 ion and subsequent loss of water corresponds to the *m/z* 159 ion. Two molecules of water

are readily lost from the $[M + H]^+$ ion (the fragment ions *m/z* 404 and 386), which is typical of vicinal hydroxy groups.

Kinetic studies were performed under aerobic conditions with NADPH as coenzyme and substrate concentrations 0.01–1.0 mmol/l. Concentrations of metabolites M2, M3 and M5 were measured. The curves obtained are presented in Fig. 4. Kinetic parameters – apparent K'_m and V'_{max} and metabolic efficiency Cl_{int} (defined as V_{max}/K_m ratio) – were calculated using GraphPad Prism 3.0 software. Data are shown in Table I.

Q (concentrations 0.05, 0.2 and 0.5 mmol/l) was incubated with rat cytosol under aerobic or anaerobic conditions. NADH or NADPH was used as a coenzyme. No metabolites were detected in incubation mixtures (data are not shown).

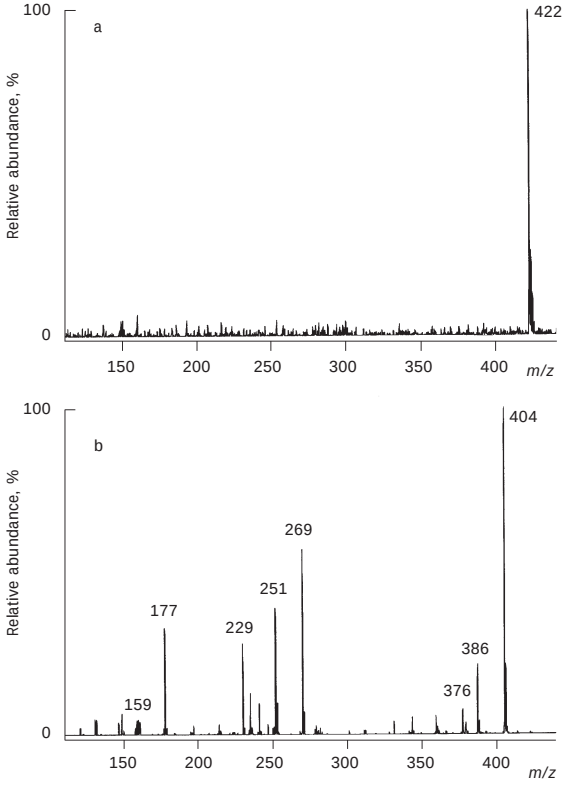

FIG. 3
ESI-MS spectra of quinlukast metabolites M3: a full scan, b MS/MS spectrum

TABLE I
Apparent kinetic parameters of the respective biotransformation enzymes in rat liver microsomal fraction

Metabolite	V'_{max}	K'_m	Cl_{int}
M2	1820 ± 54	18.8 ± 2.6	96.8
M3	271 ± 6	13.8 ± 1.7	19.6
M5	321 ± 8	14.2 ± 1.9	22.6

The values represent the average of 4–6 determinations. V'_{max} in pmol/30 min (per mg of protein), K'_m in μmol/l, Cl_{int} (metabolic efficiency, defined as V_{max}/K_m ratio) in μl/30 min (per mg of protein).

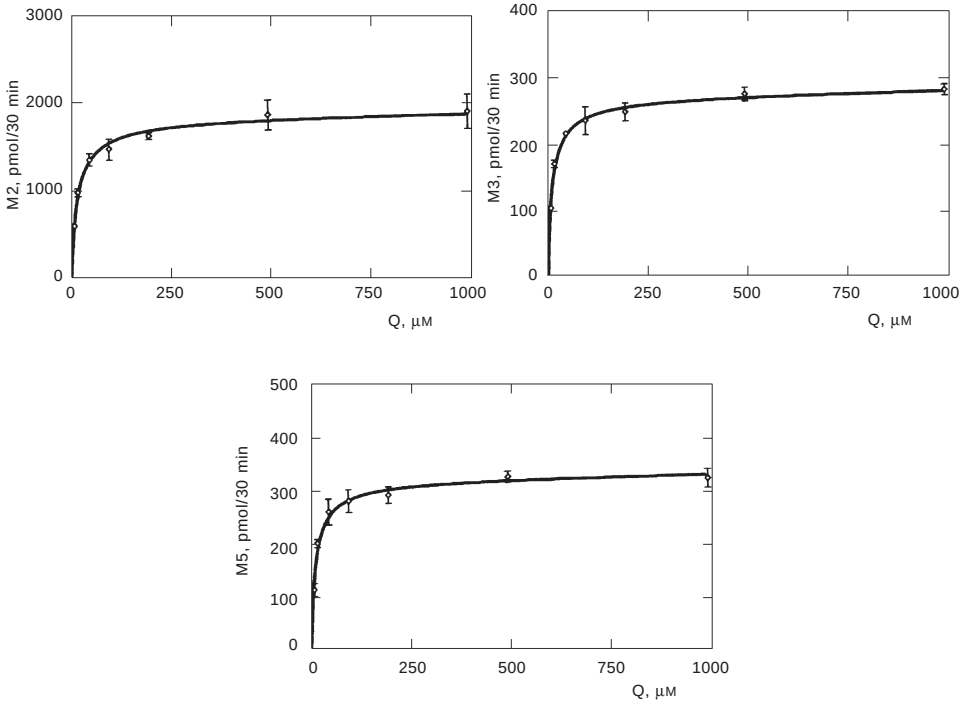

FIG. 4
Rate of formation of Q metabolites versus quinlukast concentration in rat liver microsomes. Each point represents the average and S.E.M. of 4–6 determinations. Data are normalized for 1 mg of protein

Metabolism of Quinlukast in Rat Hepatocytes

Primary cultures of rat hepatocytes were incubated with 0.05 or 0.1 mM Q and aliquots of the medium were collected and analysed. Four metabolites were detected in culture medium. Three of them were identical to metabolites found in incubation of Q with microsomes. No Q sulfone, a minor metabolite observed in microsomes, was detected in culture medium. On the other hand, another metabolite (M1) was detected in hepatocyte medium. Based on polarity and spectra analysis, M1 seems to be a conjugate of Q or its metabolite. Its structure and kinetics will be under study in the next project concerning phase II of Q metabolism.

The time-dependent (0, 2, 4, 8 and 24 h) formation of metabolites is presented in Fig. 5.

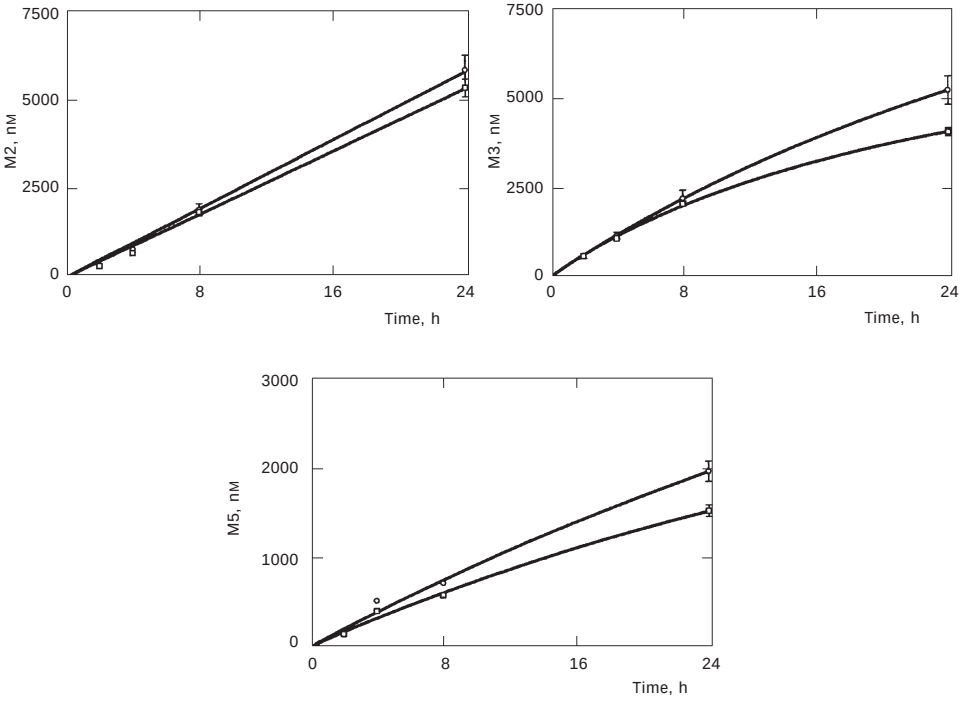

FIG. 5

Time dependent (0, 2, 4, 8 and 24 h) formation of M1, M2, M3 and M5 in culture of the rat hepatocyte medium for two concentrations of Q (50 (□) and 100 (○) μmol/l). Each point represents the average and S.E.M. of 4–6 determinations. Data are normalized for 1 million of cells

For kinetic studies, various concentrations of substrate (0.005–0.1 mmol/l) were used. Concentrations of metabolites M1, M2, M3 and M5 were measured in culture medium after 24-h incubation. The curves obtained are presented in Fig. 6. Kinetic parameters – apparent K'_m and V'_{max} – together with Hill coefficient were calculated using GraphPad Prism 3.0 software. Kinetic parameters obtained served for calculation of metabolic efficiency Cl_{int}. Data are shown in Table II.

Q was shown to be non-cytotoxic in the concentration range tested (0.005–0.1 mmol/l) in primary cultures of rat hepatocytes.

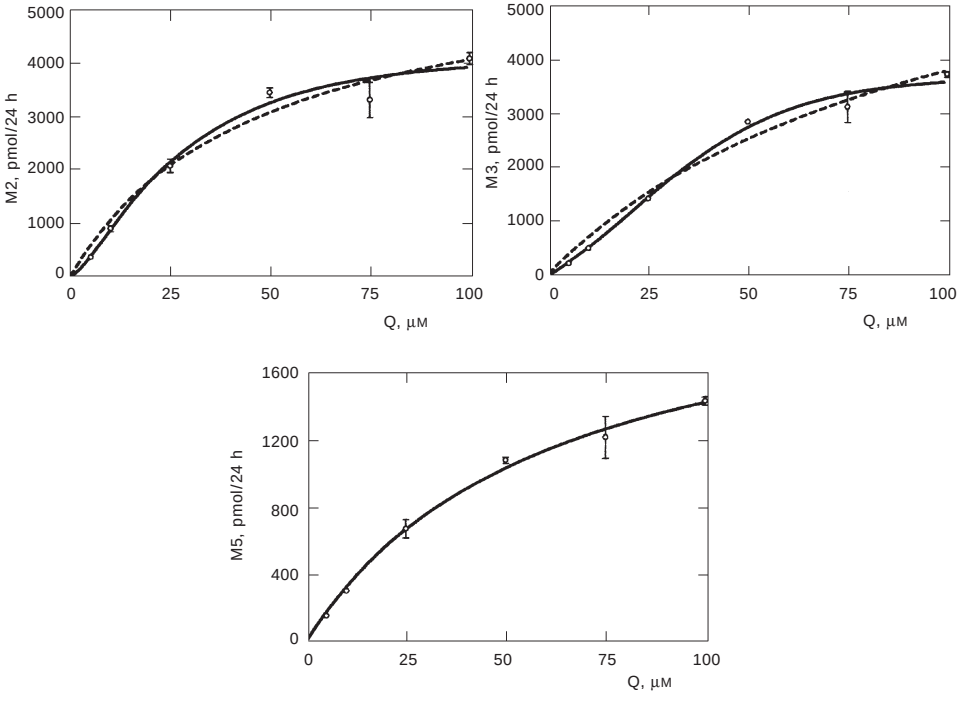

FIG. 6

Rate of formation of Q metabolites versus quinlukast concentration after 24-h incubation in 1 ml of culture medium. The dotted line indicates the Michaelis–Menten kinetics and the full line shows a better fit for sigmoidal dose-response kinetics. Each point represents the average and S.E.M. of 4-6 determinations. Data are normalized for 1 million of cells

DISCUSSION

Recently, several Cys-LT1 receptor antagonists are available for clinical management of asthma. Their metabolic pathways have been studied and ascertained. Dicarboxylic acid, acyl glucuronide, sulfoxides, hydroxylated and methylhydroxylated metabolites are the montelukast metabolites formed in humans[5,13]. Biotransformation of zafirlukast in rats, dogs and mice includes hydrolysis, hydroxylation and demethylation[14]. Hydroxylation, sulfur oxidation and conjugation of verlukast with glucuronic acid and glutathion were reported[15,16]. The identification of the main metabolic pathways of new potential antileukotrienic drug Q was necessary for starting its pharmacokinetic tests and clinical trials.

Two in vitro models were used for this purpose: subcellular fractions (microsomes and cytosol) of rat liver homogenate and primary cultures of rat hepatocytes. Four metabolites were revealed in rat microsomes. Q sulfoxide represented the principle one. A relatively high metabolic efficiency Cl_{int} indicates high metabolic efficiency of sulfur oxidation of Q. Similarly to verlukast[17], also in Q oxygen is incorporated into the structure in the form of relatively unstable Q epoxides. These epoxides are then very quickly converted probably by epoxide hydrolase to the corresponding Q dihydrodiols (metabolites M3 and M5). The mass of these Q dihydrodiols was confirmed by mass spectrometry (MS and MS2). The position of hydroxyl groups was proposed on the basis of metabolic similarity with verlukast[17] and taking into account different retention times in the HPLC system used. Just M5 is probably able to form a five-membered ring that

TABLE II
Apparent kinetic parameters of the respective biotransformation enzymes in rat hepatocyte medium

Metabolite	V'_{max}	K'_m	Cl_{int}	Hill coeff.
M2	4435 ± 431	26.0 ± 3.3	170.6	1.48 ± 0.27
M3	4239 ± 390	36.3 ± 4.6	116.8	1.68 ± 0.23
M5	1915 ± 180	42.2 ± 5.1	45.4	1.16 ± 0.17

The values represent the average of 4–6 determinations. V'_{max} in pmol/24 h (per million of cells), K'_m in μmol/l, Cl_{int} (metabolic efficiency, defined as V_{max}/K_m ratio) in μl/24 h (per million of cells).

produces less hydrogen bonds with mobile phase, which can be explanation for its higher retention time in comparison to the other dihydrodiol M3. As only negligible amount of Q sulfone was formed, structure of Q probably defended sulfur atom against second oxidation. Finding no metabolites in liver cytosol corresponded to our expectation of no reductive or hydrolytic transformation of Q.

In primary cultures of rat hepatocytes, four metabolites were also detected. Three of them were identical to metabolites found in incubation of Q with microsomes. Q sulfone, a minor metabolite observed in microsomes, was not found in hepatocytes probably due to a substantially lower concentration of the substrate used in hepatocytes than in microsomes. On the other hand, another metabolite (M1) was detected in hepatocyte medium. Based on polarity of the HPLC system and spectral analysis ($[M + H]^+$ ion *m/z* 515), M1 seems to be a conjugate of Q or Q metabolite. While in microsomes the formation of metabolites M3 and M5 was 5–8 less extensive than sulfur oxidation of Q, the amount of M3 detected in hepatocyte medium was similar to the amount of Q sulfoxide. Comparing the two models used – microsomes and hepatocytes – several factors might shift proportion of metabolites: secondary metabolic transformation, stability and orientation of enzymes, cooperation of enzymes, accessibility of substrate etc.[11].

Concentration of all metabolites increased during 24-h Q incubation in hepatocytes. While formation of Q sulfoxide was linear up to 24 h (in addition, the chemical stability during the 24-h incubation was confirmed), metabolites M1, M3 and M5 increased linearly only for 4–8 h. Exhaustion of substrate, damage of enzymes or secondary metabolic transformation might affect metabolite concentration detected in medium. Chemical stability during the 24-h incubation for M1, M3 and M5 was not measured because these metabolites were not available as standards.

No or low differences between concentration of metabolites formed in hepatocytes incubated with 0.05 and 0.1 mM Q was observed in all the time intervals tested. This finding was in accordance with low values of apparent K_m calculated from kinetic curves for all metabolites. While the shape of kinetic curves for M2, M3 and M5 in microsomes corresponded well with the Michaelis–Menten kinetics, certain sigmoidal deformation of curves was observed for these metabolites in hepatocyte culture. For this reason, two fittings of experimental points were made: first corresponding to the Michaelis–Menten kinetics and second corresponding to the sigmoidal dose-response kinetics. Hill coefficients 1.5 and 1.7 characterized the formation of metabolites M2 and M3, respectively, in primary cultures of rat

hepatocytes. This finding can either be due to partial cooperation of enzyme systems in their formation or to a contribution of transport proteins in their release into medium.

In conclusion, the in vitro study of Q metabolism revealed five Q metabolites in rat. Based on our results the metabolic pathways for Q in rat liver microsomes and hepatocytes were proposed (Fig. 7). Phase I metabolites were identified (M2 and M4) or their structures were suggested on the basis of ESI-MS spectra (M3 and M5), and kinetic parameters of their in vitro formation were calculated and evaluated.

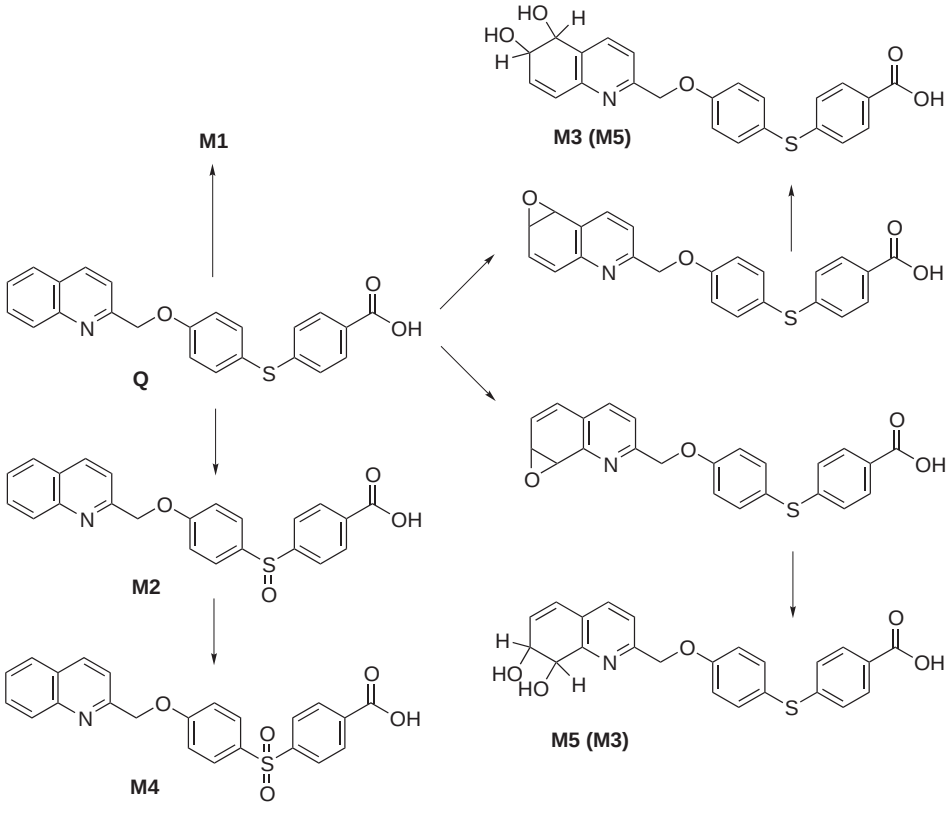

FIG. 7
Proposed biotransformation pathways for quinlukast in rat liver microsomes and hepatocytes

This project was supported by the Ministry of Education, Youth and Sports of the Czech Republic (Research Centre LN00B125 and project No. 253100002).

REFERENCES

1. Dahlen B., Hedquist S., Hammarstrom S., Samuelsson B.: *Nature (London)* **1980**, *288*, 484.
2. Jain N. K., Kulkarni S. K., Singh A.: *Eur. J. Pharmacol.* **2001**, *423*, 85.
3. Claesson H. E., Dahlen B.: *J. Intern. Med.* **1999**, *245*, 205.
4. Chung K. F., Barnes P. J.: *Drugs Today* **1998**, *34*, 375.
5. Chiba M., Xu X., Nishime J. A., Balani S. K., Lin J. H.: *Drug Metab. Dispos.* **1997**, *25*, 1022.
6. Kuchar M., Kmonicek V., Panajotova V., Brunova B., Jandera A., Jirickova H., Bucharova V.: U.S. 6,303,612 B1, 2001; *Chem. Abstr.* **2000**, *132*, 49797.
7. Gillette J. R.: *Fundamentals of Drug Metabolism and Drug Disposition*, p. 400. The Williams and Wilkins, Baltimore 1971.
8. Markwell M. A., Haas S. M., Bieber L. L., Tolbert N. E.: *Anal. Biochem.* **1978**, *87*, 206.
9. Berry M. N., Edwards A. M., Barritt G. J.: *Laboratory Techniques in Biochemistry and Molecular Biology*, pp. 1–470. Elsevier Science, Amsterdam 1991.
10. Isom H. C., Georgoff I.: *Proc. Natl. Acad. Sci. U.S.A.* **1984**, *8*, 6378.
11. Maurel P.: *Adv. Drug Deliv. Rev.* **1996**, *22*, 105.
12. Denizat F., Lang R.: *J. Immunol. Methods* **1986**, *89*, 271.
13. Balani S. K., Xu X., Pratha V., Koss M. A., Amin R. D., Dufresne C., Miller R. R., Arison B. H., Doss G. A., Chiba M., Freeman A., Holland S. D., Schwartz J. I., Lasseter K. C., Gertz B. J., Isenberg J. I., Rogers J. D., Lin J. H., Baillie T. A.: *Drug Metab. Dispos.* **1997**, *25*, 1282.
14. Savidge R. D., Bui K. H., Birmingham B. K., Morse J. L., Spreen R. C.: *Drug Metab. Dispos.* **1998**, *26*, 1069.
15. Nicol-Griffith D. A., Yergey J., Trimble L., Williams H., Rasori R., Zamboni R.: *Drug Metab. Dispos.* **1992**, *20*, 383.
16. Nicol-Griffith D. A., Gupta N., Twa S. P., Williams H., Trimble L., Yergey J. A.: *Drug. Metab. Dispos.* **1995**, *23*, 1085.
17. Grossman S. J., Herold E. G., Drey J. M., Alberts D. W., Umbenhauer D. R., Patrick D. H., Nicoll-Griffith D., Chauret N., Yergey J. A.: *Drug Metab. Dispos.* **1993**, *21*, 1029.

II

Available online at www.sciencedirect.com
SCIENCE DIRECT®
Analytical Biochemistry 341 (2005) 105–112
ANALYTICAL BIOCHEMISTRY
www.elsevier.com/locate/yabio

Rapid simultaneous determination of metabolic clearance of multiple compounds catalyzed in vitro by recombinant human UDP-glucuronosyltransferases

Kati S. Hakala [a], Bohumila Suchanova [b], Leena Luukkanen [c], Raimo A. Ketola [a], Moshe Finel [a], Risto Kostiainen [a,c,*]

[a] *Viikki Drug Discovery Technology Center (DDTC), Faculty of Pharmacy, University of Helsinki, 00014 Helsinki, Finland*
[b] *Department of Biochemical Sciences, Faculty of Pharmacy in Hradec Kralove, Charles University in Prague, Heyrovskeho 1203, 50005 Hradec Kralove, Czech Republic*
[c] *Department of Pharmaceutical Chemistry, Faculty of Pharmacy, University of Helsinki, 00014 Helsinki, Finland*

Received 17 January 2005
Available online 17 March 2005

Abstract

The purpose of this study was to test the applicability of *n*-in-one (cocktail) incubations in the determination of intrinsic clearance (Cl_{int}) as the slope of the linear portion of the Michaelis–Menten curve (velocity V vs. substrate concentration [S]) where substrate concentrations were low. A rapid, sensitive, and selective liquid chromatography tandem mass spectrometry (LC/MS/MS) method was developed for the analysis of samples produced by single-substrate and *n*-in-one (seven substrates: entacapone, 17β-estriol, umbelliferone, 4-methylumbelliferone, tolcapone, hydroxyquinoline, and paracetamol) incubations conducted in 96-well plates with different recombinant UDP-glucuronosyltransferases (UGTs). The Cl_{int} values obtained with *n*-in-one incubations were compared with those obtained in single-compound incubations and with V_{max}/K_m values determined by estimating the enzyme kinetic parameters V_{max} and K_m from the Michaelis–Menten curve. When substrate concentrations were well below their K_m values, Cl_{int} values determined as the slope of the linear part of the Michaelis–Menten fitting correlated well with the values determined as V_{max}/K_m ratios from the Michaelis–Menten curve. The correlation between Cl_{int} values determined in single-substrate and *n*-in-one incubations was high as well. Together, the *n*-in-one incubations, the determination of Cl_{int} values as the slope of the linear part of the Michaelis–Menten fitting, and LC/MS/MS as an analytical method proved to be effective approaches for increasing throughput in the first-phase screening of metabolic properties.

Keywords: UDP-glucuronosyltransferases; LC/ESI/MS/MS; *n*-in-one cocktails; Intrinsic clearance

Poor pharmacokinetics is a major reason for the withdrawal of many drug candidates from clinical trials [1]. Therefore, there is an urgent need for investigation of pharmacokinetic properties and the recognition of unsuitable drug candidates as early as possible in the drug development process. New effective synthesis techniques, such as drug design in silico, combinatorial synthesis, and high-throughput screening (HTS),[1] have increased the number of drug candidates and target molecules in the early phase of drug discovery. Thus,

* Corresponding author. Fax: +358 9 19159556.
E-mail address: risto.kostiainen@helsinki.fi (R. Kostiainen).

[1] *Abbreviations:* HTS, high-throughput screening; UGT, UDP-glucuronosyltransferase; ADME, absorption, distribution, metabolism, and elimination; LC/MS, liquid chromatography mass spectrometry; LC/MS/MS, liquid chromatography tandem mass spectrometry; UDPGA, uridine 5′-diphosphate glucuronic acid; DMSO, dimethyl sulfoxide; MRM, multiple reaction monitoring; ESI, electrospray ionization; RSD, relative standard deviation.

0003-2697/$ - see front matter © 2005 Elsevier Inc. All rights reserved.
doi:10.1016/j.ab.2005.03.003

developing in vitro methods that could provide pharmacokinetic information on much larger sets of compounds than is currently possible is an important and timely challenge. Such methods should allow a more specific selection of lead candidates with acceptable metabolic stability and permeability.

Metabolic stability is an important parameter in classifying potential lead compounds as poorly, moderately, or rapidly metabolizing. Clarification of the metabolic stability of a drug candidate is essential because metabolism can significantly alter the pharmacokinetics of the drug, resulting in poor in vivo exposure or even toxic effects if drugs are metabolized too rapidly or if active metabolites are present. Metabolic stability results are typically reported as measures of either parent disappearance or metabolite formation. Parent disappearance can be reported as $t_{1/2}$ or percentage disappearance at a single time point. In vitro intrinsic clearance can be obtained by estimating the maximal reaction rate of metabolite formation (V_{max}) and Michaelis constant (K_m) and calculating intrinsic clearance (Cl_{int}) as V_{max}/K_m. This approach is time-consuming, however, and a large number of measurements are needed to optimize the incubation conditions and perform the experiments at several substrate concentrations. An alternative and more rapid method for determining Cl_{int} in vitro from the half-life is the so-called depletion method, in which the initial substrate concentration is low and its subsequent decline is monitored at regular intervals [2,3].

Liver slices, hepatocytes, liver microsomes, and recombinant enzymes all have been used as in vitro model systems for testing metabolic stability. Liver slices and hepatocytes are whole cell systems that offer a more reliable in vivo/in vitro correlation of the metabolic clearance than do subcellular systems. They are not easily applicable to higher throughput screening, however, due to poor availability and a number of practical limitations. Instead, liver microsomes, which are well adapted to higher throughput, are widely used in screening of metabolic properties. Additional advantages of microsomal fractions are easy preparation and use, stability during storage, and high concentrations of the main drug-metabolizing enzymes.

Recombinant enzymes that are expressed individually provide an interesting testing system because they can give structure–activity information on the individual isoenzymes involved in the metabolism of a given drug candidate. Furthermore, mixing of exact proportions of different isoforms makes it possible to keep the enzyme levels constant, whereas this is not always possible with other in vitro models. UDP-glucuronosyltransferases (UGTs) are membrane-bound enzymes of the endoplasmic reticulum. They catalyze the glucuronidation of various endogenous and exogenous compounds, converting the substrate molecules into more polar glucuronides, thereby stimulating their excretion rate [4,5]. The human genome encodes at least 16 different UGTs that are divided into families (1 and 2) and subfamilies (2A and 2B) according to the degree of sequence identities and genomic organization [4,6,7]. Most UGTs are expressed in the liver, the organ that is considered to be the major site of glucuronidation, but some UGTs are extrahepatic enzymes and many of the liver UGTs are also found in other tissues [4].

Despite recent developments in assay technologies that have increased the speed of ADME (absorption, distribution, metabolism, and elimination) screening, the screening capacity is still several orders of magnitude lower than the HTS methods that are used in bioactivity screening of drug candidates. The highest throughput in metabolic stability screening with reliable results is dozens of compounds per day and is currently achieved by liquid chromatography mass spectrometry (LC/MS) [8–10]. These assays use a 96-well plate format, a robotic system, multiple injectors, a dual-column system, and effective online data processing. LC/MS is a sensitive and selective detector and allows multicomponent analysis that, in combination with *n*-in-one (cocktail) experiments, provides a highly effective technique for increasing throughput. Recently, the *n*-in-one strategy and liquid chromatography tandem mass spectrometry (LC/MS/MS) have been used successfully in high-throughput inhibition screening of human cytochrome P450 enzymes [11,12] and in Caco-2 permeability studies [13].

The aims of this study were (i) to develop a sensitive and fast LC/MS/MS method for the simultaneous analysis of a set of glucuronides, (ii) to investigate the applicability of *n*-in-one incubations in kinetic studies with recombinant human UGT isoenzymes by analyzing the formation of glucuronides of seven substrates (entacapone, 17β-estriol, umbelliferone, 4-methylumbelliferone, tolcapone, hydroxyquinoline, and paracetamol) (Fig. 1) as a mixture and as single incubations, and (iii) to introduce an alternative method for the determination of intrinsic clearances (Cl_{int}) as the slope of the linear portion of a velocity (V) versus substrate concentration ([S]) plot.

Materials and methods

Chemicals and reagents

Umbelliferone (7-hydroxycoumarin), 4-methylumbelliferone, estriol, 8-hydroxyquinoline, 4-methylumbelliferyl-β-D-glucuronide, estriol-17β-D-glucuronide, 8-hydroxyquinoline glucuronide, paracetamolglucuronide, D-saccharic acid 1,4-lactone, and uridine 5′-diphosphoglucuronic acid (UDPGA) were purchased from Sigma–Aldrich Chemie (Steinheim, Germany). Umbelliferone glucuronide was purchased from Ultrafine (Manchester, UK). Entacapone, tolcapone, and paracetamol were obtained from

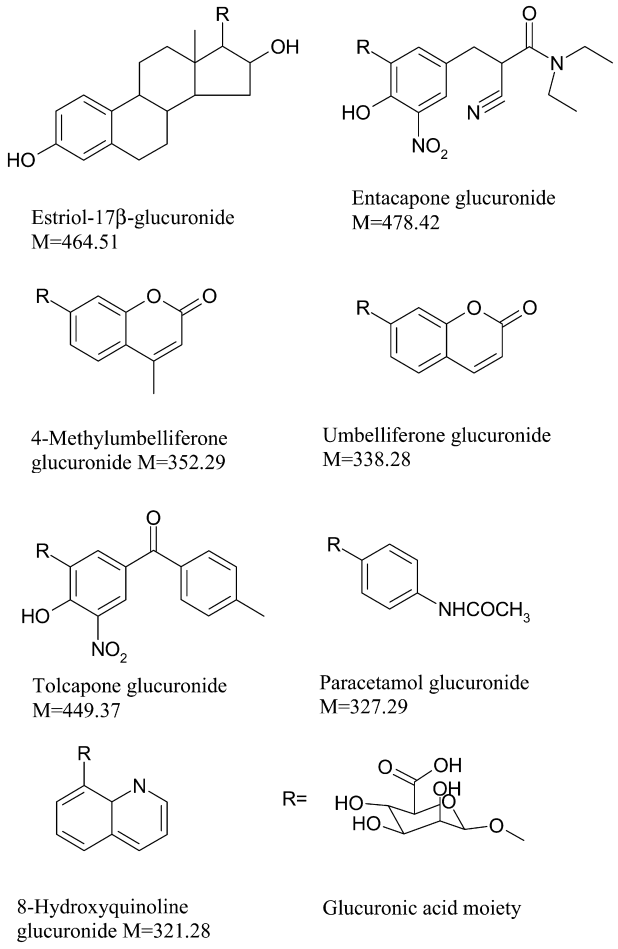

Fig. 1. Glucuronides studied. M, molecular weight (g/mol).

Orion Pharma (Espoo, Finland), and entacapone 3-*O*-glucuronide and tolcapone-3-*O*-glucuronide were synthesized at the Division of Pharmaceutical Chemistry (Faculty of Pharmacy, University of Helsinki) by a method described previously [14].

Disodium hydrogen phosphate dihydrate, magnesium chloride hexahydrate, perchloric acid (70–72%), and ammonium acetate were purchased from Merck (Darmstadt, Germany). Sodium dihydrogen phosphate dihydrate was obtained from Fluka Chemie (Buchs, Germany), PLC-grade methanol was obtained from J.T. Baker (Deventer, The Netherlands), and 98–100% formic acid was obtained from Sigma–Aldrich Chemie.

Human UGTs were cloned and expressed in baculovirus-infected insect cells as His-tagged proteins in our laboratory [15,16]. Protein concentrations were determined with the BCA Protein Assay Kit (Pierce Chemical, Rockford, IL, USA).

Determination of Cl_{int} (slope)

The different intermediate concentrations of substrates for incubations were prepared by dilution of a 25 mM stock solution of each substrate with buffer or dimethyl sulfoxide (DMSO) so that the final concentration of DMSO in the incubation solution (total volume 100 µl) was 2%. The final substrate concentrations in incubation mixtures were 100, 150, 200, 250, and 300 µM for paracetamol and either 0.25, 0.50, 0.75, 1.00, and 1.25 µM or 2.5, 5.0, 7.5, 10.0, and 12.5 µM for the other substrates. Substrate concentrations in the corresponding *n*-in-one incubations were the same.

Then 40 µl of 50 mM sodium phosphate buffer (pH 7.4) and 5 mM $MgCl_2$, 10 µl of 50 mM D-saccharic acid 1,4-lactone, and 20 µl of intermediate solution of each substrate or mixture of substrates were administered to a 96-well plate and mixed. The plate was cooled on ice before the addition of 20 µl UGT isoform (2.5 mg/ml protein). The reaction was started by adding 10 µl of 10 mM stock solution of UDPGA as quickly as possible and transferring the plate to a thermal bath at 37 °C. The incubation reaction was terminated after 60 min by the addition of 10 µl of 4 M perchloric acid and cooling on ice for 15 min, followed by centrifugation in a well plate centrifuge (Labofuge, Heraeus Sepatech, Germany) for 10 min at 2500 rpm. The samples were injected to LC/MS/MS either directly from the wells or after pooling single incubations together.

The LC instrument was an Agilent 1100 HPLC system equipped with a switching valve option (Agilent Technologies, Germany). The column was an endcapped reversed-phase Purospher STAR RP-18 column (55 × 4 mm i.d., particle size 3 µm) (Merck). The eluent flow of 1.5 ml/min was split postcolumn in a ratio of 1:16 before MS. The HPLC eluent system consisted of 0.1% aqueous formic acid (eluent A) and of 0.1% formic acid in MeOH (eluent B). The gradient profile was started with a linear gradient from 5 to 90% B in 3 min, followed by an isocratic step at 90% B for 1 min and eventually a linear gradient from 90% B back to the initial 5% B in 1 min. The column was equilibrated for 5 min before each analysis. The injection volume was 50 µl. To avoid contamination of the ion source, nonvolatile, early eluting buffer components were diverted to waste before mass analysis by diverting the first minute of the eluent flow to waste with a switching valve and flow at 1.5 ml/min (95:5 A:B) from an auxiliary pump (LKB 2150 HPLC pump, LKB Produkter, Bromma, Sweden).

Analyses were carried out with a Sciex API 3000 triple quadrupole mass spectrometer with a commercial turbo ionspray (Applied Biosystems, Canada). MS and MS/MS behavior of glucuronides and ion optics parameter optimization were examined using flow injection analysis via a syringe pump at a flow rate of 10 µl/min and 10 µM solutions (0.1% HCOOH water:MeOH 70:30) of single glucuronides. The main ion optics parameters—declustering potential (*DP*), collision energy (*CE*), and collision cell exit potential (*CXP*)—were determined for each multiple reaction monitoring (MRM) transition to find the best sensitivity.

The optimal parameters were $DP = 20$–40 V, $CE = 9$–30 V, and $CXP = 10$–15 V. The ion source was used without turbo gas or elevated temperature. All other parameters were the same as in the LC/MS/MS method described below.

In the LC/MS/MS method, all of the glucuronides were detected by positive ion MRM. The dwell time was 50 ms for each ion pair. The electrospray ionization (ESI) ionspray voltage was 5000 V. Nitrogen (Whatman 75-720 nitrogen generator) was used as the curtain, collision, and turbo gas. Compressed air (Atlas Copro air dryer, Wilrijk, Belgium) was used as a nebulizer gas. The flow rates of the curtain and nebulizer gases were 1.2 L/min. The turbo gas pressure and temperature were 75 bar and 350 °C, respectively. The data were collected with a Dell Optilex computer and were processed with PE Sciex Analyst 1.3 software.

Determination of kinetic parameters V_{max} and K_m

Kinetic parameters $V_{\max}$ and K_{m} were determined using optimized incubation conditions, and reactions were linear in terms of protein concentration and time. Enzyme assays (total volume 250 µl) contained 50 mM phosphate buffer (pH 7.4), 5 mM $MgCl_2$, 5 mM saccharolactone, 1 mM UDPGA, 1–50 µg UGT isoform, and substrates in concentrations ($n = 6$–8) ranging from $0.5 \times K_{\mathrm{m}}$ to $5 \times K_{\mathrm{m}}$. Reactions were performed at 37 °C. Incubation time varied, within a linear range, from 10 to 60 min. Reactions were terminated by the addition of 25 µl of 4 M perchloric acid. The reaction mixtures were centrifuged (5 min at 14,000 rpm, EBA 12, rotor 1412, Hettich, Tuttlingen, Germany), and the supernatants were analyzed by the Agilent 1100 HPLC system with UV 310 nm (entacapone glucuronide), fluorescence (4-methylumbelliferone glucuronide, umbelliferone glucuronide, $\lambda_{\mathrm{ex}} = 316$ nm, $\lambda_{\mathrm{em}} = 382$ nm) or MS detection (8-hydroxyquinoline glucuronide, method same as above). The quantitation was based on authentic reference standards. Entacapone glucuronide was eluted with isocratic 0.5% acetic acid:acrylonitrile (65:35) and a flow rate of 1.0 ml/min. The column was Hypersil BDS-C18 (150×4.6 mm, 5 µm particle size). 4-Methylumbelliferone glucuronide and umbelliferone glucuronide were analyzed isocratically with Chromolith SpeedROD RP-18e (50×4.6 mm) column. 4-Methylumbelliferone glucuronide was eluted with 50 mM phosphate buffer (pH 3.0):MeOH (80:20) and flow (2 ml/min), and umbelliferone glucuronide was eluted with 50 mM phosphate buffer (pH 3.0):MeOH (85:15) and flow (1.5 ml/min). The run time was 7–10 min in each case. Data analysis was performed by SigmaPlot Enzyme Kinetics Module 1.1S.

Results and discussion

Analysis

A fast linear gradient (3 min) and a short column with 3 µm particle size provided high sensitivity and fast partial separation of the seven glucuronides. Paracetamol and 8-hydroxyquinoline eluted concurrently but were separated by different MS/MS reactions. All of the glucuronides were eluted within 3.5 min, with total analysis time being 10 min (including the equilibration step). The LC method was robust, with repeatable peak shape after the analysis of hundreds of samples. Very good repeatability was obtained for the retention times, with the relative standard deviations (RSDs) being within 0.3–1% ($n = 90$) for all of the glucuronides. A faster analysis with a steeper gradient (2 min) was used at the beginning, but the robustness of the method was poor after a few dozen injections due to impaired chromatography.

ESI, rather than atmospheric chemical ionization, was chosen for analyte ionization because ESI is a more sensitive and softer ionization technique for the analysis of glucuronide conjugates [17]. All of the glucuronides produced an intense protonated molecule, which was chosen as precursor ion for positive ion MS/MS studies. All of the MS/MS spectra except that for estriol glucuronide showed abundant product ion formed by the cleavage of glucuronic acid moiety (Glu), $[M + H - Glu]^+$, which was chosen for the MRM. The MS/MS spectrum of estriol glucuronide showed more fragments, and the most intense product ions, $[M + H - H_2O]^+$ and $[M + H - H_2O - Glu]^+$, were monitored in MRM.

Table 1
Validation of the LC/MS/MS method

	Linearity (nM)	R	Limits of detection (nM)	Between-day repeatability (RSD %, $n = 4$) (250 nM)	Within-day repeatability (RSD %, $n = 6$)		
					25 nM	250 nM	1000 nM
Entacapone-3-*O*-glucuronide	10–2000	0.9990	0.5	3.4	6.5	5.3	4.6
Umbelliferone glucuronide	5–2000	0.9994	0.5	3.0	14.5	6.5	7.2
4-Methylumbelliferone glucuronide	10–2000	0.9984	0.5	6.0	12.3	6.7	8.1
Tolcapone-3-*O*-glucuronide	25–10,000	0.9976	1.0	3.0	3.7	2.7	5.1
Hydroxyquinoline glucuronide	10–2000	0.9980	0.5	6.6	6.8	3.4	5.2
Estriol-17β-glucuronide	10–5000	0.9984	5.0	12.7	7.0	5.1	4.6
Paracetamol glucuronide	10–2000	0.9981	0.5	8.2	13.1	10.4	5.7

Limits of detection by LC/MS/MS (Table 1) were less than 1 nM, and limits of quantitation were less than 2.5 nM for nearly all glucuronides. This is adequate sensitivity for metabolism studies. Good sensitivity was necessary because the concentrations of metabolites are low, especially for the substrates with very low K_m and V_{max} values. Furthermore, in *n*-in-one incubations, the initial substrate concentration levels must be low to avoid cross-effects.

Three calibration curves (2.5–250, 10–2000, and 1000–7500 nM) were prepared for the glucuronides. The correlation coefficient values (r) were greater than 0.995 and RSDs for individual points are less than 15%, indicating good linearity of the method. The within-day repeatability of the LC/MS/MS method was evaluated at three concentration levels (25, 250, and 1000 nM), and the between-day repeatability was evaluated at one concentration level (250 nM). RSDs in the within- and between-day experiments remained less than 15%, indicating acceptable precision of the analytical method (Table 1).

Cl_{int} values

The intrinsic clearance ($Cl_{int} = V_{max}/K_m$) is usually determined by estimating the enzyme kinetic parameters V_{max} and K_m from the Michaelis–Menten curve (Cl_{int}(M–M)). The Cl_{int} can also be determined as the slope of the linear part of the Michaelis–Menten fitting (Cl_{int}(slope)) if the substrate concentration is well below its K_m value. The use of the highly sensitive LC/MS/MS method enables Cl_{int}(slope) determination for several substrates simultaneously (*n*-in-one) because the cross-effects are expected to be minimal at very low concentrations. In the drug discovery phase, the determinations of Cl_{int}(slope) values must be fast. Therefore, incubation conditions in determination of Cl_{int}(slope) were not optimized separately for each experiment. On the other hand, it is impossible to select universal incubation parameters, such as substrate concentration, protein concentration, and incubation time, for all experiments because enzyme activities may vary by several orders of magnitude between different substrates.

In this study, the substrate concentrations were either 0.5–2.5 μM or 5–25 μM; these values, according to other studies in our laboratory, are less than the respective K_m values [18]. The consumption of the substrate that is controlled by incubation time and protein concentration should not exceed 10% because the Michaelis–Menten equation is based on the assumption that the substrate concentration is constant during the reaction. Because of this, the protein concentrations had to be well below the concentration of the substrate but still high enough to allow a detectable product formation. The incubation time is another critical parameter because the reaction rate as a function of the reaction time is linear only up to a certain time point and too long an incubation may result in underestimation of Cl_{int}. However, the incubation time had to be long enough for a detectable amount of metabolite to be formed. Thus, the incubation time in all experiments was 60 min.

The Cl_{int}(slope) values for all substrates were determined as the slope of the linear part of the plots of substrate concentration [S] versus glucuronidation rate (Fig. 2). The linearity of the plots was satisfactory, with the correlation coefficients (r^2) being equal to or above 0.94. The Cl_{int}(slope) values were compared with the Cl_{int}(M–M) values obtained by determining V_{max}/K_m from Michaelis–Menten curves (Table 2). The reactions followed Michaelis–Menten kinetics as evaluated on the basis of residual plots and standard deviations of the parameter estimates. The r^2 values were typically greater than 0.94 (Table 2). As an example, Fig. 3 presents Michaelis–Menten fitting for glucuronidation of entacapone. The correlation between Cl_{int}(slope) and Cl_{int}(M–M) values was very good (the variation was less than threefold) in cases where the substrate consumption in the reactions determining the Cl_{int}(slope) values was less than 10%. In cases where the substrate consumption was greater than 10%, the

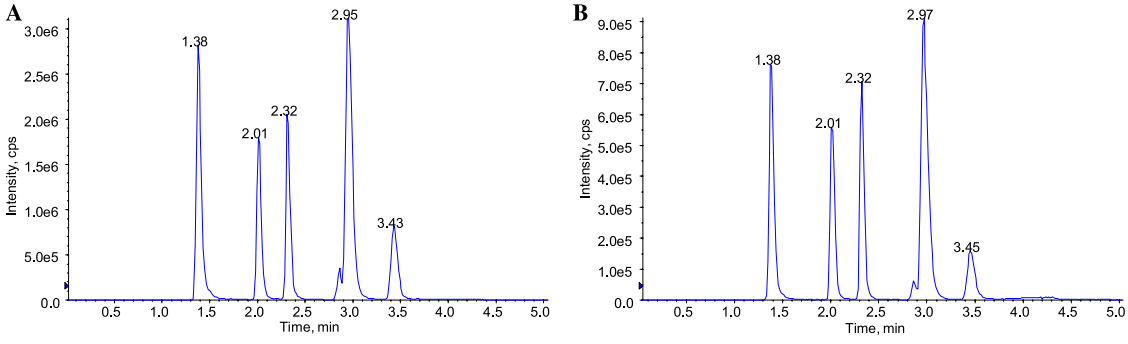

Fig. 2. Extracted ion chromatograms for samples from incubation with UGT 1A8 containing glucuronides of 8-hydroxyquinoline ($t_R = 1.3$ min, m/z 322 → 146), umbelliferone ($t_R = 2.0$ min, m/z 339 → 163), methylumbelliferone ($t_R = 2.3$ min, m/z 353 → 177), entacapone ($t_R = 2.9$ min, m/z 482 → 306), and tolcapone ($t_R = 3.4$ min, m/z 450 → 274). The initial substrate concentration was 15 μM, and the incubation time was 60 min. (A) All seven substrates incubated together as a mixture. (B) Substrates incubated separately and pooled together for analysis.

Table 2
Comparison between Cl_{int} (slope) values determined as slope of the linear portion of Michaelis–Menten curves and V_{max}/K_m calculated from kinetic parameters (V_{max} and K_m) determined from Michaelis-Menten fittings

Substrate	Enzyme	Michaelis–Menten parameters ($n = 3$)				Determination of Cl_{int} as slope of the linear part of Michaelis–Menten fitting			
		K_m (μM)	V_{max} (pmol/min/mg)	$V_{max}/K_m = Cl_{int}$ (M–M) (μl/min/mg)	R^2	Cl_{int} (slope) (μl/min/mg)	Intercept	R^2	Substrate consumption[a] (%)
4-Methylumbelliferone	1A1	115	459	4.0	0.974	2.63	+0.96	0.995	<10
Umbelliferone	1A1	294	462	1.6	0.919	2.87	–0.75	0.994	<10
Entacapone	1A3	259	622	2.40	0.981	2.58	+0.27	0.927	<10
8-Hydroxyquinoline	1A3	494	22	0.045	0.984	0.05	+0.03	0.984	<10
4-Methylumbelliferone	1A3	335	989	3.0	0.965	1.21	+0.02	0.996	<10
8-Hydroxyquinoline	1A6	6.5	705	108.0	0.990	9.03	+74.3	0.972	44
4-Methylumbelliferone	1A6	157	7870	50.0	0.995	9.23	+51.3	0.968	37
Entacapone	1A9	21	10,171	351.0	0.910	29.10	+2.37	0.999	100
8-Hydroxyquinoline	1A9	0.48	49	102.0	0.984	12.68	+0.41	0.987	35
4-Methylumbelliferone	1A9	18	1388	77.0	0.940	10.76	+3.15	0.974	42
Umbelliferone	1A9	111	2282	21.0	0.983	9.41	+2.26	0.956	30
8-Hydroxyquinoline	2B7	301	371	1.2	0.930	0.33	+0.28	0.987	<10
8-Hydroxyquinoline	2B15	16	33	2.1	0.884	0.31	+0.31	0.988	<10
4-Methylumbelliferone	2B15	149	40	0.27	0.936	0.071	+0.24	0.967	<10
Umbelliferone	2B15	339	25	0.074	0.970	0.032	+0.03	0.985	<10

[a] Approximate values for substrate consumptions are estimated from initial concentration of substrates and final concentration of glucuronides in the incubations.

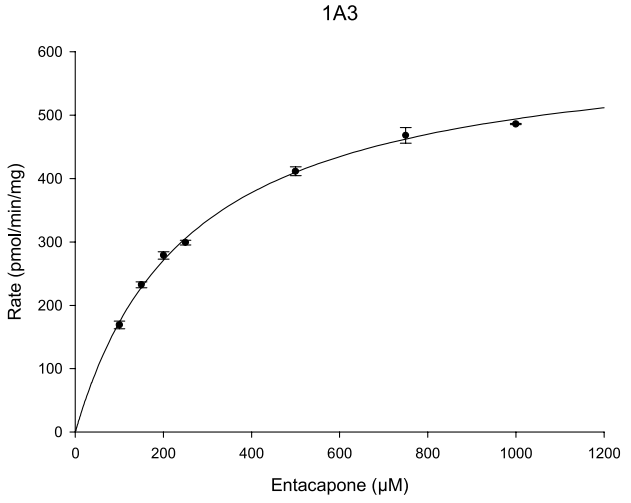

Fig. 3. Michaelis–Menten fitting of enzyme kinetics of entacapone glucuronidation by UGT 1A3.

Cl_{int}(slope) values were typically 1/5th to 1/20th of the Cl_{int}(M–M) values, showing that too high substrate consumption led to underestimation of Cl_{int} (Table 2). It may be noted here that in the determination of Cl_{int}(slope) values for 8-hydroxyquinoline with UGTs 1A6 and 1A9, the substrate concentrations (5–25 μM) were well above the K_m values (Table 2). This resulted in significantly reduced Cl_{int}(slope) values relative to the Cl_{int}(M–M) values. Interestingly, either too high substrate consumptions or too high substrate concentrations in the incubations were clearly recognized as higher intercept values in the plots of substrate concentration [S] versus glucuronidation rate V

Table 3
Cl_{int} (slope) values obtained from n-in-one (Cl_{int} (mix)) and single-compound (Cl_{int} (single)) incubations

Substrate	Enzyme	Cl_{int} (single) (μl/min/mg)	Cl_{int} (mix) (μl/min/mg)
Entacapone	1A3	2.58	4.10
8-Hydroxyquinoline	1A3	0.05	0.13
4-Methylumbelliferone	1A3	1.21	1.36
Tolcapone	1A3	43.60	53.65
Umbelliferone	1A3	0.45	0.50
8-Hydroxyquinoline	1A6	9.03	3.82
4-Methylumbelliferone	1A6	9.23	4.54
Tolcapone	1A6	0.83	0.99
Umbelliferone	1A6	9.66	3.43
Entacapone	1A7	32.90	11.55
8-Hydroxyquinoline	1A7	1.85	3.53
4-Methylumbelliferone	1A7	11.89	6.23
Tolcapone	1A7	28.75	33.71
Umbelliferone	1A7	11.03	7.67
Entacapone	1A8	10.45	5.25
8-Hydroxyquinoline	1A8	4.98	3.87
4-Methylumbelliferone	1A8	3.48	1.59
Tolcapone	1A8	6.65	7.43
Umbelliferone	1A8	2.63	2.15
Entacapone	1A9	29.10	35.01
8-Hydroxyquinoline	1A9	12.68	16.73
4-Methylumbelliferone	1A9	10.76	11.19
Paracetamol	1A9	0.006	n.d.
Tolcapone	1A9	42.37	33.65
Umbelliferone	1A9	9.41	7.72
Entacapone	1A10	30.24	19.35
8-Hydroxyquinoline	1A10	6.38	3.60
4-Methylumbelliferone	1A10	16.42	17.18
Paracetamol	1A10	0.075	0.025
Tolcapone	1A10	38.64	32.68
Umbelliferone	1A10	15.80	8.40

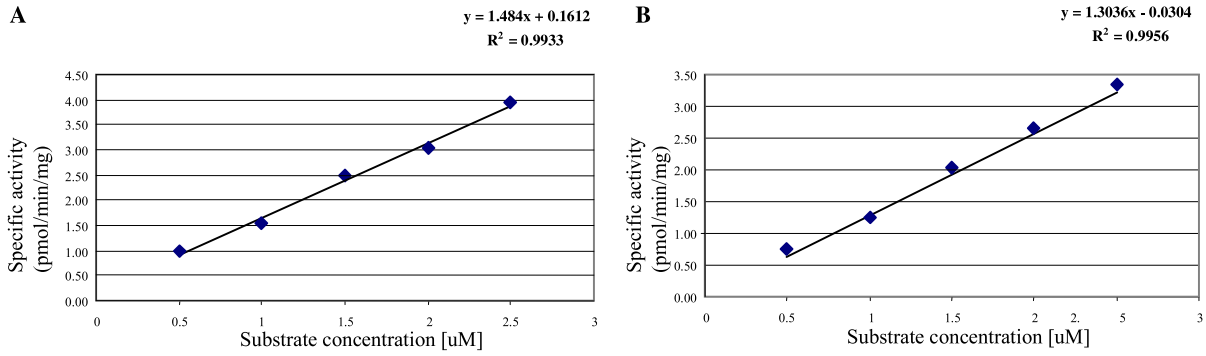

Fig. 4. Linear fittings of enzyme kinetics of 4-methylumbelliferone glucuronidation by UGT 1A3. (A) 4-Methylumbelliferone incubated in a mixture of seven substrates. (B) 4-Methylumbelliferone incubated separately and analyzed in a pooled mixture of substrates.

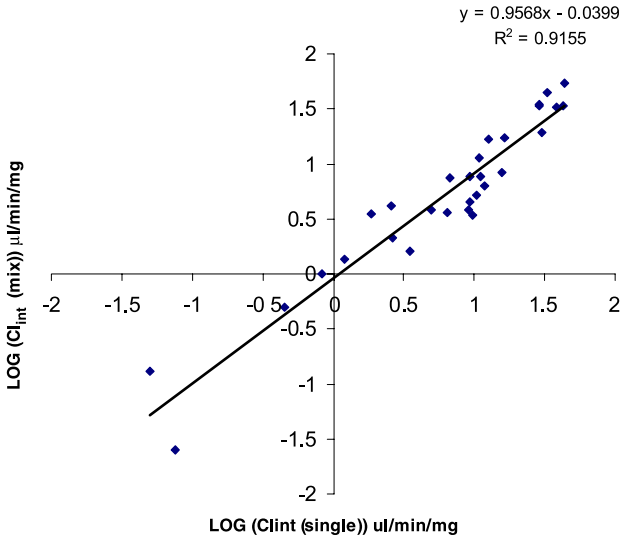

Fig. 5. Correlation between single (Cl_{int}(single)) and *n*-in-one (Cl_{int}(mix)) incubations of seven substrates with six isoenzymes.

(Table 2). Accordingly, the intercept value offers an indicator to estimate the authenticity of the experimental conditions, and in cases where the intercept is very high in proportion to the slope, the experiment should be repeated under acceptable experimental conditions.

Single-substrate versus n-in-one incubations

Our basic assumption was that if the substrate concentrations in the incubations are low enough, it should be possible to avoid cross-effects and determine Cl_{int}(slope) values using *n*-in-one incubations. To test this possibility, incubations were carried out using both a mixture of seven substrates and each substrate individually. The concentration of a substrate in the mixture was the same as its concentration in the single-compound incubations and well below the K_m values. The Cl_{int}(slope) values obtained from the mixture incubations correlated well ($r^2 = 0.9155$) with those obtained with the single-compound incubations (Table 3 and Figs. 4 and 5). The results do not give any indication of cross-effects between substrates in the *n*-in-one experiments. The deviations between single-compound and *n*-in-one experiments were within experimental errors. Thus, the results show that Cl_{int}(slope) values can be determined using the *n*-in-one experiments when the substrate concentrations are kept sufficiently low. This approach could significantly decrease the time needed for experiments to screen metabolic properties of new substrates in the early phase of drug discovery.

Conclusions

We have shown that Cl_{int} values determined as the slope (Cl_{int}(slope)) of the linear part of the Michaelis–Menten fitting correlated well with Cl_{int}(M–M) values determined as V_{max}/K_m from the Michaelis–Menten curve provided that the substrate consumptions in the reactions determining Cl_{int}(slope) values were less than 10% and the substrate concentrations were well below their K_m values. The good correlation between Cl_{int}(slope) values determined as single-substrate and *n*-in-one incubations shows that significant cross-effects do not occur in *n*-in-one experiments when the substrate concentrations in the mixture are low enough. The determination of Cl_{int}(slope) values by *n*-in-one experiments significantly reduces the time needed to screen metabolic behavior of compounds early in the discovery phase. However, the method requires highly sensitive and specific analytical techniques such as LC/MS/MS.

Acknowledgments

This work was supported by the National Technology Agency of Finland, Orion Pharma, Juvantia Pharma, and United Laboratories.

References

[1] R.A. Prentis, Y. Lis, S.R. Walker, Pharmaceutical innovation by the seven UK-owned pharmaceutical companies (1964–1985), Br. J. Clin. Pharmacol. 25 (1988) 387–396.

[2] D.J. Carlile, A.L. Stevens, E.I.L. Ashforth, D. Waghela, J.B. Houston, In vivo clearance of ethoxycoumarin and its prediction from in vitro systems: Use of drug depletion and metabolite formation methods in hepatic microsomes and isolated hepatocytes, Drug Metab. Dispos. 26 (1998) 216–221.

[3] R.S. Obach, J.B. Baxter, T.E. Liston, B.M. Silber, B.C. Jones, F. Macintyre, D.J. Rance, P. Wastall, Prediction of hepatic extraction ratio from in vitro measurement of intrinsic clearance, J. Pharmacol. Exp. Ther. 200 (1997) 420–424.

[4] R.H. Tukey, C.P. Strassburg, Human UDP-glucuronosyltransferases: expression and disease, Annu. Rev. Pharmacol. Toxicol. 40 (2000) 581–616.

[5] A. Radominska-Pandya, P.J. Czernik, J.M. Little, E. Battaglia, P.I. Mackenzie, Structural and functional studies of UDP-glucuronosyltransferases, Drug Metab. Rev. 31 (1999) 817–899.

[6] B. Burchell, D.W. Nebert, D.R. Nelson, K.W. Bock, T. Iyanagi, P.L. Jansen, D. Lancet, G.J. Mulder, J.R. Chowdhury, G. Siest, T.R. Tephly, P.I. Mackenzie, The UDP glucuronosyltransferase gene superfamily: suggested nomenclature based on evolutionary divergence, DNA Cell Biol. 10 (1991) 487–494.

[7] R.H. Tukey, C.P. Strassburg, Genetic multiplicity of the human UDP-glucuronosyltransferases and regulation in the gastrointestinal tract, Mol. Pharmacol. 59 (2001) 405–414.

[8] J.S. Janiszewski, K.J. Rogers, K.M. Whalen, M.J. Cole, T.E. Liston, E. Duchoslav, H.G. Fouda, A high-capacity LC/MS system for the bioanalysis of samples generated from plate-based metabolic screening, Anal. Chem. 73 (2001) 1495–1501.

[9] W.A. Korfmacher, C.A. Palmer, C. Nardo, K. Dunn-Meynell, D. Grotz, K. Cox, C. Lin, C. Elicone, C. Liu, E. Duchoslav, Development of an automated mass spectrometry system for the quantitative analysis of liver microsomal incubation samples: a tool for rapid screening of new compounds for metabolic stability, Rapid Commun. Mass Spectrom. 13 (1999) 901–907.

[10] P.J. Eddershaw, M. Dickins, Advances in in vitro drug metabolism screening, Pharm. Sci. Technol. Today 2 (1999) 13–19.

[11] H.Z. Bu, L. Magis, K. Knuth, P. Teitelbaum, High-throughput cytochrome P450 (CYP) inhibition screening via a cassette probe-dosing strategy: VI. Simultaneous evaluation of inhibition potential of drugs on human hepatic isoenzymes CYP2A6, 3A4, 2C9, 2D6, and 2E1, Rapid Commun. Mass Spectrom. 15 (2001) 741–748.

[12] S.A. Testino, G. Patoway, High-throughput inhibition screening of major human cytochrome P450 enzymes using an in vitro cocktail and liquid chromatography–tandem mass spectrometry, J. Pharm. Biomed. 30 (2003) 1459–1467.

[13] K.S. Hakala, L. Laitinen, A.M. Kaukonen, J. Hirvonen, R. Kostiainen, T. Kotiaho, Development of LC/MS/MS for cocktail dosed Caco-2 samples using atmospheric pressure photoionization and electrospray ionization, Anal. Chem. 75 (2003) 5969–5977.

[14] L. Luukkanen, I. Kilpelaeinen, H. Kangas, P. Ottoila, E. Elovaara, J. Taskinen, Enzyme-assisted synthesis and structural characterization of nitro-chatecol glucuronides, Bioconj. Chem. 10 (1999) 150–154.

[15] M. Kurkela, J.A. Garcia-Horsman, L. Luukkanen, S. Moersky, J. Taskinen, M. Baumann, R. Kostiainen, J. Hirvonen, M. Finel, Expression and characterization of recombinant human UPD-glucuronosyltransferases (UGTs), J. Biol. Chem. 278 (2003) 3536–3544.

[16] T. Kuuranne, M. Kurkela, M. Thevis, W. Schanzer, M. Finel, R. Kostiainen, Glucuronidation of anabolic androgenic steroids by recombinant human UPD-glucuronosyltransferases, Drug Metab. Dispos. 31 (2003) 1117–1124.

[17] H. Keski-Hynnilä, L. Luukkanen, J. Taskinen, R. Kostiainen, Mass spectrometric and tandem mass spectrometric behavior of nitrocatechol glucuronides: a comparison of atmospheric pressure chemical ionization and electrospray ionization, J. Am. Soc. Mass Spectrom. 10 (1999) 537–545.

[18] L. Luukkanen, J. Taskinen, M. Kurkela, R. Kostiainen, J. Hirvonen, M. Finel, Kinetic characterization of the 1A subfamily of recombinant human UDP-glucuronosyltransferases, Drug Metab. Dispos. (2005) submitted.

III

JPP Journal of Pharmacy and Pharmacology

JPP 2005, 57: 405–410

Received September 22, 2004
Accepted December 8, 2004
DOI 10.1211/0022357055678
ISSN 0022-3573

The stereoselective biotransformation of the anti-obesity drug sibutramine in rat liver microsomes and in primary cultures of rat hepatocytes

Marek Link, Romana Novotná, Bohumila Suchanová, Lenka Skálová, Vladimír Wsól and Barbora Szotáková

Abstract

Sibutramine is an anti-obesity drug sold as a racemic mixture under the trademark Meridia or Reductil. With the aim of evaluating the stereoselectivity in phase I of sibutramine biotransformation, the formation of the main metabolites from *R*-sibutramine, *S*-sibutramine and *rac*-sibutramine was studied in rat microsomes and primary cultures of hepatocytes. A novel analytical method for the determination of sibutramine and its phase I metabolites in culture medium and microsomal incubates using isocratic reversed-phase liquid chromatography with UV detection was developed. Only two metabolites, mono-desmethylsibutramine (M1) and di-desmethylsibutramine (M2), were found in the rat microsomes incubated with sibutramine and NADPH. The kinetics of M1 and M2 formation slightly differed depending on the enantiomeric form of the sibutramine used. The stereoselectivity in sibutramine biotransformation was much more evident in primary cultures of rat hepatocytes. While *R*-sibutramine incubation led to the formation of M1 and M2 metabolites only, the incubation of *S*-sibutramine or *rac*-sibutramine (to a lesser extent) resulted in four major metabolites (M1, M2, M3 and M4) and 2 or 3 minor metabolites. On the basis of our results, *R*-sibutramine might represent the more advantageous sibutramine enantiomer from the pharmacokinetic standpoint.

Department of Biochemical Sciences, Research Centre LN00B125, Faculty of Pharmacy, Charles University, Heyrovského 1203, CZ 50005 Hradec Králové, Czech Republic

Marek Link, Romana Novotná, Bohumila Suchanová, Lenka Skálová, Vladimír Wsól, Barbora Szotáková

Correspondence: B. Szotáková, Department of Biochemical Science, Faculty of Pharmacy, Charles University, Heyrovského 1203, Hradec Králové, CZ-500 05 Czech Republic.
E-mail: szotako@faf.cuni.cz

Acknowledgement and funding: The authors wish to thank Dr M. Kuchar for providing sibutramine enantiomers and Dr Radan Schiller for synthesis of *rac*-sibutramine and metabolites M1 and M2. The Ministry of Education, Youth and Sports of the Czech Republic, Research Centre LN00B125, supported this project.

Introduction

Nowadays, obesity represents a serious problem, especially in American and European populations. Pharmacotherapy in combination with a reduced calorie diet is recommended for obese patients as a multi-modal approach to weight loss. Sibutramine hydrochloride monohydrate represents one of the few established and well-proven agents available for treatment of obesity (Arterburn et al 2004; Ryan 2004). Sibutramine (*N*-{1-[1-(4-chlorophenyl)cyclobutyl]-3-methylbutyl}-*N*,*N*-dimethylamine) is a tertiary amine with one chiral centre. It is sold as a racemic mixture under the trade-name Meridia or Reductil. It acts as a monoamine-reuptake inhibitor. The weight loss of patients induced by sibutramine is thought to be due to a combination of serotonin- and noradrenaline (norepinephrine)-mediated mechanisms that increase both satiety and energy expenditure (Stock 1997; Heal et al 1998; Luque & Rey 1999).

In organisms sibutramine is rapidly demethylated to form metabolites M1 (*N*-{1-[1-(4-chlorophenyl)cyclobutyl]-3-methylbutyl}-*N*-methylamine) and M2 (1-[1-(4-chlorophenyl)cyclobutyl]-3-methylbutylamine). M1 and M2 undergo hydroxylation and conjugation to form inactive metabolites (Stock 1997; Hind et al 1999; Chen et al 2003). The pharmacological effects of sibutramine are mostly attributable to the M1 and M2 metabolites as these metabolites inhibit monoamine reuptake in-vitro more effectively than the parent drug (Connoley et al 1999). Sibutramine itself has several undesirable effects, the most problematic of which is increases in blood pressure and heart rate (Stock 1997). From this point of view, the M1 and M2 metabolites are considered to be safer than the parent compound (Glick et al 2000).

Sibutramine and both M1 and M2 metabolites are chiral compounds. The enantioselective pharmacodynamic profile of these enantiomers has been reported. The

R-enantiomers act as more potent monoamine reuptake inhibitors than the *S*-enantiomers (Glick et al 2000).

The aim of this study was to evaluate the stereoselectivity in phase I of sibutramine biotransformation in rat. The in-vitro formation of the main metabolites from *R*-sibutramine, *S*-sibutramine and *rac*-sibutramine were studied and compared. Primary cultures of rat hepatocytes and microsomal fraction of rat liver homogenates were used as model systems. A novel analytical method for determination of sibutramine and its phase I metabolites in culture medium and microsomal incubates, using isocratic reversed-phase liquid chromatography with UV detection, was developed.

Materials and Methods

Chemicals

Sibutramine hydrochloride, desmethylsibutramine hydrochloride (metabolite M1) and didesmethylsibutramine hydrochloride (metabolite M2) were prepared as racemic mixture using the experimental procedure according to Jeffery et al (1996) at the Department of Organic chemistry, Faculty of Pharmacy (Hradec Králové, Czech Republic). *R*- and *S*-sibutramine hydrochloride enantiomers (purity ≥ 99%) were obtained from the Research Institute for Pharmacy and Biochemistry (Prague, Czech Republic). Ethyl acetate and toluene for extraction (liquid chromatography grade), acetonitrile and methanol (all of the purity grade for LC) were obtained from Merck (Darmstadt, Germany). All other chemicals were analytical grade.

Animals

Male Wistar rats (10–12 weeks) were obtained from BioTest (Konárovice, Czech Republic). They were kept on standard rat chow with free access to tap water, in animal quarters under a 12-h light–dark cycle. The rats were cared for and used in accordance with the Guide for the Care and Use of Laboratory Animals (Protection of Animals from Cruelty Act, no. 246/92, Czech Republic). The ethical committee approval no. 28999/2001-30 for the study is deposited at the Ministry of Education, Youth and Sports of the Czech Republic.

Isolation of microsomal fraction

Livers of 6 male Wistar rats (10–12 weeks) were used as the source of microsomes. The microsomal fractions were prepared by a procedure described by Gillette (1971) with slight modification (Szotáková et al 2004). The protein content was determined by the bicinchoninic acid method (Smith et al 1985).

Isolation of hepatocytes

Hepatocytes were obtained from the livers of 6 male rats by a two-step collagenase method (Berry et al 1991) and the isolated hepatocytes were mixed together. Three million viable (85–90%) cells in 3 mL of culture medium were placed into 60-mm plastic dishes pre-coated with collagen as described elsewhere (Szotáková et al 2004). The cultures were kept at 37°C in an atmosphere of humid air with 5% CO_2.

Incubation of microsomal fraction with *R*-, *S*- and racemic sibutramine

The stock solutions (3 mM) of each substrate and NADPH were prepared by dissolving the corresponding amount of salt in re-distilled water. The other solutions of the substrates were prepared by diluting the stock solution with water. The reaction mixture consisted of 50 μL microsomal fraction (0.1 mg of proteins/mL), 100 μL NADPH (final concentration 1 mM), 100 μL substrate (final concentration 0.01–1 mM) and 50 μL 0.1 M sodium phosphate buffer, pH 7.4. The total volume of the reaction mixture was 300 μL. The standard incubation lasted 20 min. All the incubations were performed at 37°C. The reaction was stopped by alkalization and cooling in ice.

Incubation of hepatocytes primary culture with *R*-, *S*- and racemic sibutramine

The stock solutions (3 mM of the substrates in water) were added into a fresh culture medium. The concentration of water in culture medium did not exceed 3% (v/v). Hepatocyte monolayers (18–24 h after isolation) were incubated with substrates at 37°C in an atmosphere of humid air with 5% CO_2. The kinetic study was performed with substrate concentrations of 10, 20, 35 and 50 μM, and the incubation lasted 4 h. In the time-dependence study, 35 μM substrate was used and 0.5-mL samples of medium were collected at intervals of 1, 2, 4 and 8 h. The medium samples were stored frozen at −80°C before their extraction.

Cytotoxicity assay

Cytotoxicity was assayed using the MTT (dimethylthiazol diphenyl tetrazolium bromide) test as described by Denizat & Lang (1986). The cells seeded in 96-well plates were incubated with the substrate at various concentrations (5–70 μM) for 8 h. The absorbance of formazan at 595 nm in the cells treated with substrate was compared with that in control cells exposed to medium with 3% v/v water alone.

Extraction

Before the extraction procedure, the pH of sibutramine incubates was adjusted. The best recovery of metabolites from the culture medium and microsomal incubates (approx. 80% and 94%, respectively) was obtained after alkalization of samples with sodium hydroxide (0.1 M) to pH 9.6–9.7.

All the incubates were extracted twice with double volumes of ethyl acetate. The extracts were pooled and evaporated to dryness using a rotary vacuum concentrator

Eppendorf 5301 at 30°C. The dry samples were dissolved in the mobile phase prior to the injection in HPLC apparatus.

Chromatography conditions

The HPLC analyses of sibutramine and its metabolites, M1 and M2, were performed on an Agilent technologies 1100 series liquid chromatograph with a diode array detector. The chromatographic separation was performed using a Zorbax Eclipse XDB-C8 column, 4.6×150 mm with 5 μm particles (Agilent Technologies, USA). The mobile phase consisted of ammonium phosphate buffer (20 mM, pH 6.0 adjusted with phosphoric acid)–acetonitrile–methanol (42:22:36 v/v/v), the flow rate was 1.5 mL min^{-1}, temperature 25°C and detection wavelength 223 nm.

Identification of metabolites of sibutramine

The metabolites M1 and M2 were collected separately into glass test tubes after chromatographic separation using the conditions described above. After basification with sodium hydroxide, the analytes were extracted twice with double volumes of toluene. The extracts were pooled and evaporated to dryness. The residue was dissolved in a mixture of water–methanol (2:3 v/v) and analysed using an LCQ Advantage mass spectrometer (ThermoFinnigan, USA). The samples were injected into the ion source (ESI) using a 250-μL syringe and positive ion mass spectra, MS and MS/MS, were recorded.

Statistical analysis

The differences in the biological properties of the individual compounds were statistically determined using a one-way analysis of variance in conjunction with a Dunnett's post-hoc test.

Results

HPLC method

An analytical column with high pure silica gel and end-capped stationary phase Zorbax Eclipse XDB-C8 was chosen to avoid the peak-tailing problem due to the basic character of sibutramine and its metabolites. It was found that the resolution of the metabolites strongly depended on the pH of the buffer and an accuracy of pH 6.00 ± 0.05 was necessary. The retention time of sibutramine, M1, M2, M3 and M4 was 31.0, 7.7, 9.1, 4.4 and 6.1 min, respectively.

Incubation of microsomal fraction with *R*-, *S*- and *rac*-sibutramine

The rat hepatic microsomes were incubated with substrate (*rac*-sibutramine, *R*-sibutramine or *S*-sibutramine) and coenzyme NADPH. The metabolites M1 and M2 were found to be the only biotransformation products of sibutramine in rat microsomes. The kinetics of M1 and M2 formation was studied within the substrate concentration range of 0.01–1.0 mM. A blank sample was analysed simultaneously and no peak interfering with sibutramine and its metabolites was found.

Figure 1A demonstrates the plots of rate of M1 formation vs substrate concentration. Detailed analysis showed that the data are described better by a sigmoidal dose–response curve rather than by the Michaelis–Menten equation. The apparent kinetic parameters for microsomal M1 formation and intrinsic clearance were calculated

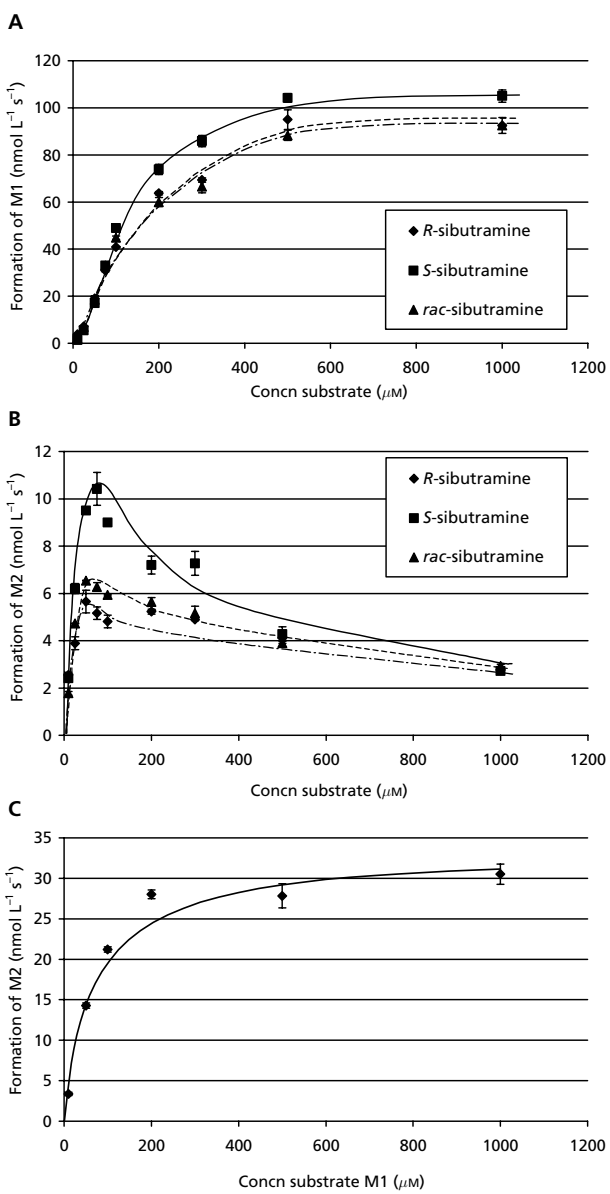

Figure 1 Velocity of formation of metabolites, depending on substrate concentration, in rat microsomes. Formation of M1 from *R*-, *S*- or *rac*-sibutramine (A), formation of M2 from *R*-, *S*- or *rac*-sibutramine (B), formation of M2 from M1 (C).

Table 1 Apparent kinetic parameters for M1 and M2 formation from *R*-, *S*-, *rac*-sibutramine and for M2 formation from *rac*-M1 in rat hepatic microsomes

Substrate	K_m' ± s.d. (μmol L^{-1})		V_{max}' ± s.d. (μmol L^{-1} s^{-1})		Cl_{int} (10^{-4} s^{-1})	
	M1	M2	M1	M2	M1	M2
R-Sibutramine	173.1 ± 35.48	25.5 ± 9.7	0.118 ± 0.009*	0.008 ± 0.001*	6.8	3.1
S-Sibutramine	171.0 ± 45.08	49.6 ± 17.0	0.134 ± 0.003*	0.018 ± 0.003*	7.8	3.7
rac-Sibutramine	167.1 ± 28.07	54.9 ± 25.0	0.114 ± 0.007	0.014 ± 0.004	6.8	2.6
rac-M1	—	57.6 ± 10.5	—	0.033 ± 0.001	—	5.7

Each value represents the mean ± s.d. of three independent experiments (n = 3). The microsomes were obtained from livers of six rats. *$P \leq 0.05$ in *R*- vs *S*-enantiomer.

using software GraphPad Prism version 3.00 (1999; GraphPad Software Inc., San Diego CA); the data are presented in Table 1. No significant differences in K_m' between sibutramine enantiomers were observed. On the other hand, microsomal enzymes displayed slightly, but significantly ($P < 0.05$), higher V_{max}' for *S*-sibutramine as compared with *R*- or *rac*-sibutramine.

The plots of the rate of M2 formation vs sibutramine concentration are shown in Figure 1B. The curves obtained were non-hyperbolic. At low sibutramine concentration, the velocity of M2 formation linearly increased with increasing concentration of sibutramine to reach the maximum, and then it decreased with increasing sibutramine concentration. When M1 was used as the substrate instead of sibutramine, the plots of M2 formation approached the classical hyperbolic curve (Figure 1C). The apparent kinetic parameters for microsomal M2 formation calculated are presented in Table 1. Microsomal enzymes displayed significantly higher values of K_m' and V_{max}' for *S*-sibutramine than for *R*-sibutramine. When M1 was used as the substrate instead of sibutramine, a significantly higher value of V_{max}' was found. Intrinsic clearance was not affected by enantiomeric form of sibutramine.

Incubation of hepatocytes with *R*-, *S*- and racemic sibutramine

Before the biotransformation study, the cytotoxicity of sibutramine in primary cultures of rat hepatocytes was assayed using the MTT test. No significant decrease in the viability of cells caused by *R*-, *S*- or *rac*-sibutramine was observed up to a concentration of 50 μM.

The time and concentration dependence of phase I biotransformation of *R*-, *S*- and *rac*-sibutramine was studied in hepatocytes. When *R*-sibutramine was used as the substrate, M1 and M2 represented the only main metabolites in the culture medium. In addition to M1 and M2, two other major metabolites (denoted as M3 and M4) and 2 or 3 minor metabolites were found as biotransformation products of *S*- and *rac*-sibutramine. By means of mass spectroscopy, M3 ($Mr = 267\ g\ mol^{-1}$) was identified as a hydroxy derivative of M2. The precise position of the OH-group in M3 is not yet known, and also the structure of M4 ($Mr = 309\ g\ mol^{-1}$) is under study. M1 and M2 were quantified using calibration curves of standards. The area under the peak was used for semi-quantification of the metabolites M3 and M4 as no standards were available.

The time dependence of formation of metabolites M1, M2, M3 and M4 is presented in Figure 2. The concentration of active metabolites M1 and M2 increased with incubation time and culminated in 2 and 4 h, respectively. A longer time of incubation led to lowering of the concentrations of these metabolites in the medium. When *S*-sibutramine was used as the substrate, the concentration of active metabolites M1 and M2 after 8 h incubation was significantly lower than when *R*- and *rac*-sibutramine were used. While the production of M4 metabolite also culminated in 2 h, the concentration of M3 increased until the end of the incubation (8 h).

The concentration dependence of formation of metabolites was tested using a concentration range of substrates 0–50 μM. No significant differences in M1 and M2 kinetics between the enantiomeric forms of sibutramine used were observed (data not shown). The results of the kinetic study of M3 and M4 formation are presented in Figure 3. Both metabolites were formed only when *S*-sibutramine or *rac*-sibutramine were used as the substrate. While the curves obtained for M3 metabolite corresponded to Michaelis–Menten kinetics (Figure 3A), those obtained for M4 metabolite corresponded to the sigmoidal dose–response kinetics (Figure 3B), which can be explained either by the dimeric form of the respective native biotransformation enzyme or by the fact that M4 is formed by participation of more than one biotransformation enzyme.

Discussion

Sibutramine is a chiral drug administered as the racemate. When the effectiveness of the enantiomers of sibutramine and its main metabolites was compared, the stereoselectivity in biological activity was reported (Glick et al 2000). This study of the biotransformation of sibutramine enantiomers was initiated with the aim of evaluating the stereoselectivity in sibutramine metabolism. Primary cultures of rat hepatocytes and rat liver microsomes were used as model systems. At the beginning of the study, it was necessary to develop appropriate analytical methods for

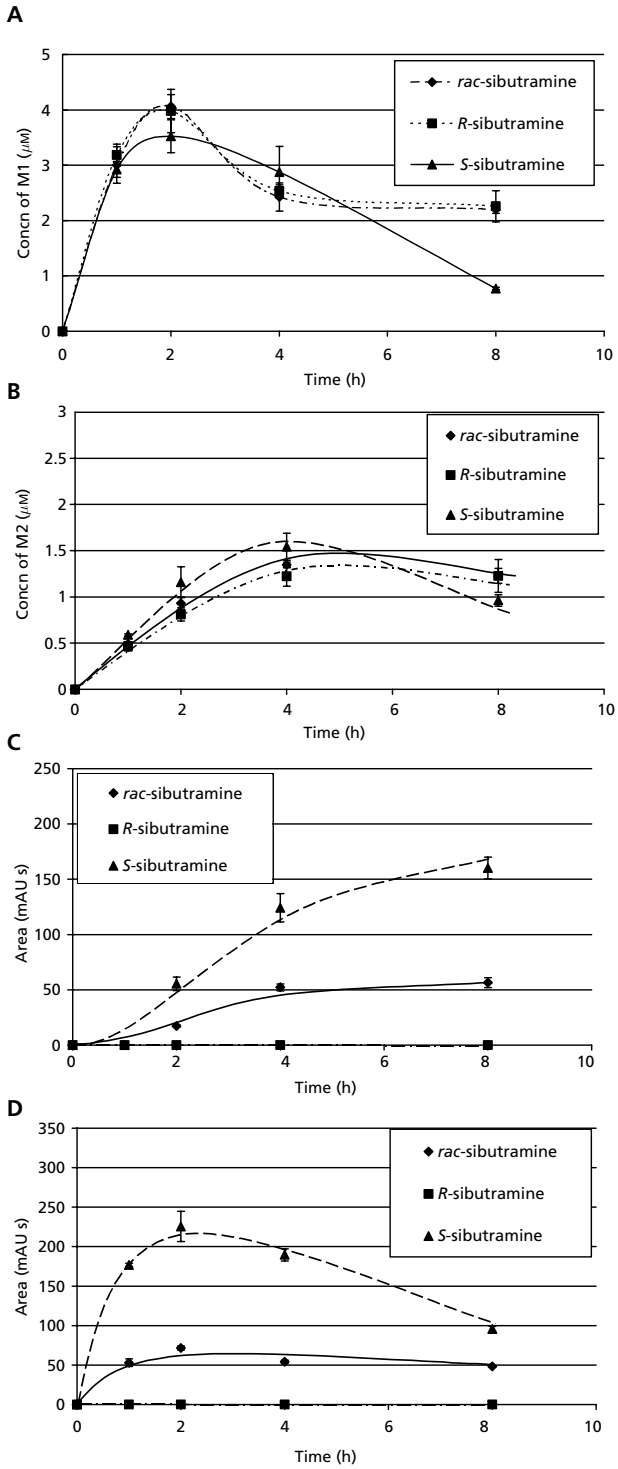

Figure 2 Time dependence of formation of M1 (A), M2 (B), M3 (C) and M4 (D) from *R*-, *S*- or *rac*-sibutramine in primary cultures of rat hepatocytes.

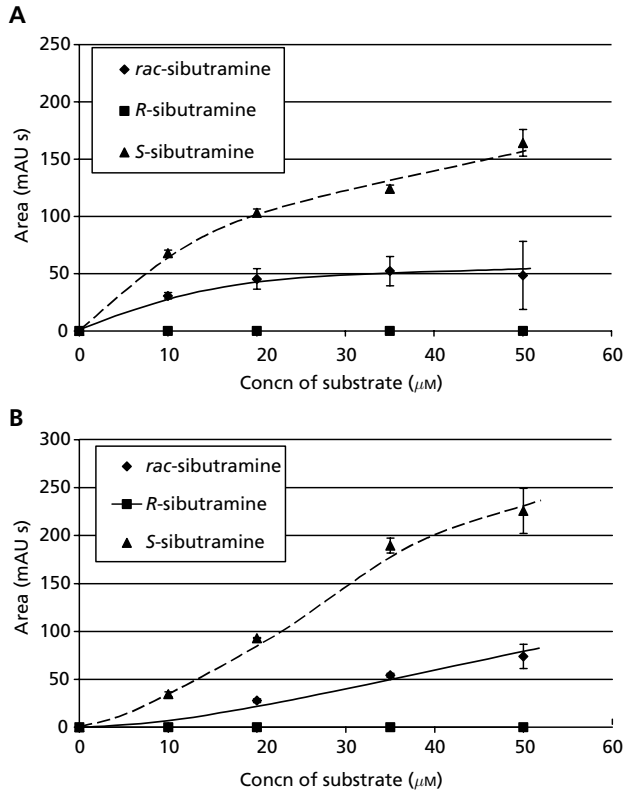

Figure 3 Concentration dependence of formation of M3 (A) and M4 (B) from *R*-, *S*- or *rac*-sibutramine in primary cultures of rat hepatocytes.

separation and quantification of sibutramine and its metabolites. The methods previously reported (Radhakrishna et al 2000; Chen et al 2003; Ding et al 2003) were not suitable for an in-vitro biotransformation study. The novel method described herein allows the separation and quantification of sibutramine and its phase I metabolites in culture medium and microsomal incubates.

Only two metabolites, M1 (desmethylated sibutramine) and M2 (didesmethylated sibutramine), were detected in incubates of sibutramine with microsomes and NADPH regardless of the enantiomeric form of substrate used. Sibutramine acted as an inhibitor of the enzyme, which catalysed M2 formation from M1. On the other hand, pronounced stereoselectivity of sibutramine biotransformation was found in primary cultures of rat hepatocytes. While *R*-sibutramine incubation led to formation of two main metabolites (M1 and M2) only, incubation of *S*-sibutramine or *rac*-sibutramine (to a lesser extent) resulted in four major metabolites (M1, M2, M3 and M4) and 2 or 3 minor metabolites. On the basis of these results, *R*-sibutramine could be considered as being the enantiomer with less extensive biotransformation than the *S*-enantiomer by rat hepatocytes in-vitro. Lower biotransformation might mean slower deactivation and a lower risk of drug–drug interactions and inter-individual variability. Moreover, both *R*-desmethylsibutramine and *R*-didesmethylsibutramine were clearly more potent in depressing food intake and decreasing body weight than the *S*-enantiomers (Glick et al 2000). Thus, *R*-sibutramine might represent the more advantageous sibutramine enantiomer from a pharmacokinetic as well as a pharmacodynamic point of view. The results

obtained in rat should be considered as preliminary with respect to well-known inter-species differences in activity, stereoselectivity and stereospecificity of biotransformation enzymes. Our results presented here seem to be so promising that a biotransformation study of sibutramine using human samples should be initiated.

Conclusion

This biotransformation study of the new anti-obesity drug sibutramine in rat liver microsomes and in primary cultures of rat hepatocytes indicates that the phase I metabolism of sibutramine is stereoselective. In hepatocytes, *R*-sibutramine incubation led to formation of M1 and M2 metabolites only (as well as in microsomes); incubation of *S*-sibutramine resulted in four major metabolites (M1, M2, M3 and M4). Lower biotransformation of *R*-sibutramine, together with its higher effectiveness in depressing food intake and decreasing body weight (Glick et al 2000), could make this enantiomer more advantageous.

References

Arterburn, D. E., Crane, P. K., Veenstra, D. L. (2004) The efficacy and safety of sibutramine for weight loss. A systematic review. *Arch. Intern. Med.* **9**: 994–1003

Berry, M. N., Edwards, A. M., Barritt, G. J. (1991) Isolated hepatocytes – preparation, properties and applications. In: van der Vliet, P. C., Pillai, S. (eds) *Laboratory techniques in biochemistry and molecular biology*. Elsevier Science, Amsterdam, pp 1–470

Chen, J., Lu, W., Zhang, Q., Jiang, X. (2003) Determination of the active metabolite of sibutramine by liquid chromatography-electrospray ionization mass spectrometry. *J. Chromatogr. B* **785**: 197–203

Connoley, I. P., Liu, Y. L., Frost, I., Reckless, I., Heal, D. J., Stock, M. J. (1999) Thermogenic effects of sibutramine and its metabolites. *Br. J. Pharmacol.* **126**: 1487–1495

Denizat, F., Lang, R. (1986) Rapid colorimetric assay for cell growth and survival. *J. Immunol. Methods* **89**: 271–277

Ding, L., Hao, X., Huang, X., Zhang, S. (2003) Simultaneous determination of sibutramine and its N-desmethyl metabolites in human plasma by liquid chromatography-electrospray ionization-mass spectrometry. Methods and clinical application. *Anal. Chim. Acta* **492**: 241–248

Gillette, J. R. (1971) Techniques for studying drug metabolism in vitro. In: La Du, B. N., Mandel, H. G., Way, E. L. (eds) *Fundamentals of drug metabolism and drug disposition*. The Williams and Wilkins Company, Baltimore, pp 400–418

Glick, S. D., Haskew, R. E., Maisonneuve, M. (2000) Enantioselective behavioral effects of sibutramine metabolites. *Eur. J. Pharmacol.* **397**: 93–102

Heal, D. J., Aspley, S., Prow, M. R., Jackson, H. C., Martin, K. F., Cheetham, S. C. (1998) Sibutramine: a novel anti-obesity drug. A review of the pharmacological evidence to differentiate it from D-amphetamine and D-fenfluramine. *Int. J. Obesity* **22**: S18–S28

Hind, I. D., Mangham, J. E., Ghani, S. P. (1999) Sibutramine pharmacokinetics in young and elderly healthy subjects. *Eur. J. Clin. Pharmacol.* **54**: 847–849

Jeffery, J. E., Kerrigan, F., Miller, T. K., Smith, G. J., Tometzki, G. B. (1996) Synthesis of sibutramine, a novel cyclobutylalkylamine useful in the treatment of obesity, and its major human metabolites. *J. Chem. Soc. Perkin Trans.* **1**: 2583–2590

Luque, C. A., Rey, J. A. (1999) Sibutramine: a serotonin-norepinephrine reuptake inhibitor for the treatment of obesity. *Ann. Pharmacother.* **33**: 968–978

Radhakrishna, T., Narayana, C. L., Rao, D. S., Vyas, K., Reddy, G. O. (2000) LC method for determination of assay and purity of sibutramine hydrochloride and its enantiomers by chiral chromatography. *J. Pharm. Biomed. Anal.* **22**: 627–639

Ryan, D. H. (2004) Clinical use of sibutramine. *Drugs Today* **40**: 41–54

Smith, P. K., Krohn, R. I., Hermanson, G. T., Mallia, A. K., Gartner, M. D., Provenzano, M. D., Fujimoto, E. K., Goeke, N. M., Olson, B. J., Klenk, D. C. (1985) Measurement of protein using bicinchoninic acid. *Anal. Biochem.* **150**: 76–85

Stock, M. J. (1997) Sibutramine: a review of the pharmacology of a novel anti-obesity agent. *Int. J. Obesity* **21**: S25–S29

Szotáková, B., Skálová, L., Baliharová, V., Dvorščáková, M., Štorkánová, L., Šišpera, L., Wsól, V. (2004) Characterization of enzymes responsible for biotransformation of the new anti-leukotrienic drug quinlukast in rat liver microsomes and in primary cultures of rat hepatocytes. *J. Pharm. Pharmacol.* **56**: 205–212

IV

Available online at www.sciencedirect.com
SCIENCE DIRECT
Analytica Chimica Acta 573–574 (2006) 273–283
ANALYTICA CHIMICA ACTA
www.elsevier.com/locate/aca

Liquid chromatography–tandem mass spectrometry in chiral study of amlodipine biotransformation in rat hepatocytes

Bohumila Suchanova, Ludek Sispera, Vladimir Wsol *

Department of Biochemical Sciences, Faculty of Pharmacy in Hradec Kralove, Charles University in Prague, Heyrovskeho 1203, CZ-500 05 Hradec Kralove, Czech Republic

Received 29 November 2005; received in revised form 17 May 2006; accepted 22 May 2006
Available online 2 June 2006

Abstract

A high proportion of drugs are chiral compounds used as racemic mixtures in a clinical practice. Very often only one of two enantiomers exhibits a desired pharmacological effect. Amlodipine, 2-[(2-aminoethoxy)methyl]-4-(2-chlorophenyl)-3-ethoxycarbonyl-5-methoxycarbonyl-6-methyl-1,4-dihydropyridine, is a chiral calcium channel blocker, currently used as a racemate in clinical practice. Racemic mixture is used even though it is known that *R*- and *S*-amlodipine do not have the same biological activity and only *S*-amlodipine possesses vasodilating properties.

In this work a novel reversed phase liquid chromatography (RP-LC) separation method for amlodipine and its metabolites was developed. Based on this separation chiral aspects of amlodipine biotransformation were studied by incubation of amlodipine and its two individual enantiomers with primary culture of rat hepatocytes. Structure of the metabolites was elucidated using a liquid chromatography (LC) separation with ultraviolet (UV) and mass spectrometry (MS) detection. An LC–tandem MS (MS/MS) method was used to establish fragmentation pattern of amlodipine and its metabolites. Eight metabolites presented in the highest amount were identified and semiquantified by employing an LC separation. Basically two types of metabolites were detected, reduced type – dihydropyridine metabolites and oxidized type – pyridine metabolites. Other metabolic modification included changes of functional groups, e.g., methylester hydrolysis or acetylation of amino group. The results exhibited that *R*-amlodipine was stereoselectively metabolized by the respective biotransformation enzymes in rat liver hepatocytes and it is also demonstrated by greater extent of *R*-amlodipine conversion into metabolites where the values for *R*-amlodipine are for the most metabolites higher than those for metabolites of *S*-amlodipine.

Keywords: Liquid chromatography–tandem mass spectrometry; Data dependent acquisition; Amlodipine; Stereoselective metabolism; In vitro; Chiral switching

1. Introduction

Chirality is one of the main features of biology, and many processes essential for life are stereospecific, meaning that one of two isomers may work best in a particular physiological situation. Because living systems themselves are chiral, each of the enantiomers of a chiral drug can behave very differently *in vivo*. Approximately 50% of marketed drugs are chiral, and of these approximately 50% are mixtures of enantiomers rather than single enantiomers. The enantiomers of a chiral drug may differ significantly in their bioavailability, rate of metabolism, metabolites, excretion, potency and selectivity for receptors, transporters and/or enzymes, and toxicity. The use of single enantiomer drugs can potentially lead to simpler and more selective pharmacologic profiles, improved therapeutic indices, simpler pharmacokinetics due to different rates of metabolism of the different enantiomers, and decreased drug interactions. For example, one enantiomer may be responsible for therapeutic effects of a drug whereas the other enantiomer is inactive or/and contributes to undesirable effects. In such case, use of the single enantiomer would provide a superior medication and should be preferred over the racemic form of the drug [1–3]. This can be demonstrated in case of citalopram, where escitalopram has been shown to have greater efficacy in non-clinical experiments than equivalent doses of citalopram, which is attributed to a counteracting effect of the *R*-enantiomer on the *S*-enantiomer [4].

Chirality has emerged as a key issue in drug design, discovery and development. Chiral switches are drugs that are already approved and claimed as racemates but that have been redevel-

* Corresponding author. Tel.: +420 495067370; fax: +429 495512665.
E-mail address: vladimir.wsol@faf.cuni.cz (V. Wsol).

0003-2670/$ – see front matter © 2006 Elsevier B.V. All rights reserved.
doi:10.1016/j.aca.2006.05.065

oped as single enantiomers. The issues of intellectual property involved in chiral switches are by no means straightforward, and the legal picture of patentability in a chiral switch scenario is far from being unequivocal [5]. The principle of switching from a racemate to an active isomer can be extended to replacement of a drug with an active metabolite, and, ideally, the more active metabolite. A recent example of such a switch is the substitution of terfenadine with its active metabolite fexofenadine, which retains the antihistaminic activity of the parent drug but is virtually devoid of cardiac side-effects. A powerful stimulus for chiral switching is the fact that many blockbuster drugs have been developed and licensed as racemate, and their substitution with single isomers could be seen as an ideal way of extending patent franchise and protecting against generic competition with racemate. Thus a well-timed chiral switch can offer enhanced therapy and further profitability as a line extension of major racemic drug with patents that are expiring. There are now several examples of successful chiral switches, e.g. omeprazol to esomeprazol, albuterol to levalbuterol, bupivacaine to levobupivacaine, citalopram to escitalopram as well as examples of failed chiral switches fenfluramine to dexfenfluramine or aborted chiral switch of fluoxetine [6–8].

On the other side most new drugs are marketed as single enantiomers but many older agents are still available in racemic form. As these drugs reach the end of their patent life manufacturers become interested in marketing single enantiomer equivalents. It has been claimed that it will bring clinical benefits in terms of improved efficacy, more predictable pharmacokinetics or reduced toxicity. According to another opinion claims of increased efficacy were based on comparisons of non-equivalent doses and any advantages seemed small and clinically unimportant. Authors have predicted that although chiral switching has not been a success for scientific medicine, it has been a success for scientific marketing and prices for racemates will decrease further, but enantiomer prices will remain high because of patent protection and perception of superiority based more on promotion than on real advantages [9].

Amlodipine, (*R*,*S*)-2-[(2-aminoethoxy)methyl]-4-(2-chlorophenyl)-3-ethoxycarbonyl-5-methoxycarbonyl-6-methyl-1,4-dihydropyridine (AML) (Fig. 1) is a chiral dihydropyridine calcium channel blocker used in therapy of hypertension and ischemic heart disease. *In vitro* studies have suggested that the dihydropyridine calcium antagonists act as antioxidants by directly quenching several radical species and that AML reduces leukocyte-induced oxidation of low-density lipoproteins (LDL) [10]. Further, in human fibroblasts, AML can modulate the expression of hydroxymethylglutaryl-coenzyme A (HMG-CoA) reductase and LDL receptors genes. AML has been shown to modulate many of the biochemical events involved in vascular hypertrophy and therefore to interfere with the mechanism involved in hypertension and atherosclerosis [11]. Moreover, AML has a capability to inhibit binding of the oxidized LDL lipids as a result of its high lipophilicity and positively charged amino group (pK_a 9.02) [12].

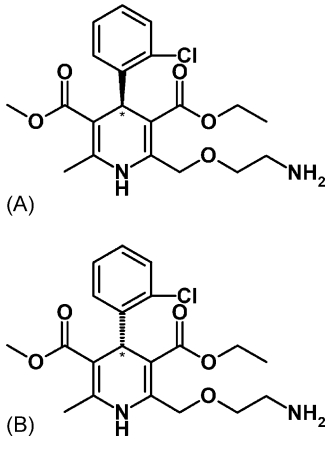

Fig. 1. Chemical structure of (A) *R*-AML and (B) *S*-AML.

AML is slowly cleared with an elimination half-time of 40–50 h. The relatively long plasma elimination half-time of AML distinguishes it from other calcium channel blocking agents. Although structurally related to other dihydropyridine derivatives, AML displays significantly different pharmacokinetic characteristics and is suitable for administration in a single daily dose.

AML molecule contains a chiral carbon. Metabolites with sustained dihydropyridine core can exert optical activity too. The optical activity ceases after dehydrogenation of dihydropyridine core. No racemization occurred *in vivo* in human plasma after single enantiomer administration as published in pharmacokinetic study of AML enantiomers in human [13]. Chiral separation of AML metabolites was not described. Concerning the biotransformation, previous studies have reported that AML is extensively metabolized in the liver [14] and biotransformation primarily involves oxidation to the pyridine derivative with species differences in humans, rats, and dogs [15–18]. However, no information on stereoselective metabolism of AML has been published yet. In the present study, biotransformation of AML and its two enantiomers was investigated using isolated rat hepatocytes. The aim of the study was to develop a liquid chromatography separation method on-line coupled via electrospray interface with mass spectrometry detection (LC/ESI-MS) for identification of main metabolic changes and an LC separation method with ultraviolet detection (LC-UV) for determination of differences in kinetic profiles of metabolites formation with respect to their stereoselectivity.

2. Experimental

2.1. Chemicals

Racemic amlodipine (*rac*-AML, M_w 408.89) and its enantiomers *R*- and *S*-AML, as well as synthetic derivatives of AML, 4-(2-chlorophenyl)-3-ethoxycarbonyl-5-methoxycarbonyl-2(carboxymethoxy)methyl-6-methylpyridine (D_1, M_w 421.84), 4-(2-chlorophenyl)-3-ethoxy-carbonyl-5-methoxycarbonyl-2(carboxymethoxy)methyl-6-methyl-1,4-dihydropyridine (D_2, M_w 423.85), and 2-(aminoethoxy)methyl-4-(2-chlorophenyl)-3-ethoxycarbonyl-5-methoxy-carbonyl-6-methylpyridine (D_3, M_w 406.87) were obtained from the Research Institute for Pharmacy and Biochemistry (Prague, Czech Republic). During

routine analysis (LC-UV) system suitability was controlled by injecting standard solution consisting of the mixture of 5.07 μM *rac*-AML and 4.82 μM D_2 in 10 mM ammonium acetate–acetonitrile (MeCN) (9:1, v/v). Chiral separation of AML was used to control chiral purity of enantiomers, as described earlier [19]. MeCN HPLC grade, Ham F12 medium, William's E medium, foetal calf serum, antibiotics, insulin and collagen were purchased from Sigma–Aldrich (Prague, Czech Republic). Water was purified in a Milli-Q water purification system (Millipore, Molsheim, France). High purity nitrogen and helium were supplied by Linde Gas (Prague, Czech Republic). The other chemicals were of the highest purity commercially available.

2.2. Animals

Male Wistar rats (age of 10–12 weeks) were obtained from the BioTest (Konarovice, Czech Republic). They were kept on a standard rat chow with free access to tap water in animal quarters under a 12-h light–dark cycle. Rats were treated in accordance with the *Guide for the care and use of laboratory animals* (Protection of Animals against Cruelty Act. No. 246/92 Coll., Czech Republic).

2.3. Instrumentation

2.3.1. LC-UV system

Semiquantitative LC analysis was carried on a fully automated LC system consisting of the following Shimadzu units (Prague, Czech Republic): LC-10AD_{VP} gradient pump, SIL-10AD_{VP} auto-injector with temperature control (10 °C), FCV-10AL_{VP} solvent mixer, CTO-10AC_{VP} column oven (25 °C), SCL-10A_{VP} system controller and SPD-M10A_{VP} UV–VIS photodiode array detector with detection set at 230–400 nm range and fluorescent detector RF-10Axl. The chromatographic data were acquired and analyzed using Chromatography Laboratory Automated Software System Class VP (version 6.12) from Shimadzu (Prague, Czech Republic).

The separation was performed on a 5 μm BDS Hypersil C_{18} column (250 mm × 4 mm) protected by 5 μm BDS Hypersil C_8 guard column (10 mm × 4 mm, both from Thermo Electron Corporation) with a flow rate of 1 mL min^{-1}. Mobile phase A consisted of 25 mM ammonium acetate (pH 4.8 adjusted with acetic acid)–water (4:6, v/v); mobile phase B consisted of 25 mM ammonium acetate (pH 4.8)–MeCN (4:6, v/v). The gradient profile was programmed as follows: from 0 to 42 min, the ratio of mobile phase A to B was linearly changed from 84:16 (v/v) to 16:84 (v/v); from 42 to 43 min, the mobile phase was returned to its initial composition and allowed to equilibrate with column for 17 min. The gradient was formed using low-pressure mixing and the delay volume was 5.3 mL. Volume of injected samples was 50 μL.

2.3.2. LC/ESI-MS system

Data-dependent LC/ESI-tandem MS in time (LC/ESI-MS/MS in time) analyses were carried on using a 5 μm BDS Hypersil C18 column (150 mm × 2.1 mm) protected by 5 μm BDS Hypersil C_8 guard column (10 mm × 4 mm) (both from Thermo Electron Corporation) at a flow rate 0.2 mL min^{-1}. The mobile phases were A: 10 mM ammonium acetate (pH 4.8 adjusted with acetic acid)–water (4:6, v/v) and B: 10 mM ammonium acetate (pH 4.8)–MeCN (4:6, v/v) with the following linear B gradient: 16 → 84% in 40 min, then back to 16% in 1 min, and re-equilibrated for 9 min. Total analysis time was 50 min. The samples in 10 mM ammonium acetate–MeCN (9:1, v/v) were kept at 10 °C in the auto-sampler to avoid loses of metabolites exceeding 10% before injected via 20-μL loop. The structure elucidation of the metabolites was carried out using a Surveyor HPLC system comprising a Surveyor MS pump, autosampler Surveyor AS with temperature control (10 °C), photodiode array detector Surveyor PDA with detection set at 230–400 nm range. The LC–MS and LC–MS/MS analyses were performed with a LCQ Advantage ion-trap mass spectrometer equipped with electrospray interface (Thermo Finnigan). The ion-trap mass spectrometer was operated in a positive mode and the tune source parameters were optimized using direct infusion of 0.1 mM solution of *rac*-AML. Samples were analyzed using a spray voltage of 4.5 kV, capillary heater temperature was held at 275 °C, sheath gas was held at 0.6 L min^{-1}, and auxiliary gas at 6.0 L min^{-1}. Ions were sampled into the mass spectrometer at a maximum injection time of 300 ms. The first scan event was operated in full scan mode with mass range from 250 to 750 amu. The second scan event was set as a list-dependent double stage MS/MS (MS^2) using a normalized collision energy of 30% with wideband activation and dynamic exclusion features enabled. Precursor mass list and reject mass list were designed according to a prior simple LC–MS analysis in which ion currents were reconstructed and the most intense background ions detected. The product ion spectra of the metabolites in a list-dependent mode included the *m/z* 365, 393, 407, 423, 437, 449, 470, 483, 495, 509, 542, 584, 643. Reject mass list included the *m/z* 265, 280, 294, 298, 355, 359, 391, 429, 454, 503, 511, 600, 685, 737. Dynamic data exclusion repeat count was 5 with repeat duration 0.2 min with exclusion lasting for 2 min with exclusion mass width of 2 amu. Data were acquired using Xcalibur™ software (version 1.2) and processed by Qual Browser (version 1.2) (both from Finnigan Corp.).

2.4. Hepatocytes isolation

Hepatocytes were prepared by two-step collagenase method [20]. In the first step the liver was rinsed with 150–200 mL of solution without calcium in order to remove the rest of blood and to weaken the cell-junction. In the second step the hepatocytes were released by action of collagenase (50 mg/100 mL) in perfusion solution. Second perfusion lasted for 5–6 min (recirculation system). Isolated hepatocytes were rewashed three times and mixed with culture medium. The culture medium consisted of a mixture of Ham F12 and William's E 1:1, supplemented as described earlier [21,22].

2.5. Incubation of hepatocytes with AML

A 100 mM stock solutions of *R*-, *S*-, and *rac*-AML dissolved in 10 mM ammonium acetate–MeCN (6:4, v/v) were added to

fresh medium. The final concentrations of *R*-, *S*-, and *rac*-AML used for incubation were 10, 20, 30, and 40 μM. About 0.5 mL of samples were taken in 2, 4, 8, 12 and 24 h intervals, frozen and kept at −20 °C. Identically as AML samples medium was incubated with hepatocytes without substrate and *R*-, *S*- and *rac*-AML was incubated in medium without hepatocytes in blank samples and control samples, respectively.

2.6. Cytotoxicity test

The cytotoxic effect of AML on rat hepatocytes was assessed after 24 h exposure, using the dimethylthiazolyl diphenyltetrazolium bromide (MTT) test as described earlier [23]. The absorbance of the product formazan in cell treated with AML was compared to that in control cells exposed to medium itself. Cytotoxicity was measured for 10 and 50 μM AML with viability 100% and 20%, respectively.

2.7. Sample pretreatment procedure

Solid phase extraction (SPE) was used for sample pretreatment. The defrosted medium sample (0.5 mL) was mixed with 0.6 mL of 20 mM phosphate buffer (pH 6.9), then centrifuged at 10,000 rpm for 10 min. One milliliter of the mixture was passed through preconditioned (2 mL MeCN, 2 mL water) Sep-Pak Vac tC18 cartridges (100 mg sorbent, Waters, Prague, Czech Republic) using Visiprep SPE Vacuum Manifold (Supelco, Sigma–Aldrich, Prague, Czech Republic) with a flow rate of approximately 1 drop s^{-1}. The cartridge was washed with 2 mL of 10 mM ammonium acetate, then the aqueous phase was removed using an air stream and finally, the analytes were eluted from the cartridges with 1 mL of 25% NH_3–MeCN (1:9, v/v). The eluates were evaporated to dryness at 45 °C under the reduced pressure. The residue was dissolved in 150 μL of 10 mM ammonium acetate–MeCN (9:1, v/v). Dissolved residues were kept at 10 °C in the auto-sampler and should be injected into the column within 24 h to avoid loses of metabolites exceeding 10%.

Deproteination was used as reference method in order to evaluate the extraction efficiency of the SPE method. Melted medium sample (0.5 mL) was mixed with 1 mL of MeCN and 20 μL of 0.25 M phosphoric acid, then centrifuged at 10,000 rpm for 10 min. The supernatants (1.4 mL) were evaporated to dryness at 45 °C under the reduced pressure. Further the residues were treated same as in case of SPE.

3. Results and discussion

3.1. Metabolites identification and structure elucidation

An RP-LC method was developed to separate metabolites of AML. Different chromatographic conditions (buffers, organic solvents and stationary phases) were tested. The best conditions for separation are described in Section 2 and a representative LC-UV chromatogram is shown in Fig. 2.

From the metabolites detected in the incubation of AML with primary culture of rat liver hepatocytes, eight metabolites presented in the highest amounts (M_1–M_8) were chosen for identification and semiquantification. The assumption they are metabolites of AML was based comparison with blank and control samples, incubation of rat hepatocytes without AML and incubation of AML without rat hepatocytes, respectively. Then all eight metabolites were divided into two groups, 1,4-dihydropyridines and pyridines, based on findings whether they display their absorption maximum at 275 nm (pyridines) or 360 nm (1,4-dihydropyridines). In addition, 1,4-dihydropyridine's metabolites gave signal at fluorescent detection (λ_{ex} 360 nm, λ_{em} 445 nm). Moreover, their full scan mass spectra in positive ionization mode showed molecular ions accompanied by characteristic chlorine isotopic peaks with two unit higher mass to

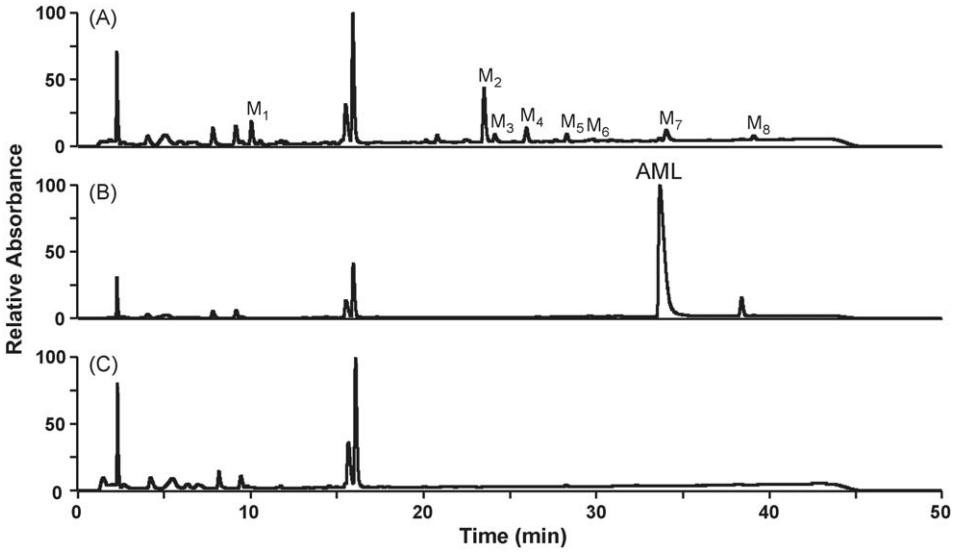

Fig. 2. Representative UV-chromatograms (240 nm) referring to the separation of AML and its metabolites M_1–M_8 on BDS Hypersil C18 column. (A) Sample: 40 μM *rac*-AML with primary culture of rat hepatocytes; (B) control: 40 μM *rac*-AML in medium without hepatocytes; (C) blank: hepatocytes without substrate incubated for 24 h. Chromatographic conditions specified in experimental-LC-UV system.

charge ratio. Thus, the assumption was even enhanced. Detection of metabolites was also tested in negative mode; however, the ionization of analytes was markedly better in positive mode with exception of M_5, which exerted enough ionization in both positive and negative mode.

The structure elucidation of AML metabolites was performed by employing data-dependent LC/ESI-MS^2 method. Product ion spectra of AML and synthetic derivatives D_1–D_3 of AML whose structures are shown in Fig. 3 were measured in order to determine a characteristic fragmentation pattern. Different fragments were found for reduced and oxidized derivatives, thus two distinctive fragmentation patterns were established. Product ion spectrum of AML with the identification of product ions and the mechanisms of fragmentation is shown in Fig. 4. Further product ion spectra of metabolites M_1–M_8 were measured, compared with product ion spectra of AML and synthetic derivatives and identified whether reduced or oxidized. Assigning to reduced or oxidized type was not always straightforward based on fragmentation pattern. Besides product ions, also data from PDA detector were considered when the suggestion whether there is reduced or oxidized type ring in the metabolite structure. Based on individual metabolites fragmentation functional groups were defined as demonstrated for M_6 in Fig. 5. Characteristic product ions seen for synthetic derivatives of AML, AML itself, and metabolites M_1–M_8 together with identification and retention times are summarized in Table 1. Acquired product ion spectra of the eight studied metabolites were compared with product ion spectra of knowledge-based predicted metabolites [24] with corresponding masses (generated by Mass Frontier). From theoretically possible structures of metabolites were chosen those in which measured and theoretical product ion spectra matched the best. Structures shown in Fig. 6 were assigned to studied metabolites and metabolic pathways suggested.

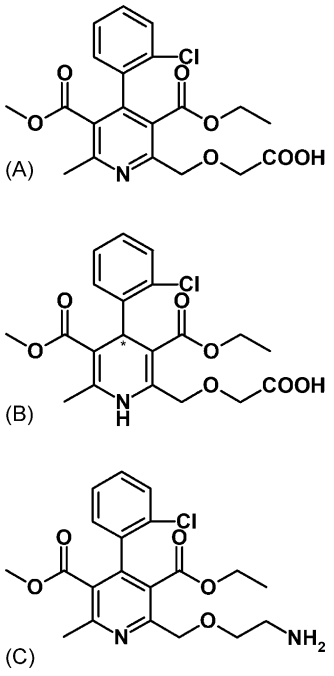

Fig. 3. Chemical structures of amlodipine derivatives: (A) D_1, (B) D_2, and (C) D_3.

Table 1
LC–MS/MS characteristics of synthetic derivatives D_1–D_3, AML, and metabolites M_1–M_8

Analyte	t_R UV (min)	t_R MS (min)	M_w	Precursor ion (*m/z*)	Product ions (*m/z*)
D_1	25.1	25.3	421	422	376 (–C_2H_5OH); 346 (–$OHCH_2COOH$); 318 (–$OHCH_2COOH$; –C_2H_4); 286 (–CH_3OH; –C_2H_4; $OHCH_2COOH$)
D_2	29.3	29.4	423	424	392 (–CH3OH); 378 (–C_2H_5OH); 348 (–$OHCH_2COOH$); 320 (–$OHCH_2COOH$; –C_2H_2); 288 (–C_2H_5OH;–CH_3OCH_2COOH); 244 (–C_2H_5OH; –CH_3OCH_2COOH; —CO_2)
D_3	29.3	29.7	406	407	390 (–NH_3); 364 (–$C_2H_2NH_3$); 346 (–$OHC_2H_4NH_2$); 318 (–$OHC_2H_4NH_2$; –C_2H_4); 286 (–$OHC_2H_4NH_2$; –OHC_2H_3O)
AML	33.7	33.8	408	409	392 (–NH_3); 366 (–$C_2H_3NH_2$); 348 (–$OHC_2H_4NH_2$); 320 (–$OHC_2H_4NH_2$; –C_2H_4); 288 (–$OHC_2H_4NH_2$; –C_2H_3OH; –CH_4)
M1	10.1	10.1	392	393	376 (–NH_3); 350 (–$C_2H_3NH_2$); 332 (–$OHC_2H_4NH_2$); 304 (–$OHC_2H_4NH_2$; –C_2H_4); 286 (–$OHC_2H_4NH_2$; –C_2H_5OH); 280 (–$C_2H_3OC_2H_2NH_2$; –C_2H_2); 260 (–$OHC_2H_4NH_2$;–$HCOOC_2H_3$); 168 (–C_6H_5Cl; –$HCOOC_2H_3$; –C_2HNH_2); 149 (–C_6H_5Cl; –OC_2H_2NH; –NH_3; –CHCOOH)
M_2	23.5	23.6	394	395	352 (–$C_2H_3NH_2$); 334 (–$OHC_2H_4NH_2$); 306 (–$OHC_2H_4NH_2$; –C_2H_4)
M_3	24.1	24.2	424	425	393 (–CH_3OH); 382 (–$C_2H_3NH_2$); 346 (–$OHC_2H_4NH_2$; –H_2O); 320 (–$OHC_2H_4NH_2$; –C_2H_3OH); 310 (–$OHC_2H_4NH_2$; –H_2O; HCl); 286 (–$OHC_2H_4NH_2$; –CH_4; –OHC_2H_4OH); 276 (–$HCOOC_2H_4OH$; –$OC_2H_3NH_2$); 252 (–C_6H_5Cl; –NH3; –C_2H_3OH); 238 (–C_6H_5Cl; CH_3OH; –$C_2H_3NH_2$); 229 (–$C_6H_4ClC_2H_2COOCH_3$)
M_4	26.0	26.0	422	423	391 (–CH_3OH); 377 (–OCHOH); 347 (–CH_3OH); 338 (–C_2H_3OH; –$C_2H_3NH_2$)
M_5	28.3	28.4	436	437	419 (–H_2O); 393 (–CH_4; –C_2H_4); 352 (–$C_2H_3NHCOCH_3$); 308 (–H_2O; –$OHC_2H_2NHCOCH_3$)
M_6	29.3	29.7	406	407	390 (–NH_3); 364 (–$C_2H_2NH_3$); 346 (–$OHC_2H_4NH_2$); 318 (–$OHC_2H_4NH_2$; –C_2H_4); 286 (–$OHC_2H_4NH_2$; –OHC_2H_3O)
M_7	34.0	34.3	448	449	431 (–H_2O); 417 (–CH_3OH); 407 (–C_2H_2O); 390 (–NH_2COCH_3); 364 (–$C_2H_3NHCOCH_3$); 346 (—$OHC_2H_4NHCOCH_3$); 318 (–$OHC_2H_4NHCOCH_3$; C_2H_4); 286 (–$OHC_2H_4NHCOCH_3$; C_2H_4; CH_3OH)
M_8	39.1	39.3	450	451	419 (–CH_3OH); 366 (–$C_2H_3NHCOCH_3$); 348 (–$OHC_2H_4NHCOCH_3$); 334 (–CH_3OH; –$C_2H_3NHCOCH_3$)

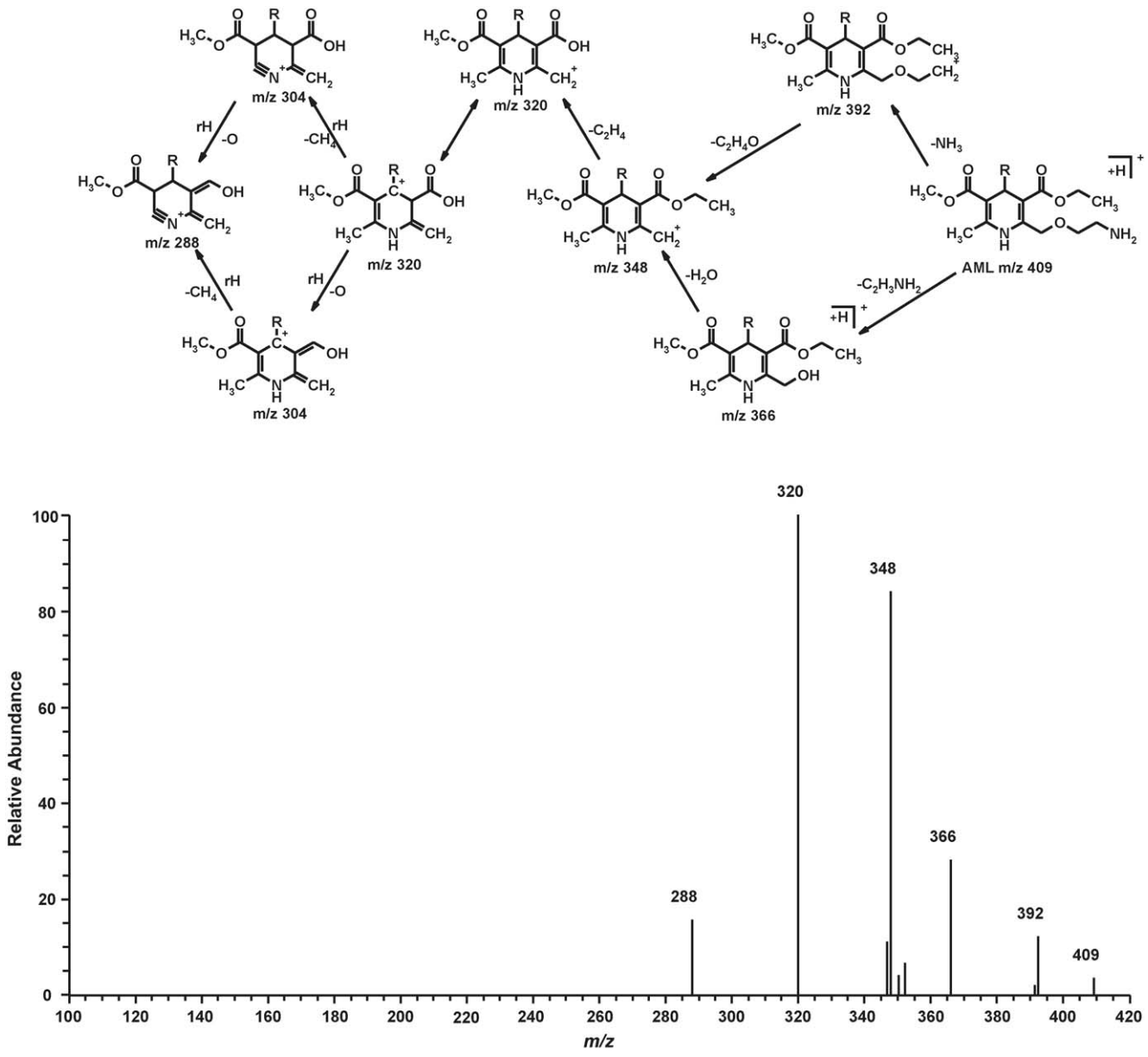

Fig. 4. Product ion spectrum of AML with identification of ions and fragmentation pathways: rH, hydrogen rearrangements; *R*, 2-chlorphenyl. The product ion at 304 *m/z* is included for the explanation, it was not observed.

3.2. Method performance

3.2.1. Biological quality controls

Analytical standards for semiquantified metabolites were not available, thus biological quality control (BQC) samples were used instead of spiked quality control (SQC) samples to control quality of the data generated. For these purposes 100 μM *R*-AML were incubated with hepatocytes for 24 h. After incubation, the hepatocyte medium was pooled and consequently divided into 0.5 mL aliquots. Injection of pooled hepatocyte media in between analyses of determined samples was used as BQC of acquired data. Extraction efficiency, precision of the method, as well as intraday, interday precision and stability was calculated from repeated analyses of BQC samples (aliquots mentioned).

Limit of semiquantitation (LOQ) was assessed as 19.5 pmol mL^{-1} amlodipine concentration equivalent units for analytes and ensures acceptable precision (relative standard deviation $\leq 20\%$). The estimated LOQ corresponds to the peak area of 10,000 integration units (I.U.) and the value 1016 I.U. $pmol^{-1}$ for amlodipine. Integration of peak areas was found to be the crucial step of semiquantitation since minority impurities eluting close to peaks of metabolites were not completely separated. Peaks with area lower than 8000 I.U. failed to be integrated by algorithm of chromatographic software. Therefore LOQ 10,000 I.U. was assessed to be optimal for routine analyses. Quality of data generated during the study was controlled with analyses of standard solution of 5.07 μM *rac*-AML and 4.82 μM D_2, and BCQ. The mean deviation did not exceed 1.4% and 1.3% for *rac*-AML and D_2, respectively.

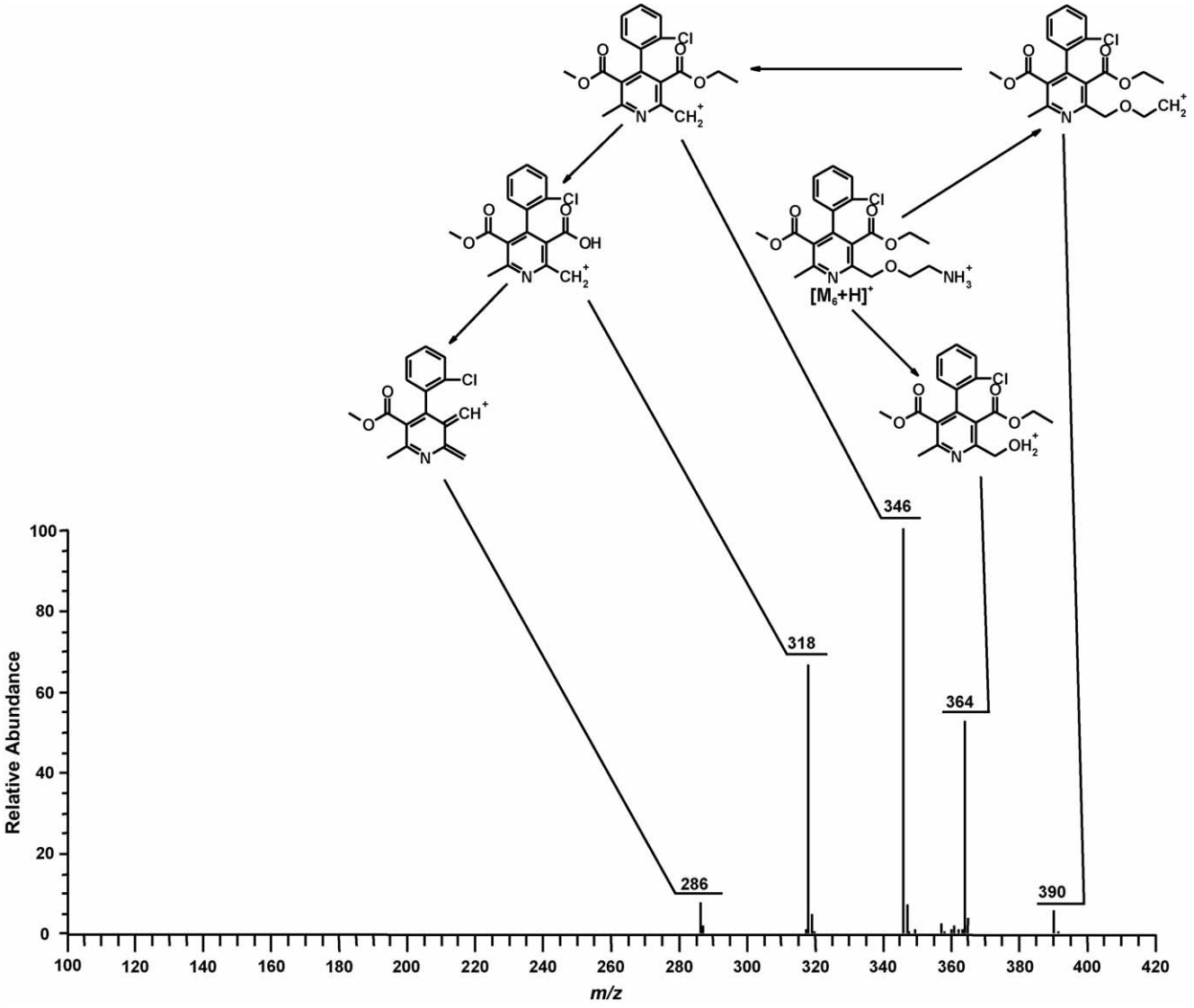

Fig. 5. Representative product ion spectrum of metabolite M_6 with explanation of fragments.

3.2.2. Recovery study

An alternative approach to determination of extraction recoveries was employed due to inaccessibility of analytical standards of semiquantified metabolites. BCQ were pretreated with SPE and compared with BCQ pretreated with deproteination. Instead of absolute recovery, relative recoveries for SPE were determined.

UV detection at 240 nm was used for semiquantitation. In chromatograms of samples processed with both deproteination and SPE measurable concentrations were found for AML and its metabolites M_1–M_8. Relative recovery of analyzed metabolites ranged from 78.0% to 111.8% as presented in Table 2. For parent compound relative recovery only 45% was found.

According to literature AML is strongly bonded to proteins and cell membranes [14]. Samples were centrifuged before SPE pretreatment, whereas in deproteination procedure MeCN was initially added directly to medium sample containing hepatocytes, thus AML bonded to cell membranes may be solubilized. Therefore it is advisable to separate cells and their fractions by

Table 2
Comparison of SPE with deproteination

Analyte	Deproteination ($n=3$)		SPE ($n=3$)		R^b (%)
	Mean (pmol mL^{-1})	CV[a] (%)	Mean (pmol mL^{-1})	CV[a] (%)	
AML	2633	16.87	1169.19	8.31	45.0
M_1	303	3.34	334.012	0.89	111.8
M_2	753	0.09	745.088	5.68	100.3
M_3	377	4.55	341.94	2.06	91.9
M_4	434	0.36	409.153	3.21	95.4
M_5	264	0.30	242.404	6.43	93.0
M_6	63	2.76	57.4843	1.88	92.2
M_7	93	3.62	89.7977	0.83	97.9
M_8	454	0.32	349.172	2.36	78.0

100 μM *R*-AML incubated with rat hepatocytes.

[a] Coefficient of variation.

[b] Relative recovery for SPE, $R = 100 \times$ mean (SPE)/mean (deproteination) $\times f$, where f is a correction coefficient for incomplete loading of samples on cartridges (1.1/1.0) and for incomplete transfer of supernatant for evaporation (1.52/1.4), thus $f = 1.013$.

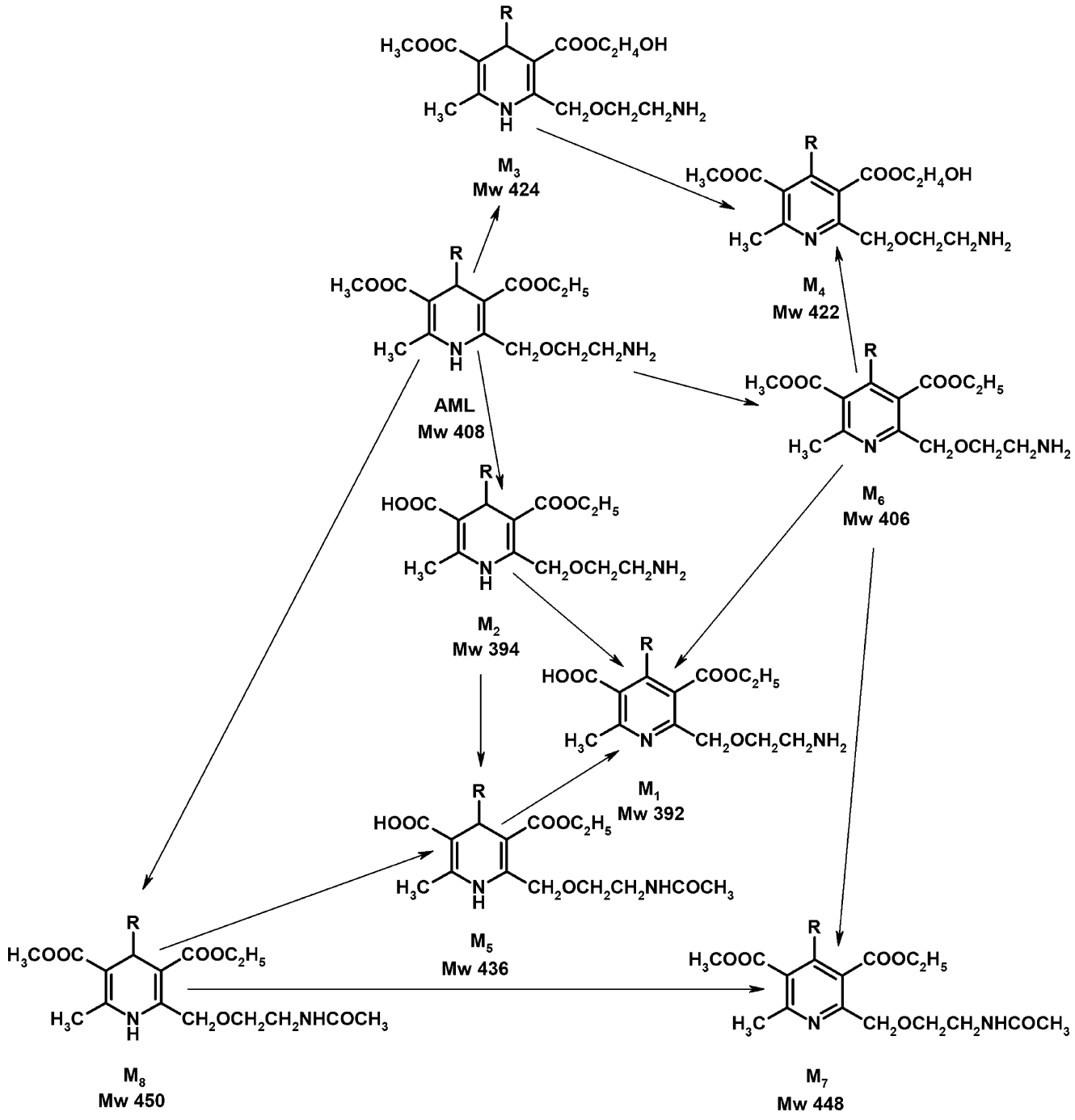

Fig. 6. Structures of AML metabolites and suggested scheme of biotransformation in rat.

centrifugation in order to achieve objective comparison of recoveries of both extraction procedures. Low relative recovery of the most lipophilic metabolite M_8 may be explained in compliance with binding to cell membranes as well. Recovery > 110% in M_1 indicates that oxidation of dihydropyridine core may occur during SPE sample pretreatment.

3.2.3. Intraday/interday precision and stability studies

BCQ were analyzed in triplicates in order to assess intraday precision and stability of samples in autosampler at 10 °C. Reconstituted samples were stored in autosampler at 10 °C for 24 h and then reanalyzed. Intraday precision was expressed as the coefficient of variation (CV) for each of the metabolites. None of the mean deviations exceeded value of 4.31%. The mean deviation in parent drug was 6.45%. Quality of data generated during the study was controlled as well and interday precision assessed. *In vitro* samples obtained by incubation of *R*-, *S*-, and *rac*-AML with rat hepatocytes were divided into nine batches. One BQC sample was incorporated into each batch. Responses of metabolites M_1–M_8 in chromatograms of BQC samples were used for estimation of interday precission. Coefficient of variations ranged from 2.19% for M_8 to 5.59% for M_3. The mean

Table 3
Precision data of the LC method for separation of AML and its metabolites calculated from the analyses of three BCQ aliquots (pooled samples)

Analyte	Intraday precision ($n=3$)		Interday precision ($n=9$)		Stability, 10 °C 24 h ($n=3$)		
	Mean (pmol mL^{-1})	CV[a] (%)	Mean (pmol mL^{-1})	CV[a] (%)	Mean$_t$[b] (pmol mL^{-1})	CV[a] (%)	RD[c] (%)
AML	1194	6.45	4829	12.15	1179	6.87	−1.23
M_1	331	0.39	92.1	4.86	343	0.16	3.68
M_2	789	2.05	216	5.59	741	1.45	−6.12
M_3	343	2.40	56.5	4.14	367	0.49	7.02
M_4	414	0.50	200	3.38	406	0.53	−1.80
M_5	255	1.94	94.0	2.24	229	1.31	−10.17
M_6	58.1	4.31	186.5	3.84	62.5	1.8	7.56
M_7	88.9	1.62	114.3	2.74	86.1	2.87	−3.20
M_8	348	1.66	1042	2.19	340	2.02	−2.39

[a] Coefficient of variation.
[b] Mean areas of peaks measured after 24 h storage at 10 °C.
[c] Relative deviation calculated as RD = 100 × (mean$_t$ − mean)/mean; meant corresponds to analysis after 24 h.

Table 4
Individual metabolites formation after incubation of 10 μM *R*-, *S*-, and *rac*-AML with rat hepatocytes

AML	Time	Concentration (pmol mL^{-1})							
		M_1	M_2	M_3	M_4	M_5	M_6	M_7	M_8
	2	ND	47.7 ± 9.7	33.1 ± 1.2	ND	ND	ND	ND	ND
	4	20.3 ± ND	137.3 ± 9.7	61.6 ± 2.9	ND	ND	ND	ND	ND
R	8	43.6 ± 2.7	259.5 ± 22.9	63.3 ± 6.4	ND	25.3 ± 2.6	ND	ND	ND
	12	73.6 ± 6.2	372.1 ± 40.4	55.5 ± 7.2	20.0 ± ND	34.5 ± 4.5	ND	ND	ND
	24	156.5 ± 13.8	494.0 ± 110.7	51.0 ± 9.2	34.2 ± 4.7	46.0 ± 5.6	ND	ND	ND
	2	ND	30.0 ± 3.5	ND	ND	ND	ND	ND	ND
	4	ND	55.0 ± ND	ND	ND	ND	ND	ND	ND
S	8	58.5 ± 5.6	232.9 ± 50.1	ND	ND	ND	ND	ND	ND
	12	119.9 ± 13.8	369.7 ± 137.7	ND	ND	ND	ND	ND	ND
	24	333.8 ± 18.6	543.8 ± 191.6	41.7 ± 7.2	23.0 ± ND	31.2 ± 10.8	ND	ND	ND
	2	ND	23.3 ± 0.2	ND	ND	ND	ND	ND	ND
	4	ND	85.7 ± 18.2	ND	ND	ND	ND	ND	ND
rac	8	55.1 ± 4.7	244.8 ± 56.8	25.9 ± 2.9	ND	22.0 ± 2.5	ND	ND	ND
	12	114.3 ± 7.9	460.6 ± 74.1	32.1 ± 4.9	29.7 ± 6.0	31.2 ± 3.0	ND	ND	ND
	24	292.2 ± 18.0	675.2 ± 166.7	52.3 ± 7.2	46.4 ± 12.4	46.4 ± 6.0	ND	ND	ND

Values are given as mean ± S.D. from $n=3$; ND, not determined. Value ± ND: S.D. not determined since only one value from triplicate determined.

Table 5
Individual metabolites formation after incubation of 20 μM *R*-, *S*-, and *rac*-AML with rat hepatocytes

AML	Time (h)	Concentration (pmol mL^{-1})							
		M_1	M_2	M_3	M_4	M_5	M_6	M_7	M_8
	2	ND	77.5 ± 5.7	65.6 ± 4.2	ND	ND	ND	ND	27.4 ± 1.6
	4	26.8 ± 3.7	210.3 ± 21.4	142.6 ± 10.5	ND	25.5 ± 2.97	ND	ND	28.2 ± 2.4
R	8	75.5 ± 0.5	500.7 ± 55.3	198.1 ± 11.1	41.3 2.7	51.0 ± 17.8	ND	ND	20.9 ± ND
	12	129.6 ± 1.6	681.1 ± 84.7	189.8 ± 10.5	65.8 ± 4.1	85.0 ± 4.54	ND	ND	ND
	24	283.4 ± 20.8	894.2 ± 49.1	144.3 ± 19.1	97.8 ± 3.6	108 ± 11.1	ND	ND	ND
	2	ND	30.7 ± 6.7	ND	ND	ND	ND	ND	27.7 ± 3.2
	4	ND	113.9 ± 14.2	ND	ND	NDND	ND	ND	43.4 ± 0.2
S	8	68.6 ± 5.4	305.8 ± 26.1	ND	ND	20.9 ± 0.18	ND	26.7 ± 5.1	51.3 ± 8.9
	12	158.3 ± 7.0	584.6 ± 63.9	28.8 ± 2.2	26.8 ± 6.8	42.3 ± 2.72	ND	27.7 ± 4.0	43.3 ± 5.6
	24	441.1 ± 20.4	1069.9 ± 207.9	58.2 ± 2.0	60.1 ± 2.0	75.7 ± 10.5	ND	ND	ND
	2	ND	25.9 ± 3.2	ND	ND	ND	ND	ND	24.5 ± 1.3
	4	ND	108.5 ± 16.7	21.1 ± 0.6	ND	ND	ND	ND	36.0 ± 1.0
rac	8	62.4 ± 6.2	331.3 ± 43.8	43.7 ± 1.6	34.1 ± 2.5	34.8 ± 5.75	ND	22.2 ± 2.8	31.7 ± 2.7
	12	144.0 ± 11.8	598.4 ± 111.5	54.2 ± 3.0	60.1 ± 4.9	60.9 ± 8.38	ND	22.9 ± 0.4	21.6 ± 1.1
	24	380.9 ± 45.1	1098.2 ± 143.2	76.6 ± 8.5	88.3 ± 16.4	89.3 ± 24.1	ND	ND	ND

Values are given as mean ± S.D. from $n=3$; ND, not determined. Value ± ND: S.D. not determined since only one value from triplicate determined.

Table 6
Individual metabolites formation after incubation of 30 μM *R*-, *S*-, and *rac*-AML with rat hepatocytes

AML	Time (h)	Concentration (pmol mL^{-1})							
		M_1	M_2	M_3	M_4	M_5	M_6	M_7	M_8
	2	ND	69.4 ± 6.1	76.2 ± 3.1	ND	ND	ND	ND	57.2 ± 8.3
	4	26.3 ± 2.4	234.2 ± 32.8	186.7 ± 10.7	21.1 ± 1.9	31.2 ± 4.6	ND	ND	79.5 ± 15.9
R	8	81.3 ± 1.3	543.2 ± 44.5	307.4 ± 4.8	76.8 ± 9.7	82.1 ± 9.0	ND	38.7 ± 0.8	76.6 ± 12.7
	12	159.7 ± 8.9	714.7 ± 110.8	338.8 ± 22.1	139.2 ± 20.8	126.0 ± 19.3	ND	38.2 ± 0.1	54.9 ± 15.5
	24	23.6 ± 23.6	944.2 ± 126.6	944.2 ± 8.6	233.3 ± 42.5	163.4 ± 50.8	ND	22.1 ± 1.4	ND
	2	ND	38.4 ± 6.4	ND	ND	ND	ND	ND	43.0 ± 6.1
	4	20.5 ± ND	123.2 ± 22.3	ND	ND	ND	ND	21.0 ± 0.9	68.5 ± 4.3
S	8	70.4 ± 8.1	334.4 ± 20.4	21.5 ± 1.7	ND	28.7 ± 3.2	ND	36.4 ± 2.4	93.7 ± 9.2
	12	156.4 ± 11.5	486.7 ± 84.6	29.5 ± 0.1	35.9 ± 5.4	51.0 ± 6.7	ND	51.6 ± 3.4	103.1 ± 12.0
	24	554.3 ± 84.5	1038.1 ± 104.6	69.1 ± 4.9	101.3 ± 9.6	124.0 ± 22.0	ND	38.9 ± 8.2	79.6 ± 40.2
	2	ND	27.7 ± 0.5	182.3 ± ND	ND	ND	ND	ND	52.9 ± 3.5
	4	ND	110.1 ± 12.3	27.9 ± 0.4	ND	ND	ND	19.5 ± ND	95.0 ± 6.5
rac	8	59.9 ± 5.7	329.9 ± 38.4	63.8 ± 2.7	56.8 ± 6.9	47.0 ± 5.5	ND	45.6 ± 1.4	116.0 ± 5.1
	12	140.5 ± 14.8	634.5 ± 39.0	89.6 ± 0.5	118.7 ± 4.5	97.0 ± 3.1	ND	58.9 ± 2.7	114.3 ± 9.2
	24	446.2 ± 9.8	742.4 ± 276.9	121.2 ± 10.7	218.8 ± 44.1	152.8 ± 49.4	ND	42.8 ± 0.2	32.7 ± 7.1

Values are given as mean ± S.D. from $n = 3$; ND, not determined. Value ± ND: S.D. not determined since only one value from triplicate determined.

deviation in parent drug was 12.15%. Thus the method ensures acceptable precision of determination of all metabolites and parent drug. The least stable metabolites M_2 and M_5 exhibited losses of 6.1% and 10.2%, respectively, after 24 h storage in autosampler at 10 °C. The limit considered to be still acceptable is 20%. Precision of the method was not impaired. Data from BQC (pooled samples) are summarized in Table 3.

3.2.4. Application of the method to hepatocytes medium samples

The developed LC-UV method was applied to primary rat hepatocytes samples incubated with *R*-, *S*-, and *rac*-AML. Metabolites formation was explored in four concentrations of the parent drug (10, 20, 30, and 40 μM) and samples were taken in five intervals (2, 4, 8, 12, and 24 h). UV detection at three wavelengths (240, 275, 360 nm) and fluorescent detection (λ_{ex} 360 nm, λ_{em} 445 nm) were employed to identify peaks of metabolites in LC analysis. Data acquired at 240 nm were used for semiquantification. Samples were analyzed in triplicates, where each of the samples in the triplicate was from the individual incubation.

The amounts of metabolites were expressed as amlodipine equivalent concentration units. The value 1016 I.U. pmol^{-1} was determined and used for calculation of amlodipine equivalent concentration in metabolites. Tables 4–7 show the average values and standard deviations acquired for individual metabolites of *R*-, *S*-, and *rac*-AML in four different concentrations. Apparently, the values obtained for *rac*-AML do not correspond to the average values of *R*- and *S*-AML. In most cases, *R*-AML is converted to its metabolites in a greater extent than *S*-AML

Table 7
Individual metabolites formation after incubation of 40 μM *R*-, *S*-, and *rac*-AML with rat hepatocytes

AML	Time (h)	Concentration (pmol mL^{-1})							
		M_1	M_2	M_3	M_4	M_5	M_6	M_7	M_8
	2	ND	67.6 ± 22.4	77.1 ± 7.2	ND	ND	25.7 ± 3.1	ND	102.1 ± 5.6
	4	30.4 ± 4.5	249.1 ± 95.8	224.3 ± 20.1	32.0 ± 4.7	34.8 ± 11.8	22.6 ± 1.1	31.4 ± 1.6	185.9 ± 3.7
R	8	86.9 ± 5.3	607.2 ± 24.7	397.4 ± 19.6	118.4 ± 14.7	105.4 ± 12.9	22.3 ± ND	63.2 ± 2.5	272.5 ± 17.2
	12	166.0 ± 9.5	883.8 ± 23.3	505.5 ± 24.4	253.2 ± 32.6	186.1 ± 34.2	ND	88.2 ± 3.3	314.6 ± 21.8
	24	464.4 ± 34.7	1259.8 ± 4.7	588.2 ± 8.2	632.7 ± 84.3	400.9 ± 3.7	26.0 ± ND	96.3 ± 14.0	211.8 ± 37.1
	2	ND	30.4 ± 4.6	ND	ND	ND	23.5 ± 2.0	ND	52.6 ± 6.0
	4	ND	113.9 ± 23.3	ND	ND	ND	24.8 ± 1.1	25.8 ± ND	97.2 ± 8.1
S	8	64.8 ± 6.6	286.9 ± 17.2	21.7 ± 0.1	ND	28.8 ± 4.7	23.3 ± 1.5	47.9 ± 4.5	156.6 ± 7.8
	12	153.2 ± 17.7	548.9 ± 45.4	35.4 ± 3.6	39.1 ± 2.2	55.2 ± 9.0	20.1 ± 0.2	69.7 ± 5.1	202.9 ± 1.0
	24	528.2 ± 61.7	1184.2 ± 51.8	75.1 ± 8.2	136.9 ± 1.7	169.3 ± 11.7	ND	80.3 ± 1.7	120.5 ± 16.2
	2	ND	27.7 ± 1.4	ND	ND	ND	24.0 ± 1.6	ND	81.7 ± 8.5
	4	ND	123.7 ± 20.0	29.1 ± 1.6	20.7 ± 0.6	ND	30.5 ± 2.6	32.3 ± 0.4	176.9 ± 12.7
rac	8	49.3 ± 3.9	314.5 ± 69.1	72.2 ± 4.8	72.7 ± 4.7	54.1 ± 4.6	31.2 ± 4.2	64.0 ± 1.3	275.2 ± 23.4
	12	123.9 ± 1.8	594.5 ± 69.1	120.0 ± 5.7	179.7 ± 17.5	124.1 ± 15.9	33.6 ± 3.0	104.7 ± 5.7	390.9 ± 23.3
	24	416.4 ± 27.8	1220.1 ± 189.6	202.5 ± 7.1	517.4 ± 34.0	297.8 ± 52.7	43.6 ± 3.9	148.1 ± 7.4	390.3 ± 54.2

Values are given as mean ± S.D. from $n = 3$; ND, not determined. Value ± ND: S.D. not determined since only one value from triplicate determined.

Table 8
Comparison of metabolites formation in *R*-, *S*-, and *rac*-AML in 24 h interval

Metabolite	Areas ratio after 24 h	AML concentration			
		10 μM	20 μM	30 μM	40 μM
M1	*R*/*rac*	0.54	0.74	0.05	1.12
	S/*rac*	1.14	1.16	1.24	1.27
	R/*S*	0.47	0.64	0.04	0.88
M2	*R*/*rac*	0.73	0.81	1.27	1.03
	S/*rac*	0.81	0.97	1.40	0.97
	R/*S*	0.91	0.84	0.91	1.06
M3	*R*/*rac*	0.98	1.89	7.78	2.90
	S/*rac*	0.80	0.76	0.57	0.37
	R/*S*	1.23	2.48	13.67	7.84
M4	*R*/*rac*	0.74	1.11	1.07	1.22
	S/*rac*	0.50	0.68	0.46	0.26
	R/*S*	1.49	1.63	2.30	4.62
M5	*R*/*rac*	0.99	1.21	1.07	1.35
	S/*rac*	0.67	0.85	0.81	0.57
	R/*S*	1.47	1.42	1.32	2.37
M6	*R*/*rac*	ND	ND	ND	0.59
	S/*rac*	ND	ND	ND	ND
	R/*S*	ND	ND	ND	ND
M7	*R*/*rac*	ND	ND	0.52	0.65
	S/*rac*	ND	ND	0.91	0.54
	R/*S*	ND	ND	0.57	1.20
M8	*R*/*rac*	ND	ND	ND	0.54
	S/*rac*	ND	ND	2.43	0.31
	R/*S*	ND	ND	ND	1.76

ND: not determined.

as illustrates Table 8 with ratios of individual metabolites formation, although type of metabolite formed, concentration of substrate, and incubation time play an important role. While metabolite M_1 is easily formed from *S*-AML, metabolites M_3, M_4, and M_5 are preferentially formed from *R*-AML. Formation of M_2, M_6, M_7, and M_8 is not strictly dependent on the 3D-arrangement of the respective enantiomers of AML (see Tables 4–7). From these data it is obvious that there is not just quantitative but also qualitative difference in the metabolism and pharmacokinetics for *S*-AML and *R*-AML.

4. Conclusions

In this study, liquid chromatography on-line coupled with mass spectrometry was proven to be a powerful tool for study of drug metabolism and provided an efficient method for identification and structure elucidation of eight major metabolites found in biological samples. The major metabolites were identified and their structure elucidated by data dependent MS/MS experiment of *in vitro* samples obtained by incubation of *R*-, *S*-, and *rac*-AML with rat hepatocytes. The developed semiquantitative LC-UV method was applied to investigate differences in metabolism of chiral drug AML. The method clearly demonstrated sufficient precision to reveal differences in AML enantiomers metabolism and stereoselectivity in amlodipine biotransformation was confirmed *in vitro*.

Acknowledgements

The authors acknowledge the financial support of the Ministry of Education, Youth and Sports of the Czech Republic (FRVS 1981/2005). We gratefully thank M. Kuchar (Research Institute for Pharmacy and Biochemistry, Prague, Czech Republic) for the kind provision of amlodipine enantiomers, T. Vontor for the supply of the synthetic derivatives, and B. Szotakova and L. Skalova (Department of Biochemical Sciences, Faculty of Pharmacy in Hradec Kralove, Charles University in Prague, Hradec Kralove, Czech Republic) for the kind provision of primary cultures of rat hepatocytes.

References

[1] T. Andersson, Clin. Pharmacokinet. 43 (2004) 279.
[2] A.J. Hutt, CNS. Spectrom. 7 (2002) 14.
[3] J. McConathy, M.J. Owens, Primary Care Companion, J. Clin. Psychiatr. 5 (2003) 70.
[4] C. Sanchez, K.P. Bogeso, B. Ebert, E.H. Reines, C. Braestrup, Psychopharmacology (Berlin) 174 (2004) 163.
[5] I. Agranat, H. Caner, Drug Discov. Today 4 (1999) 313.
[6] I. Agranat, H. Caner, J. Caldwell, Nat. Rev. Drug Discov. 1 (2002) 753.
[7] G.T. Tucker, Lancet 355 (2000) 1085.
[8] R.L. Woosley, Y. Chen, J.P. Freiman, R.A. Gillis, JAMA 269 (1993) 1532.
[9] P. Mansfield, D. Henry, A. Tonkin, Clin. Pharmacokinet. 43 (2004) 287.
[10] L. Chen, W.H. Haught, B. Yang, T.G. Saldeen, S. Parathasarathy, J.L. Mehta, J. Am. Coll. Cardiol. 30 (1997) 569.
[11] O. Stepien, L. Iouzalen, T. Herembert, D.L. Zhu, P. Marche, Int. J. Cardiol. 62 (Suppl. 2) (1997) S79–S84.
[12] J.E. Phillips, M.R. Preston, Atherosclerosis 168 (2003) 239.
[13] J. Luksa, D. Josic, M. Kremser, Z. Kopitar, S. Milutinovic, J. Chromatogr. B: Biomed. Sci. Appl. 703 (1997) 185.
[14] P.A. Meredith, H.L. Elliott, Clin. Pharmacokinet. 22 (1992) 22.
[15] A.P. Beresford, P.V. Macrae, D.A. Stopher, Xenobiotica 18 (1988) 169.
[16] A.P. Beresford, D. McGibney, M.J. Humphrey, P.V. Macrae, D.A. Stopher, Xenobiotica 18 (1988) 245.
[17] A.P. Beresford, P.V. Macrae, D. Alker, R.J. Kobylecki, Arzneimittelforschung 39 (1989) 201.
[18] D.A. Stopher, A.P. Beresford, P.V. Macrae, M.J. Humphrey, J. Cardiovasc. Pharmacol. 12 (Suppl. 7) (1988) S55–S59.
[19] P.L. Spargo, Ch. US Patent 5,750,707 (1998) to Pfizer Inc, New York, NY.
[20] M.N. Berry, G.J. Barritt, A.M. Edwards, Isolated Hepatocytes—Preparation, Properties and Applications, Elsevier Science, Amsterdam, 1991.
[21] H.C. Isom, I. Georgoff, Proc. Natl. Acad. Sci. U.S.A. 81 (1984) 6378.
[22] P. Maurel, Adv. Drug Deliv. Rev. 22 (1996) 105.
[23] F. Denizot, R. Lang, J. Immunol. Methods 89 (1986) 271.
[24] M.R. Anari, R.I. Sanchez, R. Bakhtiar, R.B. Franklin, T.A. Baillie, Anal. Chem. 76 (2004) 823.

V

Characterization of the *in vitro* metabolic profile of amlodipine in rat using liquid chromatography-mass spectrometry

Bohumila Suchanova[1,2], Risto Kostiainen[3] and Raimo A. Ketola[2,3 *]

[1] Department of Biochemical Sciences, Faculty of Pharmacy, Charles University, Heyrovskeho 1203, CZ-50005 Hradec Kralove, Czech Republic

[2] Drug Discovery and Development Technology Center (DDTC), Faculty of Pharmacy, P.O. Box 56, FI-00014 University of Helsinki, Finland

[3] Division of Pharmaceutical Chemistry, Faculty of Pharmacy, P.O. Box 56, FI-00014 University of Helsinki, Finland

[*] Corresponding author:

Raimo A. Ketola,

Division of Pharmaceutical Chemistry, Faculty of Pharmacy, P.O. Box 56, FI-00014 University of Helsinki, Finland

Tel: +358-9-191 59194, fax: +358-9-191-59556, e-mail: raimo.ketola@helsinki.fi

Running head: Metabolism of amlodipine by LC/MS

text 18, figures 4, tables 2

Abstract

In the present study, the metabolic profile of amlodipine, a well-known calcium channel blocker, was investigated employing liquid chromatography-mass spectrometric (LC/MS) techniques. Two different types of mass spectrometers – a triple-quadrupole (QqQ) and a quadrupole time-of-flight (Q-TOF) mass spectrometer – were utilized to acquire structural information on amlodipine metabolites. The metabolites were produced by incubation of amlodipine with primary cultures of rat hepatocytes. Incubations from rat hepatocytes were analyzed with LC-MS/MS, and 21 phase I and phase II metabolites were detected and their product ion spectra acquired, interpreted, and structures proposed. Accurate mass measurement using LC-Q-TOF was used to determine the elemental composition of metabolites and thus to confirm the proposed structures of these metabolites. Mainly phase I metabolic changes were observed including dehydrogenation of the dihydropyridine core, as well as reactions of side chains, such as hydrolysis of ester bonds, hydroxylation, N-acetylation, oxidative deamination, and their combinations. The only phase II metabolite detected was the glucuronide of a dehydrogenated, deaminated metabolite of amlodipine. We propose several *in vitro* metabolic pathways of amlodipine in rat, based on our analysis of the metabolites detected and characterized.

Keywords: *in vitro* metabolism, LC/MS, LC-MS/MS, rat hepatocyte, accurate mass measurement

Introduction

Absorption, distribution, metabolism, excretion, and toxicology (ADMET) studies play an important role in the drug discovery and development process. The discovery of poor bioavailability and high clearance, as well as the formation of active or toxic metabolites can set a research program back significantly. Until recently, metabolite identification occurred only after a drug candidate had been chosen for drug development, although metabolism can dictate the rate of absorption into the body, leading to the production of new and possibly toxic species or activation of the drug. Currently, data on metabolism are frequently used to optimize drug candidates, suggesting that more active compounds may be sought or supporting further toxicology studies, and are required before a new substance can advance towards the developmental stages of a new therapeutic agent.[1-3]

Due to its selectivity, sensitivity, and speed of analysis, liquid chromatography-tandem mass spectrometry (LC-MS/MS) has become the method of choice for metabolite identification in the fast-paced environment of drug discovery and development. Crude extracts of *in vitro* incubation and *in vivo* samples can be subjected to metabolite profiling and identification by LC-MS/MS directly or after purification, e.g. with solid-phase extraction (SPE). Complex metabolite mixtures are resolved chromatographically on a high-performance liquid chromatography (HPLC) column and full-scan MS and product ion scan MS/MS data are generated on-line. Thus, the molecular weight of drug metabolites and localization of the biotransformation sites can be elucidated, based on interpretation of the MS/MS data. Collision-induced dissociation (CID) mass spectra often provide sufficient information for structural assignment. However, structural characterization of drug metabolites is not always straightforward[4]; e.g. metabolites with isobaric product ions cannot be identified unambiguously. Each type of mass spectrometer has its own advantages in metabolite profiling, and more complete information on the metabolism of a drug or drug candidate can be obtained by combining data obtained with different instruments.[5] Use of additional analytical tools such as MS measurement of accurate molecular mass together with consequent determination of the elemental composition belongs to a common strategy.[6,7]

Amlodipine, (R,S)-2-[(2-aminoethoxy)methyl]-4-(2-chlorophenyl)-3-ethoxycarbonyl-5-methoxycarbonyl-6-methyl-1,4-dihydropyridine (AML) (Fig. 1) is a dihydropyridine calcium channel blocker used in therapy of hypertension and ischemic heart disease. *In vitro* studies have suggested that the dihydropyridine calcium antagonists act as antioxidants by directly quenching several radical species and that AML reduces leukocyte-induced oxidation of low-

density lipoproteins (LDLs).[8] Furthermore, in human fibroblasts AML can modulate the expression of hydroxymethylglutaryl-coenzyme A (HMG CoA) reductase and LDL receptor genes. AML modulates many of the biochemical events involved in vascular hypertrophy and therefore can interfere with the mechanism involved in hypertension and atherosclerosis.[9] Moreover, AML has the capacity to inhibit binding of the oxidized LDL lipids as a result of its high lipophilicity and positively charged amino group (pKa 9.02).[10]

AML is slowly cleared with a relatively long elimination half-time of 40-50 h, which distinguishes it from other calcium channel-blocking agents. Although structurally related to other dihydropyridine derivatives, AML displays significantly different pharmacokinetic characteristics and is suitable for administration in a single daily dose. Regarding biotransformation, previous *in vivo* studies showed that AML is extensively metabolized in the liver[11] and that biotransformation primarily involves oxidation to the pyridine derivative with species differences in human, rat, and dog.[12-15] Nevertheless, the complex metabolic pathways of AML are still not completely known.

The aim of the present study was to characterize the *in vitro* metabolic profile of amlodipine from rat hepatocyte incubations, utilizing different LC-MS techniques. Based on MS and MS/MS data we propose chemical structures for the metabolites detected, and present a chart showing the *in vitro* metabolic pathways of amlodipine.

Experimental

Chemicals

AML (M_w = 408.89), as well as its synthetic derivatives 4-(2-chlorophenyl)-3-ethoxycarbonyl-5-methoxycarbonyl-2(carboxymethoxy)methyl-6-methylpyridine (S1, M_w = 421.84), 4-(2-chlorophenyl)-3-ethoxycarbonyl-5-methoxycarbonyl-2(carboxymethoxy)-methyl-6-methyl-1,4-dihydropyridine (S2, M_w = 423.85), and 2-(aminoethoxy)methyl-4-(2-chlorophenyl)-3-ethoxycarbonyl-5-methoxycarbonyl-6-methylpyridine (S3, M_w = 406.87) were obtained from the Research Institute for Pharmacy and Biochemistry (Prague, Czech Republic). Metoprolol (as tartrate salt) was obtained from ICN Biomedicals (Irvine, CA, USA). Acetonitrile (MeCN), ammonium hydroxide (NH_4OH), and ammonium acetate (NH_4Ac), all of HPLC grade, were purchased from J.T. Baker (Mallinckrodt Baker B.V., Deventer, The Netherlands). Ham F12 medium, William's E medium, fetal calf serum, antibiotics, insulin and collagen were purchased from Sigma-Aldrich (Prague, Czech

Republic). Water was purified in a Milli-Q water purification system (Millipore, Molsheim, France). Compressed air (Atlas Copco air dryer, Wilrijk, Belgium) was used as a nebulizer gas, while nitrogen (Whatman 75-720 nitrogen generator; Whatman, Brentford, Middlesex, UK) was used as a curtain, collision, and turbogas in a triple-quadrupole mass spectrometer. High-purity nitrogen produced by a High Purity Nitrogen Generator (Inchinnan, Renfrew, Scotland) was used as a desolvation and cone gas, and argon purchased from Oy Woikoski Ab (Helsinki, Finland) was used as a collision gas in a quadrupole-time-of-flight mass spectrometer. The other chemicals were of the highest purity commercially available.

Equipment

The MS/MS experiments with unit resolution were performed with an API 3000 triple-quadrupole (QqQ) mass spectrometer equipped with a commercial turbo ion spray source (Applied Biosystems/MDS Sciex, Toronto, Ontario, Canada). The accurate masses were determined using a Micromass Q-TOF Micro mass spectrometer (Waters Micromass, Elstree, Hertfordshire, UK) equipped with a commercial dual-spray ionization source (LockSpray) for the simultaneous infusion of the lock mass reference solution with the LC eluent. Both instruments were coupled with an Agilent 1100 series LC system (Agilent Technologies, Böblingen, Germany). The column used for separation was a Symmetry Shield C_{18} 100 mm × 2.1 mm, 3.5 µm with Symmetry C_{18} Sentry Guard 10 mm × 2.1 mm, 3.5 µm as a precolumn (both from Waters, Milford, MA, USA). The lock mass reference solution was infused using a syringe pump (PHD 2000 Syringe Pump; Harvard Apparatus, Holliston, MA, USA). Analyst 1.4 software (Applied Biosystems/MDS Sciex, Canada) and MassLynx 4.0 and 4.1 software (Waters, UK) were used to provide control and data management in the LC-MS system with QqQ and the LC-MS system with Q-TOF, respectively. The samples were pretreated via SPE using an Isolute VacMaster 10 SPE vacuum manifold (International Sorbent Technology, Hengoed, Mid Glamorgan, UK) together with Sep-Pak Vac tC18 100-mg cartridges (Waters, USA).

Methods

HPLC separation

The mobile phase consisted of two eluents, solvent A: aqueous 10 mM NH_4Ac (pH 4.8 adjusted with acetic acid) and solvent B: 10 mM NH_4Ac (pH 4.8) in 60% MeCN. The column was maintained at initial conditions of 16% B and 30 °C for 5 min, followed by three steps in

the B gradient: 16% → 25% in 5 min, then 25% → 75% in 5 min, then 75% → 84% in 5 min, and finally back to 16% in 1 min, and reequilibrated for 9 min. The injection volume was 15 µl and the flow rate was 0.2 ml/min.

Mass spectrometry

The QqQ was operated in the positive ion mode with a mass-to-charge ratio (*m/z*) of 150-750 under the following optimized conditions: ion spray voltage 5500 V and source temperature 380 °C. The turbogas pressure was 75 bars, nebulizer gas flow rate was 1.58 l/min, curtain gas 1.25 l/min, declustering potential 30 V, focusing potential 133 V, entrance potential 7 V, and collision cell exit potential 15 V for full-scan data acquisition. When MS/MS was employed, a collision energy of 30 eV was applied. During the analyses, system performance was controlled by injecting a standard solution consisting of a mixture of 14.67 µM AML and 14.16 µM S2 in 10 mM NH_4Ac:MeCN (9:1, v/v). MS/MS was carried out in the product ion scanning mode only.

Accurate mass measurements were carried out in the positive ion mode. The source parameters were optimized as follows: source temperature 80 °C, desolvation temperature 300 °C, desolvation gas 500 l/h, no cone gas was used. The capillary voltage was 2100 V, sample cone voltage 27 V, extraction cone voltage 8 V, and collision energy 15 eV. The transfer optics and analyzer parameters were as follows: ion energy 1 V, tube lens 80 V, grid 0.1 V, TOF flight tube 5630 V, reflectron 1780 V, and pusher cycle time 35 ms. Argon at a pressure of 1 bar was used as the collision gas. Instrument calibration over a mass range of *m/z* 80-800 was performed and checked daily prior to accurate mass measurements using a calibration solution consisting of 0.1 M sodium hydroxide and 10% formic acid in water:MeCN (1:1 v/v). The resolution of Q-TOF varied between 5000 and 6000.

All accurate mass measurements were performed using direct infusion of a reference solution consisting of 2 µM metoprolol (*m/z* 268.1913) in water:MeCN (1:1 v/v) by syringe pump at a flow rate of 3 µl/min via the LockSpray interface to ensure accuracy. The LockSpray was configured as follows: reference scan frequency 5.0 s, reference cone voltage 27 V, and analyte-to-reference scan ratio 4:1. A mass accuracy of 5 ppm or less could be obtained with the operating parameters used.

Sample pretreatment

SPE was used for sample pretreatment. The defrosted medium sample (0.5 ml) was diluted with 0.5 ml of water and mixed, then centrifuged at 10 000 rpm for 10 min. The supernatant was passed through preconditioned (2 ml MeCN, 2 ml water) cartridges with a flow rate of approximately 1 drop per second. The cartridge was washed with 2 ml of 10 mM NH_4Ac, the aqueous phase was removed using an airstream, and finally the analytes were eluted from the cartridges with 1 ml of 25% NH_4OH:MeCN (1:9, v/v). The eluates were evaporated to dryness using nitrogen at room temperature. The residue was reconstituted in 100 µl of 10 mM NH_4Ac:MeCN (9:1, v/v) and thus also preconcentrated 5-fold prior to injection into the column.

Hepatocyte isolation

Hepatocytes were prepared, using a two-step collagenase method.[16] Isolated hepatocytes were rewashed three times and mixed with a culture medium consisting of a mixture of Ham F12 and William's E 1:1, supplemented as described previously.[17,18] Three million viable cells in 3 ml of culture medium were placed into 60-mm plastic dishes precoated with collagen. The fetal calf serum was added in culture medium (5%) to support cell attachment during the first 4 h after planting, after which fresh medium without serum was used. The cultures were maintained at 37 °C in a humid atmosphere of air and 5% CO_2.

In vitro experiments

A 1.2-µl quantity of a 100-mM stock solution of AML dissolved in 10 mM NH_4Ac:MeCN (6:4, v/v) was added to 3 ml of the fresh medium in the dish and the resulting concentration of AML used for incubation was 40 µM. Sample 0.5-ml aliquots were taken at 24-h intervals, frozen, and kept at -20 ºC. Similarly, medium without AML was used to incubate hepatocytes, while medium without hepatocytes was used to incubate AML in blank and control samples, respectively.

Cytotoxicity test

The cytotoxic effect of AML on rat hepatocytes was assessed after a 24-h exposure, using the MTT (dimethylthiazolyl diphenyltetrazolium bromide) test as described in a previous study.[19] The absorbance of the product formazan in cells treated with AML was compared

with that in control cells exposed to the medium itself. Cytotoxicity was measured for 10 μM and 50 μM concentrations of AML with viability 100% and 20%, respectively.

Animals

Male Wistar rats (age 10-12 weeks) were obtained from BioTest (Konarovice, Czech Republic). They were kept on a standard rat chow with free access to tap water in animal quarters under a 12-h light-dark cycle. The rats were treated in accordance with the *Guide for the Care and Use of Laboratory Animals* (Protection of Animals against Cruelty Act. No. 246/92 Coll., Czech Republic).

Results and discussion

The structure of AML enables a variety of metabolic modifications and their combinations. Among the most expected phase I metabolic changes are dehydrogenation of the dihydropyridine core, oxidative deamination of the side chain amino group at position 2, hydrolysis of the ester bonds in side chains at positions 3 and 5, as well as aliphatic and carboaromatic hydroxylations. Phase II metabolic changes, e.g. glucuronidation, can occur later. To be more explicit, except for dihydropyridine core dehydrogenation which was described as the main biotransformation step in *in vivo* studies,[12-15] other likely metabolic changes in the side chains of AML are demonstrated in Fig. 1.

The data were processed both manually and by the metabolite identification software Metabolite ID of Analyst. The combination of both approaches decreased risk of metabolite omission during manual processing or failure of software for identification of drug metabolites. Of the metabolites detected in the incubation of AML with primary culture of rat liver hepatocytes, 21 (M1-M21; the numbers were assigned according to retention times) were characterized and their reconstructed chromatograms as well as chromatograms of AML and S1-S3 are shown in Fig. 2. We based our assumption that they were AML metabolites on comparison of the incubation sample with the blank and control samples (incubation of rat hepatocytes without AML and incubation of AML without rat hepatocytes, respectively), as well as on the presence of molecular ions accompanied by characteristic chlorine isotopic peaks with 2-unit-higher *m/z* ratios in the mass spectra. The product ion spectra of the metabolites were interpreted and tentative structures for the metabolites proposed.

Interpretation of product ion spectra

First, the fragmentation patterns of AML and its synthetic derivatives S1-S3 were studied as shown in Fig. 3. The interpretation of the product ions of four known compounds facilitated interpretation of the 21 metabolites detected as summarized in Table 1. The structures suggested were confirmed by accurate mass determination using Q-TOF with a mass accuracy better than 4 ppm, as presented in Table 2. M1 ($[M+H]^+$ at *m/z* 393) showed a mass decrease of 16 amu compared with AML, which was assigned to dehydrogenation and hydrolysis of the methyl ester group in a side chain at position 5. A product ion at *m/z* 376 corresponded to loss of NH_3, a product ion at *m/z* 350 was explained by the neutral loss of CH_2CHNH_2, and product ions at *m/z* 332 and 314 were related to successive losses of H_2O. A product ion at *m/z* 86 accompanied by one at *m/z* 366, corresponding to the remaining part of the molecule, was observed for M2 ($[M+H]^+$ at *m/z* 451). The product ion at *m/z* 86 accompanied by the remaining part of the molecule was observed for most of the N-acetylated metabolites. In addition to N-acetylation, dehydrogenation, hydrolysis of methyl ester groups, and monooxygenation were also suggested for M2, based on the product ions observed. M3 ($[M+H]^+$ at *m/z* 435) was differentiated from M1 by a mass increase of 42 amu, corresponding to N-acetylation, while a typical product ion at *m/z* 86 accompanied by one at *m/z* 350 were also present; thus an N-acetylated and demethylated structure was designated. M4 and M6 (both showing an $[M+H]^+$ at *m/z* 365) were monooxygenated in a side chain at positions 6 and 3, respectively, with a degraded side chain at position 5. It is not clear whether a hydroxyl group (in the pyridine structure) or a carbonyl group (in the 1,4-dihydropyridine structure) is introduced into the molecules. Nevertheless, for M4 only the structure with a hydroxymethyl group at position 6 is expected to yield the most abundant product ions at *m/z* 304 and 276 after loss of $CH_2{=}CH_2$ from the side chain at position 3, whereas for M6 the presence of a product ion at *m/z* 248 can only be explained by a neutral loss of 117 amu, which corresponds to loss of both $CH_2OCH_2CH_2NH_2$ and CH_2CHOH. An isobaric metabolite with both ester bonds hydrolyzed was excluded, based on calculation of the empirical formula from accurate mass determination. The retention time of a metabolite with two carboxylic acid groups would also probably be shorter than that of an ester. For M5 ($[M+H]^+$ at *m/z* 423) the mass increase of 14 or 16 compared with AML or its pyridine analogue S3 can be assigned to monooxygenation yielding a carbonyl or hydroxyl group to the molecule, respectively. Several regioisomers corresponding to an elemental composition of $C_{20}H_{23}ClN_2O_6$, which are monooxygenated in side chains at positions 2 or 3, can lead to similar product ions, and as

with M4 it is not possible to determine the position of the hydroxyl or carbonyl groups unambiguously. For steric reasons, primary hydroxylation of the side chain at position 3 is more likely. For M7 ($[M+H]^+$ at *m/z* 425) the same product ions at *m/z* 320 and 294 as for AML were detected. The mass increase compared with that for AML was 16 amu, which corresponded to a gain of one oxygen atom; thus hydroxylation was suggested and the elemental composition was confirmed by accurate mass measurement. Based on the structure of product ions at *m/z* 320 and 294, the hydroxyl group was suggested to be in the side chain at position 3. M8 ($[M+H]^+$ at *m/z* 395) was suggested to be a 1,4-dihydropyridine analogue to M1 with hydrolysis of the methoxycarbonyl group in the side chain at position 5, because the product ions were up-shifted by 2 amu compared with M1 and the calculated empirical formula of M8 corresponded to the accurate mass measured. The tentative structure of M9 ($[M+H]^+$ at *m/z* 584) was suggested, based on a characteristic neutral loss of the glucuronic acid moiety from the protonated molecule and a relatively short retention time as evidence for a highly polar metabolic change. The precursor ion (protonated molecule) was expected to be an even-electron ion, thus having an odd number of nitrogen atoms, consistent with the nitrogen rule.[20] From the possible structures of ester and ether glucuronides, only the latter corresponded to the measured elemental composition of $C_{26}H_{31}NO_{12}Cl$. M10 ($[M+H]^+$ at *m/z* 407) showed retention time, accurate mass, and product ion spectrum identical to those of S3; thus the structure of M10 was determined unambiguously. For M11 ($[M+H]^+$ at *m/z* 349) the degradation of the side chain at position 5 was suggested, based on a mass decrease of 60 amu, and the product ions and the measured elemental composition confirmed the tentative structure as well. M12 ($[M+H]^+$ at *m/z* 422) showed retention time, accurate mass, and product ion spectrum identical to those of S1; thus the structure of M12 was determined unambiguously. M13 ($[M+H]^+$ at *m/z* 467) was suggested to be N-acetylated, based on a product ion at *m/z* 86, and monooxygenated, based on the mass difference between M2 (*m/z* 451) and M13 (*m/z* 467); this was also confirmed by accurate mass measurement. M14 ($[M+H]^+$ at *m/z* 407) had the same empirical formula as M10, but the longer retention time indicated a less polar compound. Of the possible isobaric metabolites a dehydrogenated, N-acetylated metabolite with a degraded side chain at position 5 was suggested. Unlike other N-acetylated metabolites, a complementary pair of product ions at *m/z* 104 and 304 was observed instead of a product ion at *m/z* 86 and its complementary product ion. For M15 ($[M+H]^+$ at *m/z* 433) a product ion at *m/z* 86 was observed and thus N-acetylation was suggested. M15 also showed product ions that were not observed for other metabolites. The product ions showed *m/z* values 2 amu lower than those of pyridine analogues, which was

explained by dehydrogenation of a single bond. M16 ($[M+H]^+$ at *m/z* 465) was suggested to be dehydrogenated, N-acetylated, and monooxygenated. The product ions observed were the same as those of the pyridine analogues. Although the product ion at *m/z* 86 was not observed, the neutral loss of 85 amu leading to a product ion at *m/z* 360 indicated N-acetylation. The remaining mass increase of 16 amu was assigned to hydroxylation in a side chain at position 3, in compliance with interpretation of a product ion at *m/z* 360. For M17 ($[M+H]^+$ at *m/z* 449) the typical product ion at *m/z* 86 accompanied by a complementary product ion at *m/z* 364 was detected. Other product ions were similar to those observed for S3, the pyridine analogue of AML. M17 differed from S3 by a mass increase of 42 amu, which corresponded to N-acetylation. Thus, dehydrogenation and N-acetylation were suggested for M17. For M18 ($[M+H]^+$ at *m/z* 391) a product ion at *m/z* 86 together with a complementary product ion at *m/z* 306 was observed, as for many of the N-acetylated metabolites. We proposed that loss of H_2O led to a product ion at *m/z* 288 followed by the loss of $CH_2{=}CH_2$, giving rise to a product ion at *m/z* 260. M19 and M21 (both showing an $[M+H]^+$ at *m/z* 408) showed the same unit mass as well as the same elemental composition. Based on the nitrogen rule, they were expected to be oxidatively deaminated. The product ion spectrum of M19 showed more similarity with those of the dehydrogenated standards S1 and S3, thus suggesting it to be dehydrogenated and oxidatively deaminated to a hydroxyl derivative, whereas M21 was suggested to be oxidatively deaminated to a carbonyl derivative. For M20 ($[M+H]^+$ at *m/z* 451) the characteristic product ion at *m/z* 86 was detected and the presence of an acetyl group in the molecule suggested. The product ions were up-shifted by 2 amu in comparison to M17, which was expected to be due to the dihydropyridine core of the metabolite. The gain of 42 amu compared with the molecular weight of AML corresponded to the N-acetylation of AML, which was in agreement with the accurate mass measured. As a consequence of these interpretations we suggest an *in vitro* metabolic profile for AML in rat and present a tentative scheme for biotransformation of AML in Fig. 4.

Conclusions

The present study describes the characterization of an *in vitro* metabolic profile for amlodipine, a widely used long-acting dihydropyridine calcium antagonist, in rat. The metabolites formed by incubation of AML with a primary culture of rat hepatocytes were separated by LC and the product ion spectra measured by QqQ. In the first step the product ions were interpreted and tentative structures for 21 metabolites proposed. In the second step

the proposed structures of the metabolites were further confirmed by accurate mass determination with a mass accuracy better than 4 ppm, using Q-TOF with subsequent calculation of elemental composition. Combination of the structural information provided by the product ion spectra measurement with QqQ with information on the elemental compositions of the metabolites provided by accurate mass determination with Q-TOF enabled us to characterize the metabolites of AML and to propose its *in vitro* metabolic pathways in rat.

REFERENCES

1. Clarke NJ, Rindgen D, Korfmacher WA, Cox KA. Systematic LC/MS metabolite identification in drug discovery. *Anal. Chem.* 2001; **73**: 430A.
2. Nassar AE, Talaat RE, Kamel AM. The impact of recent innovations in the use of liquid chromatography-mass spectrometry in support of drug metabolism studies: are we all the way there yet? *Curr. Opin. Drug Discov. Devel.* 2006; **9**: 61.
3. Oliveira EJ, Watson DG. Liquid chromatography-mass spectrometry in the study of the metabolism of drugs and other xenobiotics. *Biomed. Chromatogr.* 2000; **14**: 351. DOI:10.1002/1099-0801(200010)14:6<351::AID-BMC28>3.0.CO;2-2.
4. Liu DQ, Hop CE. Strategies for characterization of drug metabolites using liquid chromatography-tandem mass spectrometry in conjunction with chemical derivatization and on-line H/D exchange approaches. *J. Pharm. Biomed. Anal.* 2005; **37**: 1. DOI: 10.1016/j.jpba.2004.09.003.
5. Hakala KS, Kostiainen R, Ketola RA. Feasibility of different mass spectrometric techniques and programs for automated metabolite profiling of tramadol in human urine. *Rapid Commun. Mass Spectrom.* 2006; **20**: 2081. DOI: 10.1002/rcm.2562.
6. Deroussent A, Re M, Hoellinger H, Vanquelef E, Duval O, Sonnier M, Cresteil T. In vitro metabolism of ethoxidine by human CYP1A1 and rat microsomes: identification of metabolites by high-performance liquid chromatography combined with electrospray tandem mass spectrometry and accurate mass measurements by time-of-flight mass spectrometry. *Rapid Commun. Mass Spectrom.* 2004; **18**: 474. DOI: 10.1002/rcm.1357.
7. Nagele E, Moritz R. Structure elucidation of degradation products of the antibiotic amoxicillin with ion trap MS(n) and accurate mass determination by ESI TOF. *J. Am. Soc. Mass Spectrom.* 2005; **16**: 1670. DOI: 10.1016/j.jasms.2005.06.002.
8. Chen L, Haught WH, Yang B, Saldeen TG, Parathasarathy S, Mehta JL. Preservation of endogenous antioxidant activity and inhibition of lipid peroxidation as common mechanisms of antiatherosclerotic effects of vitamin E, lovastatin and amlodipine. *J. Am. Coll. Cardiol.* 1997; **30**: 569. DOI: 10.1016/S0735-1097(97)00158-7.
9. Stepien O, Iouzalen L, Herembert T, Zhu DL, Marche P. Amlodipine and vascular hypertrophy. *Int. J. Cardiol.* 1997; **62**: S79. DOI: 10.1016/S0167-5273(97)00244-1.

10. Phillips JE, Preston MR. Inhibition of oxidized LDL aggregation with the calcium channel blocker amlodipine: role of electrostatic interactions. *Atherosclerosis.* 2003; **168**: 239. DOI: 10.1016/S0021-9150(03)00102-3.
11. Meredith PA, Elliott HL. Clinical pharmacokinetics of amlodipine. *Clin. Pharmacokinet.* 1992; **22**: 22.
12. Beresford AP, McGibney D, Humphrey MJ, Macrae PV, Stopher DA. Metabolism and kinetics of amlodipine in man. *Xenobiotica.* 1988; **18**: 245.
13. Beresford AP, Macrae PV, Stopher DA. Metabolism of amlodipine in the rat and the dog: a species difference. *Xenobiotica.* 1988; **18**: 169.
14. Beresford AP, Macrae PV, Alker D, Kobylecki RJ. Biotransformation of amlodipine. Identification and synthesis of metabolites found in rat, dog and human urine/confirmation of structures by gas chromatography-mass spectrometry and liquid chromatography-mass spectrometry. *Arzneimittelforschung.* 1989; **39**: 201.
15. Stopher DA, Beresford AP, Macrae PV, Humphrey MJ. The metabolism and pharmacokinetics of amlodipine in humans and animals. *J. Cardiovasc. Pharmacol.* 1988; **12**: S55.
16. Berry MN, Barritt GJ, Edwards AM. Isolated Hepatocytes - Preparation, Properties and Applications in *Laboratory Techniques in Biochemistry and Molecular Biology*, van der Vliet PC, Pillai S (eds). Elsevier Science, Amsterdam: 1991; 1-470.
17. Isom HC, Georgoff I. Quantitative assay for albumin-producing liver cells after simian virus 40 transformation of rat hepatocytes maintained in chemically defined medium. *Proc. Natl. Acad. Sci. U.S.A.* 1984; **81**: 6378.
18. Maurel P. The use of adult human hepatocytes in primary culture and other in vitro systems to investigate drug metabolism in man. *Advanced Drug Delivery Reviews.* 1996; **22**: 105. DOI: 10.1016/S0169-409X(96)00417-6.
19. Denizot F, Lang R. Rapid colorimetric assay for cell growth and survival. Modifications to the tetrazolium dye procedure giving improved sensitivity and reliability. *J. Immunol. Methods.* 1986; **89**: 271. DOI: 10.1016/0022-1759(86)90368-6.
20. McLafferty FW. In *Interpretation of Mass Spectra,* Kelly A (ed). University Science Books: Mill Valley, CA, USA, 1980; 37-38.

Table 1. Characteristics of amlodipine, its metabolites, and its synthetic derivatives S1-S3. M_W = molecular weight g/mol.

Metabolite	Proposed metabolic change	t_R (min)	M_W	Major product ions
M1	dehydrogenation, 5-demethylation	8.58	393	376 350; 348; 332; 314; 304; 286; 258
M2	dehydrogenation, 5-demethylation, N-acetylation, hydroxylation	12.20	451	366; 348; 320; 302; 286; 86
M3	dehydrogenation, 5-demethylation, N-acetylation	12.35	435	376; 350; 332; 304; 286; 86
M4	dehydrogenation, degradation of methoxycarbonyl, hydroxylation (position 6)	14.09	365	320; 304; 276; 230; 62
M5	dehydrogenation, hydroxylation	14.09	423	391; 288; 276; 86
M6	dehydrogenation, degradation of methoxycarbonyl, hydroxylation (position 3)	14.26	365	304; 276; 248; 230; 62
M7	hydroxylation	14.46	425	379; 336; 320; 294; 286
M8	5-demethylation	14.61	395	352; 334; 306; 288
M9	dehydrogenation, oxidative deamination + glucuronidation	14.91	584	408; 346; 318
M10	dehydrogenation	15.37	407	390; 364; 346; 318; 286
M11	dehydrogenation, degradation of methoxycarbonyl side chain	15.41	349	332; 306; 288; 260; 232
M12	dehydrogenation, oxidative deamination to carboxylic acid	15.48	422	376; 346; 318; 314; 286
M13	N-acetylation and monooxygenation	15.54	467	364; 288; 86
M14	dehydrogenation, degradation of methoxycarbonyl, N-acetylation, hydroxylation	15.75	407	304; 276; 230; 104
M15	dehydrogenation, 5-demethylation, N-acetylation, dehydrogenation	16.47	433	374, 302; 258; 224; 98; 86
M16	dehydrogenation, N-acetylation, monooxygenation	16.62	465	406; 360; 346; 318; 286
M17	dehydrogenation, N-acetylation	17.48	449	417; 364; 346; 318; 286; 258; 86
M18	dehydrogenation, degradation of methoxycarbonyl, N-acetylation	17.55	391	306; 288; 260; 86
M19	dehydrogenation, oxidative deamination to hydroxyl	17.91	408	346; 318; 314; 286
M20	N-acetylation	19.56	451	419; 366; 334; 320; 316; 288; 260; 208; 86
M21	oxidative deamination to aldehyde	21.07	408	390; 344; 317; 286; 71
Standard				
AML		16.23	409	392; 377; 366; 334; 320; 294; 288; 248; 238; 220; 206; 170; 84
S1		15.48	422	376; 346; 318; 314; 286
S2		16.46	424	392; 378; 348; 320; 302; 288; 270; 260; 208
S3		15.37	407	390; 364; 346; 318; 286

Table 2. Retention times and accurate mass measurements of amlodipine metabolites M1-21.

Metabolite	t_R (min)	Measured mass	Theoretical mass	Error		DBE[a]	Formula
				mDa	ppm		
M1	8.58	393.1212	393.1217	-0.5	1.3	9.5	$C_{19}H_{22}N_2O_5Cl$
M2	12.20	451.1229	451.1272	0.8	-1.8	10.5	$C_{21}H_{24}N_2O_7Cl$
M3	12.35	435.1327	435.1323	0.4	0.9	10.5	$C_{21}H_{24}N_2O_6Cl$
M4	14.09	365.1261	365.1268	-0.7	-1.9	8.5	$C_{18}H_{22}N_2O_4Cl$
M5	14.09	423.1339	423.1323	1.6	3.8	9.5	$C_{20}H_{24}N_2O_6Cl$
M6	14.26	365.1259	365.1268	-0.9	-2.5	8.5	$C_{18}H_{22}N_2O_4Cl$
M7	14.46	425.1378	425.1379	0.1	0.3	8.5	$C_{20}H_{26}N_2O_6Cl$
M8	14.61	394.1378	394.1374	0.4	1.1	8.5	$C_{19}H_{20}N_2O_5Cl$
M9	14.91	584.1528	584.1535	-0.7	-1.2	11.5	$C_{26}H_{31}NO_{12}Cl$
M10	15.37	407.1384	407.1374	0.7	1.8	9.5	$C_{20}H_{23}N_2O_5Cl$
M11	15.41	349.1328	349.1319	0.9	2.6	8.5	$C_{18}H_{22}N_2O_3Cl$
M12	15.54	422.0981	422.1007	0.8	2.0	10.5	$C_{20}H_{21}NO_7Cl$
M13	15.58	467.1571	467.1585	1.4	-3.0	9.5	$C_{22}H_{28}N_2O_7Cl$
M14	15.75	407.1379	407.1374	0.5	1.3	9.5	$C_{20}H_{23}N_2O_5Cl$
M15	16.47	433.1173	433.1166	0.7	1.5	11.5	$C_{21}H_{22}N_2O_6Cl$
M16	16.62	465.1437	465.1429	0.8	1.8	10.5	$C_{22}H_{26}N_2O_7Cl$
M17	17.48	449.1496	449.1479	1.7	3.7	10.5	$C_{22}H_{26}N_2O_6Cl$
M18	17.55	391.1430	391.1425	0.5	1.4	9.5	$C_{20}H_{24}N_2O_4Cl$
M19	17.91	408.1203	408.1214	-1.1	-2.7	9.5	$C_{20}H_{23}NO_6Cl$
M20	19.56	451.1644	451.1636	0.8	1.8	9.5	$C_{22}H_{28}N_2O_6Cl$
M21	21.07	408.1223	408.1214	0.9	2.2	9.5	$C_{20}H_{23}NO_6Cl$

[a] DBE = double-bond equivalent

Figure captions

Fig. 1.

Metabolic changes expected in amlodipine.

Fig. 2.

Extracted ion chromatograms of metabolites M1-21, AML, and its synthetic derivatives S1-S3 used as standards.

Fig. 3

Product ion spectra of amlodipine and its synthetic derivatives S1-S3 used as standards.

Fig. 4.

Proposed *in vitro* metabolic pathways of amlodipine in rat.

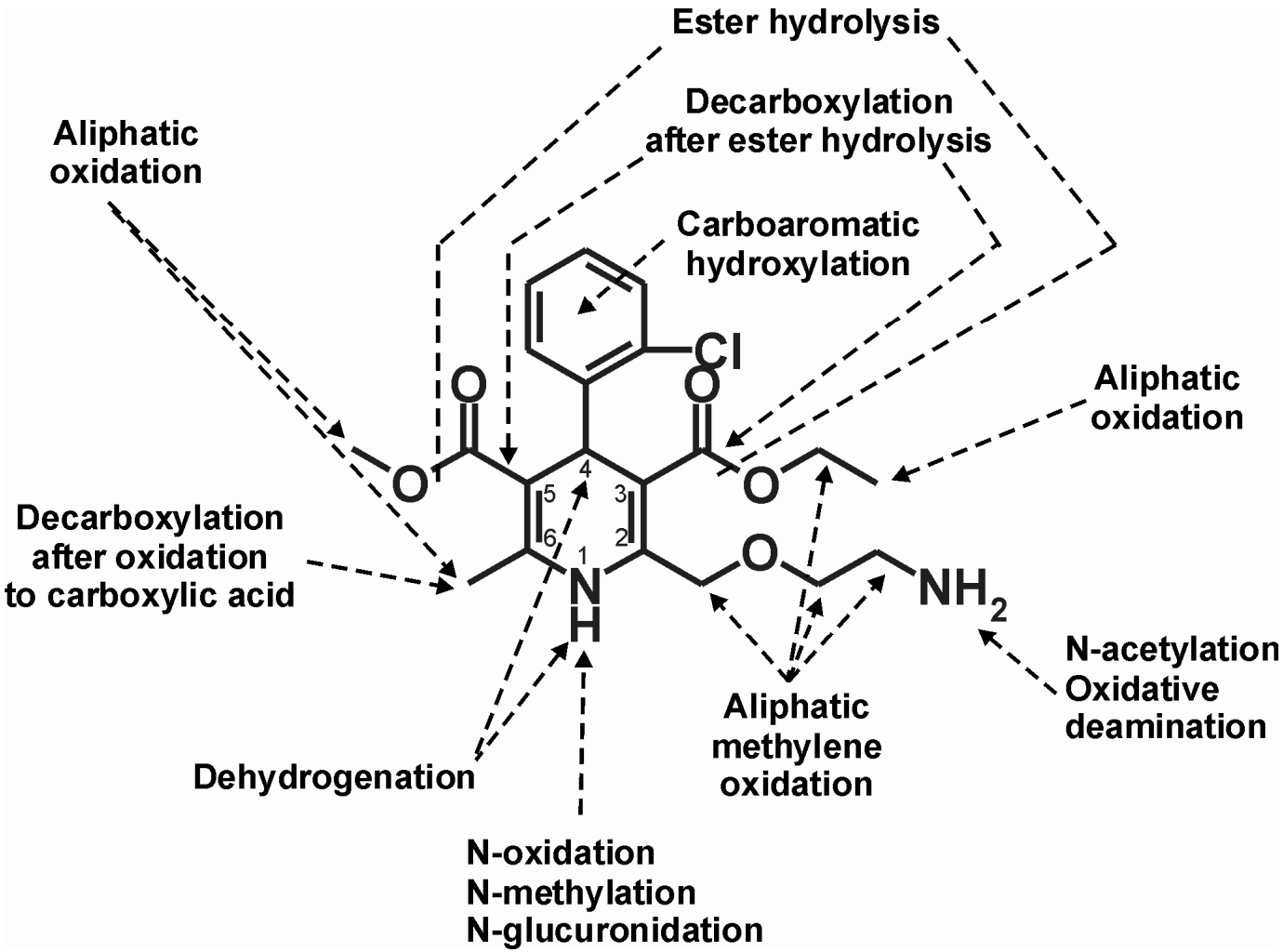
Ester hydrolysis
Decarboxylation after ester hydrolysis
Aliphatic oxidation
Carboaromatic hydroxylation
Cl
O
O
O
O
Aliphatic oxidation
Decarboxylation after oxidation to carboxylic acid
4
5
3
6
2
1
N
H
O
NH2
N-acetylation Oxidative deamination
Aliphatic methylene oxidation
Dehydrogenation
N-oxidation
N-methylation
N-glucuronidation

Figure 1

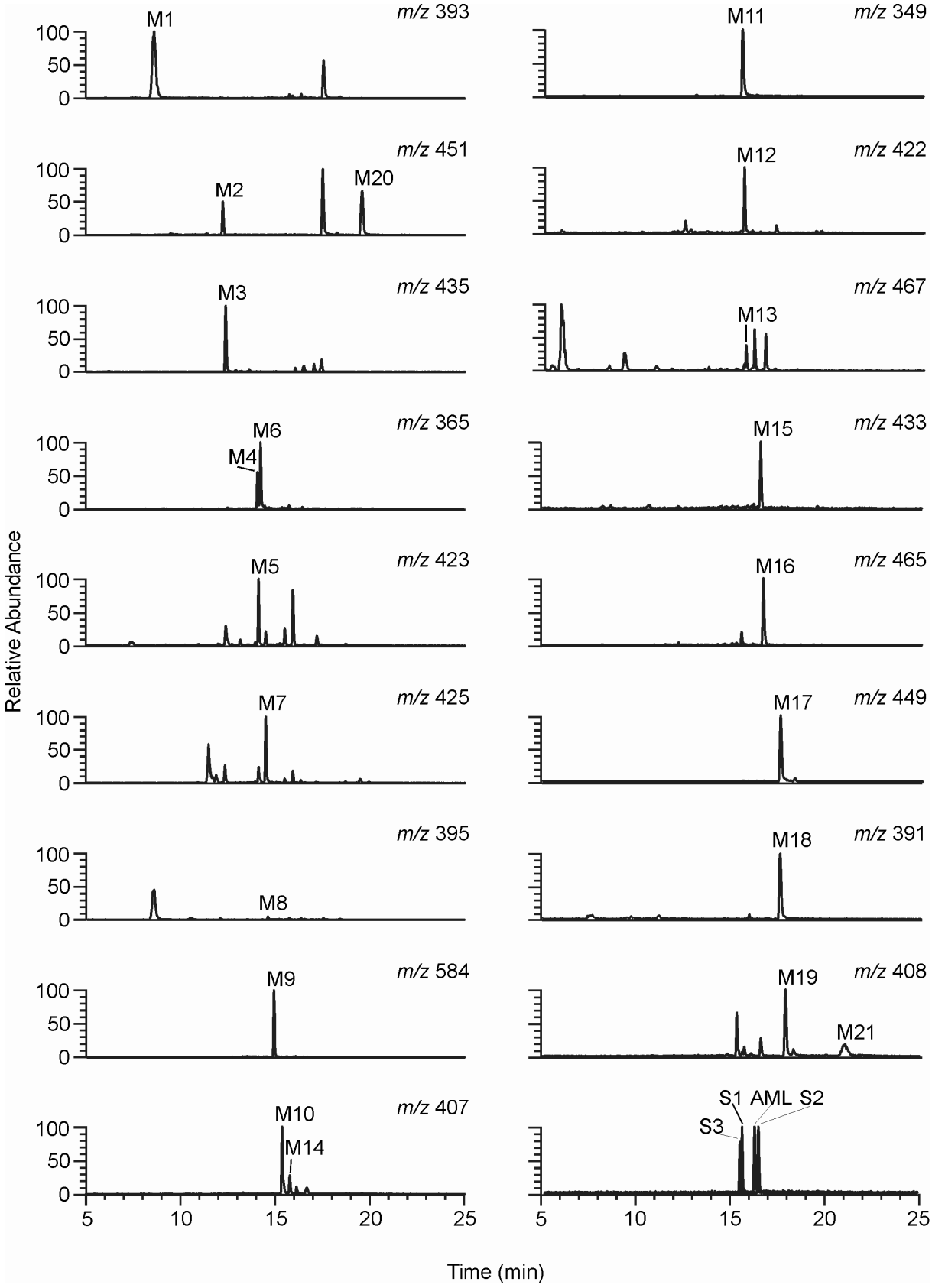
m/z 393
M1
m/z 349
M11
m/z 451
M2
M20
m/z 422
M12
m/z 435
M3
m/z 467
M13
m/z 365
M6
M4
m/z 433
M15
m/z 423
M5
m/z 465
M16
m/z 425
M7
m/z 449
M17
m/z 395
M8
m/z 391
M18
m/z 584
M9
m/z 408
M19
M21
m/z 407
M10
M14
S1
AML
S2
S3
100
50
0
5
10
15
20
25
Relative Abundance
Time (min)

Figure 2

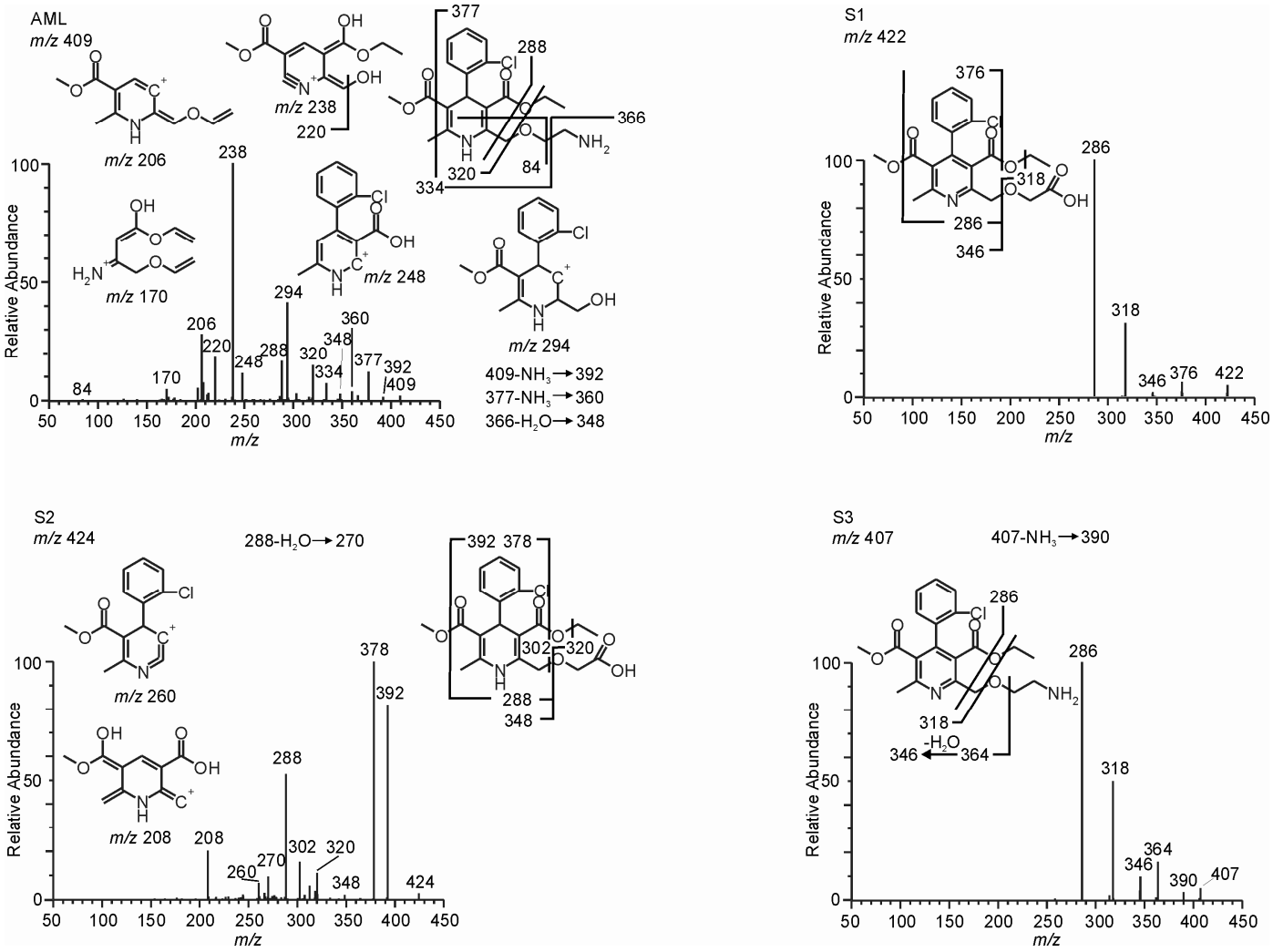
AML
m/z 409
m/z 206
m/z 238
m/z 220
m/z 170
m/z 248
m/z 294
409-NH3→392
377-NH3→360
366-H2O→348
Relative Abundance
m/z
S1
m/z 422
m/z 376
m/z 286
m/z 346
m/z 318
S2
m/z 424
288-H2O→270
m/z 260
m/z 208
S3
m/z 407
407-NH3→390
-H2O

Figure 3

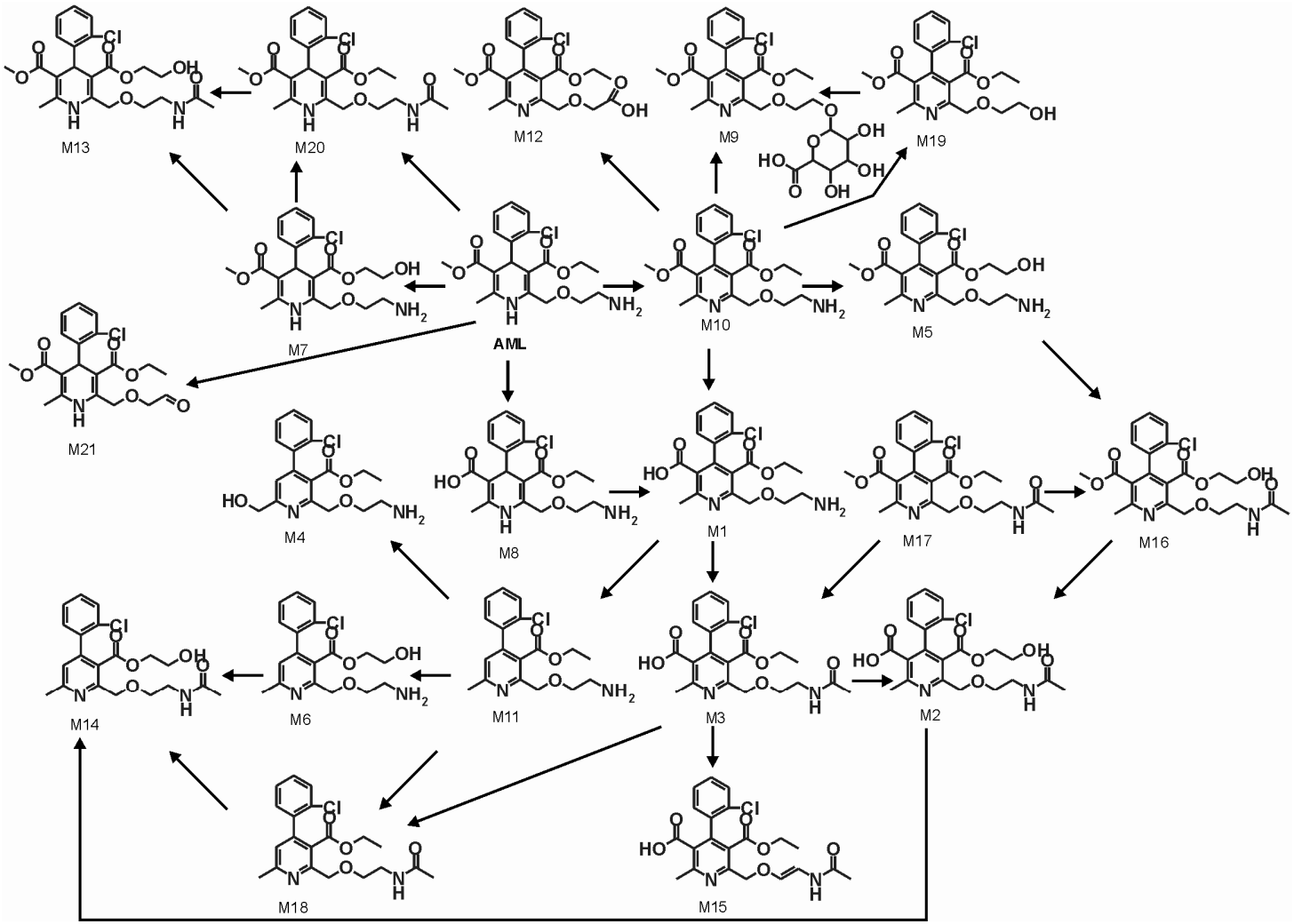
M13
M20
M12
M9
M19
M7
AML
M10
M5
M21
M4
M8
M1
M17
M16
M14
M6
M11
M3
M2
M18
M15

Figure 4